# VAGINAL DELIVERY OF MULTIVALENT ANTI-SPERM ANTIBODIES FOR EFFECTIVE NON-HORMONAL CONTRACEPTION

Bhawana Shrestha

A dissertation submitted to the faculty at the University of North Carolina at Chapel Hill in partial fulfillment of the requirements for the degree of Doctor of Philosophy in the Department of Microbiology and Immunology.

Chapel Hill
2021

Approved By:

Samuel K. Lai

Jason Whitmire

Brian Kuhlman

Brian Button

Raymond Pickles

Dirk Dittmer

**ABSTRACT**

Bhawana Shrestha: Vaginal delivery of multivalent anti-sperm antibodies for effective non-hormonal contraception
(Under the direction of Dr. Samuel Lai)

Nearly half of all pregnancies in the United States are unintended, due to poor adoption of existing methods of contraception, the majority of which are hormonal methods. Naturally occurring sperm-binding antibodies prevents fertilization in immune infertile women by trapping motile sperm in mucus through agglutination and mucin-crosslinking, thereby preventing sperm from reaching the egg. Indeed, vaginal delivery of sperm agglutinating IgM in the highly fertile rabbit model reduced embryo formation by 95%. This led us to explore the direct vaginal delivery of sperm-binding monoclonal antibodies as a strategy for effective non-hormonal contraception. In this dissertation, I worked to 1) Engineer a panel of multivalent IgGs possessing 4-10 Fabs against a unique surface antigen universally present on human sperm, 2) Assess the agglutination and trapping potency of all multivalent IgGs *in vitro* and *in vivo*, 3) Develop self-dissolving intravaginal film comprising of hexavalent sperm-binding IgG (6 Fabs per molecule; termed as "FIF") produced in cGMP-compliant *Nicotiana*-expression system and 4) Evaluate the potency of FIF-Film in reducing progressively motile sperm in the sheep vagina. Our results indicated that all multivalent IgGs produced at comparable yields and possessed identical thermal stability and homogeneity to the parent IgG. All multivalent IgGs were markedly more potent and faster at agglutinating sperm than the parent IgG, while preserving Fc-mediated crosslinking of individual spermatozoa in mucus. Especially, the highly multivalent IgGs (HM-IgGs; 6-10 Fabs per molecule) were at least 10- to 16-fold more potent and faster at agglutinating sperm than the parent IgG. The increased potencies translated to effective (>99.9%) reduction of progressively motile sperm in the sheep vagina using just 33 micrograms of the 10-Fab HM-IgG per sheep. Similarly, the polyvinyl alcohol-based water-

soluble contraceptive film formulated with *Nicotiana*-expressed 6-Fab HM-IgG enabled complete agglutination of all progressively motile sperm within 2 mins in the sheep vagina. These results not only underscore the potential of multivalent contraceptive antibodies to provide safe, effective, on-demand non-hormonal contraception but also represent a promising platform for generating potent agglutinating mAb for diverse medical applications such as anti-bacterial therapeutics.

## ACKNOWLEDGEMENTS

It would be an understatement to say Ph.D. was hard; it was a mentally- and physically-exhausting cycle of breaking down and starting all over again. Yet, if I had to redo my whole life, I would choose to do a Ph.D. all over again because at the end of the day it was completely worth it and unarguably, one of the most memorable parts of my life. However, I would not have been able to survive, let alone thrive, in Ph.D. without the support of many important human beings in my life; I call them "super-beings". First and foremost, I am very thankful for and continuously inspired by professor Samuel Lai because of his dedicated mentorship, expert guidance, and innovative mindset over the past 4 years. I am also very thankful to my thesis committee members: Jason, Dirk, Ray, Brian (Button), and Brian (Kuhlman) for not only providing crucial constructive feedback for the progression of my project, but also for looking out for my personal and professional well-being. I am very glad that I spent my 5 years in Lai Lab because I thoroughly enjoyed conducting experiments and venting when it didn't work, with an amazing team of Lai Lab members. Finally, I am incredibly grateful for all my friends and family, who repeatedly made my Ph.D. related stress go away with their magical brew of laughter and silliness, and provided all of the needed support and encouragement throughout my graduate career.

**TABLE OF CONTENTS**

## LIST OF TABLES

## LIST OF FIGURES

## LIST OF ABBREVIATIONS

Ab antibody

ALH lateral head amplitude

ANOVA analysis of variance

ASA anti-sperm antibody

BCF beat cross-frequency

BCM bovine cervical mucus

CASA computer-assisted sperm analysis

CFU colony-forming unit

cGMP current good manufacturing practice

CH constant heavy

CHO chinese hamster ovary

CHT ceramic hydroxyapatite

CL constant light

CVM cervicovaginal mucus

DSF differential scanning fluorimetry

ELISA enzyme-linked immunosorbent assay

FIF Fab-IgG-Fab

FIFF Fab-IgG-Fab-Fab

FFIFF Fab-Fab-IgG-Fab-Fab

FRT female reproductive tract

GPI glycosylphosphatidylinositol

GS glycine serine

HA hyperactivated

HC heavy chain

HCA human contraceptive antibody

HM-IgGs highly multivalent IgGs

HPLC high performance liquid chromatography

HRP horseradish peroxidase

IACUC institutional animal care and use committee

IRB institutional review board

IUD intrauterine devices

IVR intravaginal ring

LC light chain

LDS lithium dodecyl sulfate

LIN linearity

MW molecular weight

N9 nonoxynol-9

NPM non-progressively motile

PBS phosphate buffered saline

PCR polymerase chain reaction

PCT post coital test

PFA paraformaldehyde

PI propidium iodide

PM progressively motile

PVA polyvinyl alcohol

PVX potato virus X

scFv single-chain variable fragment

SDS-PAGE sodium dodecyl sulfate polyacrylamide gel electrophoresis

SEC-MALS size exclusion chromatography with multiple angle light scattering

SEM scanning electron microscopy

sIgA secretory IgA

STI sexually transmitted infections

STR straightness

Tagg aggregating temperature

TCEP tris(2-carboxyethyl) phosphine

Tm melting temperature

TMV tobacco mosaic virus

VAP average pathway velocity

VCF vaginal contraceptive film

VCL curvilinear velocity

VSL straight-line velocity

VH variable heavy

VL variable light

WHO world health organization

# CHAPTER 1: INTRODUCTION

## 1.1. Anti-sperm antibodies and infertility

The early evidence for the association of anti-sperm antibodies (ASAs) with human infertility was reported by Baskin in 1932 [1]. The controversial human trial that involved immunizing 20 fertile women with their partner's semen resulted in the detection of sperm-immobilizing activity in the serum of 19 women; only 1 woman became pregnant after 12 months when the sperm-immobilizing activity was no longer detectable in her serum. Since then, numerous investigations have characterized the incidence and the potential role of sperm-immobilizing antibodies in infertility [2–6]. ASAs are detected in the sera and genital secretions of both men and women. In men, ASAs are detected after the surgical removal of the vas deferens during vasectomy and in women, for unknown reasons, due to intolerance to their partner's sperm antigens [6]. ASAs have been detected in as many as 15% couples with otherwise unexplained infertility [3,7]. ASAs are thought to prevent fertility in women by limiting the cervical mucus penetration via two mechanisms i.e., agglutination and mucus trapping. First, at high sperm concentration, typically observed upon ejaculation, ASAs can agglutinate motile sperm into large clusters with no forward motility in the mucus [8,9]. Second, at a low concentration, ASAs can trap individual sperm in mucus without killing ("shaking phenomenon") by forming multiple low-affinity Fc-mucin bonds between sperm-bound ASA and mucin fibers [2,10–12]. Additionally, ASAs exhibit complement-dependent cytotoxicity in the presence of an external complement source but this mechanism is highly unlikely in the vaginal tract due to the low secretion of complement [13–15].

### 1.2. Anti-sperm antibodies for contraception

A few decades ago, the discovery of anti-sperm antibodies and their possible role in infertility led to significant interest in the use of sperm antigens as contraceptive vaccines. Several sperm-specific antigens such as FA-1, SP-10, CD52g etc. were identified as the potential candidates for the development of contraceptive vaccine [16,17]. ASAs elicited by vaccination with sperm antigens offered considerable contraceptive efficacy, but this approach stalled due to unresolved variability in the intensity and duration of the vaccine responses in humans, as well as concerns that active vaccination might lead to irreversible infertility [1,16,18]. Rather than active immunization, passive delivery of ASAs [19] represents the next logical method for contraception by providing identical advantages in potency and safety while overcoming the lack of predictability and potential irreversibility of active vaccination. Indeed, vaginal delivery of a sperm-agglutinating IgM reduced embryo formation by 95% in a highly fertile rabbit model [20]. Unfortunately, due to the exceedingly high costs of mAb production at the time and the emphasis on systemic administration for all mAb products on the market, cost-effective contraception by passive immunization simply was not thought feasible. However, the latest advances in bioprocessing have greatly reduced the costs of IgG production to make topical delivery of sperm-agglutinating mAbs for contraception potentially cost-effective [21,22]. Additionally, by further enhancing agglutination and muco-trapping potency of IgG-based sperm-agglutinating mAbs that is amenable to current methods of commercial-scale production, the cost, and dose of mAb contraception could be further reduced.

### 1.3. CD52g as a contraceptive target

CD52g was one of the sperm antigens submitted to the WHO workshop for the development of contraceptive vaccine [23]. CD52g, also known as SAGA-1, is a unique GPI-anchored glycoprotein that is secreted by epithelial cells lining the lumen of the epididymis and ubiquitously coated onto the sperm during sperm maturation [4,19]. CD52g is also present in the epithelium of the vas deferens, semen white blood cells, and seminal vesicles. CD52g is universally present on all human sperm while absent in all other tissues and women [19]. Both CD52g and lymphocyte GPI-anchored protein, CD52 possess an

identical core peptide of 12 amino acids but differ in N-linked glycan structures [24]. The function of CD52g is currently unknown, but it is thought to be involved in sperm maturation, preventing self-agglutination, immune (complement) protection of sperm in the female reproductive tract, and the liquefaction of semen [25]. Besides humans, this distinctive carbohydrate moiety of CD52g is only present in chimpanzees [26]. Due to such exclusivity and universality in the human male reproductive tract, CD52g remains an excellent antigen target for the development of monoclonal antibodies, which can be locally delivered to the vagina to provide safe and effective contraception in women.

### 1.4. Human Contraceptive Antibody

The human IgM antibody targeting CD52g, termed H6-3C4, was first reported and characterized by Isojima [8]. H6-3C4 was generated by immortalizing peripheral blood B cells isolated from an immune infertile woman with high sperm-immobilizing titers. The VH region of H6-3C4 was cloned into the IgG1 Heavy chain backbone and introduced into the mouse myeloma cell line for the production of the human IgG mAb against CD52g. Similarly, CD52g-binding mouse IgG, termed as S19, was isolated by John Herr by immunizing mice with human sperm [27,28]. Due to the polyvalent structure of IgM possessing 10 Fab arms and 5 Fc moieties and respectively offering the best combination of agglutination and trapping, H6-3C4 stands as the ideal molecule to develop a human contraceptive antibody (HCA). Unfortunately, large-scale manufacturing of IgM remains exceptionally costly, due to the lack of scalable processes to purify IgM while IgG is highly stable and easy to produce and purify; virtually all Ab products that are FDA approved or in clinical development are based on IgG [29,30]. IgG, though modest at mucus trapping, is a considerably weak agglutinator compared to IgM. Thus, in order to develop a potent and yet cost-effective mAb-based contraception, it is crucial to increase the potency of IgG-based ASA without compromising its much-appreciated stability and homogeneity.

### 1.5. Dissertation overview

In this dissertation, my goal is to elaborate on our recent advances in the engineering of multivalent sperm-binding IgGs and the subsequent development of intravaginal contraceptive film using the suitable mAb candidate to provide safe and effective non-hormonal contraception. This work is divided into three aims:

*Aim 1: Engineer multivalent HCA constructs for maximizing agglutination potency and maintaining trapping potency.* In this work, we designed a panel of HCA constructs comprising varying valencies (4-10) of Fab against a unique antigen present on human sperm, CD52g. The panel comprised of two 4Fab-HCAs in different orientations, 6Fab-HCA, 8Fab-HCA, and 10Fab-HCA, arranged in Fab-IgG, IgG-Fab, Fab-IgG-Fab, Fab-IgG-Fab-Fab, and Fab-Fab-IgG-Fab-Fab formats respectively. We expressed all HCA constructs using the Expi293 transfection system followed by purification using Protein A chromatography. Similarly, we rigorously characterized all constructs using (i) SDS-PAGE and size exclusion chromatography with multiple angle light scattering (SEC-MALS) for the correct assembly and (ii) DSF for thermostability and (iii) ELISA for binding activity.

*Aim 2: Measure sperm agglutination potency and trapping potency of the HCA constructs in vitro and in vivo.* We assessed the sperm agglutination potency of all HCA constructs in *vitro* by quantifying the reduction in the percentage of progressively motile sperm after treatment with HCA at different concentrations using Computer-Assisted Sperm Analysis (CASA). To determine the agglutination potency of constructs, we performed agglutination assays using whole semen, purified semen at high, average and low concentrations, and the capacitated sperm. Similarly, we assessed the trapping potency of HCA constructs *in vitro* by tracking fluorescently-labeled progressively motile sperm in HCA-treated cervicovaginal mucus. Next, we evaluated the sperm-immobilizing potency of lead HCA candidates in vivo by instilling the constructs into the vagina of female sheep followed by human semen and briefly simulated intercourse. Two minutes later, we quantified the progressively motile sperm present in the sheep vaginal fluids using a hemocytometer.

*Aim 3: Develop and assess the potency of an intravaginal film possessing HCA in vitro and in vivo.* We produced 6Fab HCA, FIF, using a cGMP-compliant Nicotiana expression system and formulated it into a water-soluble intravaginal film using polyvinyl alcohol. We assessed the agglutination and trapping potency of Nicotiana-produced FIF *in vitro* similar to Aim 2. We evaluated the potency of FIF-Film *in vivo* by instilling it into sheep's vagina followed by human semen. We immediately assessed the sheep vaginal fluids for progressively motile sperm using a hemocytometer.

# CHAPTER 2: ENGINEERING TETRAVALENT IGGS WITH ENHANCED AGGLUTINATION POTENCIES FOR TRAPPING VIGOROUSLY MOTILE SPERM IN MUCIN MATRIX[1]

## 2.1. Introduction

More antibodies (Ab) are secreted into mucus than the blood and lymph [31,32], where they are able to work in tandem with mucins to block foreign entities (virus, bacteria, cells) from permeating through the mucus layer and reaching target cells of interest [10,33]. When encountering low concentrations of foreign entities as common with most viral transmissions, the Fc domain of Ab can interact with mucins to facilitate crosslinking of virus-Ab complexes to the mucin mesh, commonly referred to as muco-trapping [10,12,33]. When encountering high concentrations of foreign entities such as bacteria and sperm, Ab (particularly polyvalent Ab) can also crosslink multiple foreign bodies together into clumps that are either too large to diffuse through mucus, or swim in a coordinated fashion towards target epithelium, a phenomenon commonly referred to as agglutination. Agglutination is particularly effective against motile species as they are much more likely to collide with each other and become agglutinated compared to diffusive species. Agglutination results in not only in an increase in hydrodynamic diameter, but more importantly an effective neutralization of the net forward motion of motile species.

Owing to its prevalence at mucosal surfaces and strong agglutination potency due to the diametrically-opposite orientation of the 4 Fab domains, sIgA represents an attractive format to develop Ab against highly motile species commonly encountered at mucosal surfaces, such as bacteria and sperm [34]. Unfortunately, there has been limited success advancing sIgA for mucosal applications in humans, in part because of manufacturing challenges and stability issues with sIgA and IgM. Recombinant

[1] This chapter is based on an article that previously appeared in Acta Biomaterialia. The original citation is as follows: Shrestha B., et al. Acta Biomaterialia (2020) 117, 226-234; https://doi.org/10.1016/j.actbio.2020.09.020

production of sIgA suffer from low production yields and stability due to its complex structure comprising 2 IgA antibodies linked together by the J chain and secretory component [35–37]. Similarly, the lack of scalable purification and homogenous expression remain the main challenges behind recombinant IgM production because of the large size and complexity of IgM structure [29,38,39]. In contrast, IgGs are highly stable and easy to produce, making IgG the most common Ab format for the development of biologics [40]. We hypothesized that we could overcome the instability and production challenges of sIgA as well as the limited agglutination potency of IgG by creating IgG molecules with 4 Fabs, identical to sIgA. This includes two different formats: "Fab-IgG" and "IgG-Fab", based on linking an additional Fab to either the N- or C- terminus respectively, of a parent IgG using a flexible glycine-serine linker (Figure 2.1A).We specifically engineered these two formats because IgG-Fab possess structural similarity to sIgA with diametrically opposite Fabs, while Fab-IgG is a commonly studied tetravalent-IgG format [21,41]. The comparison of Fab-IgG and IgG-Fab formats, which differ only in the location of the additional appended Fab fragment, could provide critical insights into the importance of geometric orientation in the agglutination potency of Abs.

As a proof-of-concept to assess agglutination potencies, we engineered the tetravalent and parent IgGs to bind sperm, as a potential approach to enable safe and effective non-hormonal contraception. Globally, over 40% of all pregnancies are unintended, which creates an enormous burden on healthcare systems [42], including over $20 billion per year in the U.S. alone [43,44]. Despite the availability of cheap and effective contraceptive methods such as progestin and/or estrogen birth control pills and intrauterine devices (IUD), many women are dissatisfied with available contraceptive methods, particularly due to real and/or perceived side-effects associated with the use of exogenous hormones, including increased risks of breast cancer, depression, prolonged menstrual cycle, nausea and migraines [45,46]. Many women are also restricted from using estrogen-based hormonal contraceptives due to medical contraindications [47–49]. Current non-hormonal contraceptives are limited to detergent-based spermicides (e.g. nonxynol-9), which are toxic to mucosal surfaces and substantially increase the risks of STI transmission, and the copper-IUD, which, though highly effective, is adopted only by a small and

declining fraction of women due to heavy menstrual bleeding and its relative invasiveness [50]. These realities strongly underscore the need for convenient non-hormonal contraceptives.

Sperm possess vigorous motility, and women are frequently exposed to a very high concentration of sperm in semen in the vagina. Interestingly, anti-sperm antibodies (ASAs) in infertile women can readily agglutinate and arrest highly motile sperm in mucus, thereby preventing sperm from permeating through mucus and reaching the egg [2,51]. Vaginal delivery of sperm agglutinating ASA exhibited considerable contraceptive efficacy in a rabbit model, reducing embryo formation by 95% in the highly fertile rabbit model [20]. Unfortunately, this approach had not been translated into a clinical setting, due to limited agglutination potencies of IgG. Previous work has shown that CD52g, a glycoform of CD52, is universally present in abundant quantities on the surface of all sperm yet absent in all other tissues and women, establishing CD52g as a highly promising target for contraceptive mAbs. Using a Fab domain isolated from an immune infertile but otherwise healthy woman [8,52], we engineered Fab-IgG and IgG-Fab against CD52g, and assessed their agglutination potencies compared to the parent IgG.

**2.2. Materials and Methods:**

***2.2.1. Study design and ethics***. All studies were performed following a protocol approved by the Institutional Review Board of the University of North Carolina at Chapel Hill (IRB-101817). Informed written consent was obtained from all male and female subjects before the collection of any material.

***2.2.2. Cloning and expression of the parent and tetravalent anti-sperm IgG Abs***. The variable heavy (VH) and variable light (VL) DNA sequences for anti-sperm IgG1 Ab were obtained from the published sequence of H6-3C4 mAb [8,52]. For light chain (LC) production, a gene fragment consisting of VL and CL sequences (Integrated DNA Technologies, Coralville, IA) was cloned into an empty mammalian expression vector (pAH, ThermoFisher Scientific) using KpnI (5') and EcoRI (3') restriction sites. For parent IgG and Fab-IgG heavy chain (HC) production, VH and VH/CH1-(G4S)6 linker-VH gene fragments (GeneArt, ThermoFisher Scientific) were respectively cloned into mammalian IgG1 expression

vector comprising of only CH1-CH2-CH3 DNA sequence using KpnI (5') and NheI (3') restriction sites. For IgG-Fab HC production, (G4S)6 linker-VH/CH1 was cloned into the parent IgG expression plasmid using BamHI (5') and MluI (3') restriction sites. The expression plasmids encoding HC and LC sequences were co-transfected into Expi293F cells using ExpiFectamine™ 293 Transfection reagents (Gibco, Gaithersburg, MD) [53]. For IgG expression, HC and LC plasmid were co-transfected using a 1:1 ratio at 1 μg total DNA per 1 mL of culture. For Fab-IgG and IgG-Fab expression, HC and LC plasmid were co-transfected using a 1:2 ratio at 1 μg total DNA per 1 mL culture. Transfected Expi293F cells were grown at 37°C in a 5% CO2 incubator and shaken at 125 r.p.m. for 3-5 days. Supernatants were harvested by centrifugation at 12,800 g for 10 min and passed through 0.22 μm filters. Briefly, Abs were purified using standard protein A/G chromatography method. 30 mL of purified supernatants were incubated with 600 μL Pierce protein A/G agarose resins (Thermofisher Scientific) overnight at 4°C and loaded into Econo-Pac® Chromatography Columns (Bio-Rad). Resins were washed three times with 1X phosphate-buffered saline (PBS) and proteins were eluted from the resins using 900 μl Pierce™ IgG Elution Buffer (Thermofisher Scientific). The eluants were immediately neutralized with 100 μL UltraPure™ 1M Tris-HCI, pH 8.0 (Thermofisher Scientific). Next, purified Abs were quantified using absorbance at 280 nm along with the corresponding protein extinction coefficients [54]. The extinction coefficients for IgG, Fab-IgG and IgG-Fab were calculated to be 245400, 415980 and 415980 respectively.

***2.2.3. Characterization of the parent and tetravalent anti-sperm IgG Abs***. The molecular size of the purified Abs was determined using sodium dodecyl sulfate–polyacrylamide gel electrophoresis (SDS-PAGE) at reducing and non-reducing conditions. For each sample, 1 μg of protein was diluted in 3.75 μL lithium dodecyl sulfate (LDS) sample buffer followed by the addition of 11.25 μL nuclease-free water. Proteins were then denatured at 70°C for 10 min. Next, 0.3 μL of 0.5 M tris (2-carboxyethyl) phosphine (TCEP) was added as a reducing agent to the denatured protein for reduced samples and incubated at

room temperature for 5 min. Bio-Rad Precision Protein Plus Unstained Standard and Novex™ Sharp Pre-stained Protein Standard were used as ladders. After loading the samples, the gel was run for 50 min at a constant voltage of 200 V. The protein bands were visualized by staining with Imperial Protein Stain (Thermo Scientific) for 1 hr followed by overnight de-staining with Milli-Q water. Image J software (Fiji) was used to adjust the brightness and contrasts of the SDS-PAGE gel for visual purposes.

Size exclusion chromatography with multiple angle light scattering (SEC-MALS) was used to determine the weight average molar weight (MW) and the homogeneity of the purified Abs [55]. The experimental setup consisted of a GE Superdex 200 10/300 column connected to an Agilent FPLC system, a Wyatt DAWN HELEOS II multi-angle light-scattering instrument, and a Wyatt T-rEX refractometer. Experiments were performed at room temperature with a flow rate maintained at 0.5 mL/min. The column was equilibrated with 1X PBS pH 7.4 containing 200 mg/L of NaN3 before sample loading. 50-100 µL of each sample (1 mg/mL) was injected onto the column, and the MALS data were collected and analyzed using Wyatt ASTRA software (Ver. 6). As the solutes moves through the SEC-MALS system, they scatter light, and the detectors placed at various angles (with respect to the LASER) measure the scattered light intensities at these angles, and the refractometer measures the concentration of the solutes (as refractive index is proportional to the concentration of the solutes) at each time point. Using these values, ASTRA software fits the data to a Debye plot [56,57] and determines the MW of the solutes eluting in different peaks, unequivocally, without using any standards.

The Tm and Tagg of the purified Abs were determined using nano differential scanning fluorimetry (nanoDSF; Nanotemper Prometheus NT.48 system) [58]. Samples were diluted to 0.5 mg/mL in 1X PBS at pH 7.4 and loaded into Prometheus NT.48 capillaries. Thermal denaturation experiments were performed from 20°C to 95°C at the rate of 1°C/min, measuring the intrinsic tryptophan fluorescence at 330 nm and 350 nm. The Tm for each experiment was calculated automatically by Nanotemper PR.Thermcontrol software by plotting the ratiometric measurement of the fluorescent signal against increasing temperature. Next, the Tagg for each experiment was also calculated automatically by Nanotemper PR.Thermcontrol software via the detection of the back-reflection intensity of a light beam

that passes through the sample. As the Ab aggregates, it scatters more light, thus, leading to a reduction of the back-reflected light.

***2.2.4. Collection and processing of semen samples***. Healthy male subjects were asked to refrain from sexual activity for at least 24 hr before semen collection. Semen was collected by masturbation into sterile 50 mL sample cups and incubated for a minimum of 15 min post-ejaculation at room temperature to allow liquefaction. Semen volume was measured, and the density gradient sperm separation procedure (Irvine Scientific, Santa Ana, CA) was used to extract motile sperm from liquefied ejaculates. Briefly, 1.5 mL of liquified semen was carefully layered over 1.5 mL of Isolate® (90% density gradient medium, Irvine Scientific) at room temperature, and centrifuged at 300 g for 20 min. Following centrifugation, the upper layer containing dead cells and seminal plasma was carefully removed without disturbing the motile sperm pellet in the lower layer. The sperm pellet was then washed twice with the sperm washing medium (Irvine Scientific) by centrifugation at 300 g for 10 min. Finally, the purified motile sperm pellet was resuspended in the sperm washing medium, and an aliquot was taken for determination of sperm count and motility using computer-assisted sperm analysis (CASA). All semen samples used in the functional assays exceeded lower reference limits for sperm count (15 x 106 total sperm/mL) and total motility (40%) as indicated by the World Health Organization guidelines [59].

***2.2.5. Sperm count and motility using CASA***. The Hamilton-Thorne computer-assisted sperm analyzer, 12.3 version, was used for the sperm count and motility analysis. This device consists of a phase-contrast microscope (Olympus CX41), a camera, an image digitizer, and a computer with a Hamilton-Thorne Ceros 12.3 software to save and analyze the acquired data. For each analysis, 4.4 μL of the semen sample was inserted into MicroTool counting chamber slides (Cytonix, Beltsville, MD) and six randomly selected microscopic fields, near the center of the slide, were imaged and analyzed for progressively motile and non-progressively motile sperm count. The parameters that were assessed by CASA for motility analysis were as follows: average pathway velocity (VAP), the straight-line velocity (VSL), the

curvilinear velocity (VCL), the lateral head amplitude (ALH), the beat cross-frequency (BCF), the straightness (STR) and the linearity (LIN). PM sperm were defined as having a minimum of 25 μm/s VAP and 80% of STR. The complete parameters of the Hamilton-Thorne Ceros 12.3 software are listed in Table 2.1 [60,61].

**Table 2.1:** The sperm motility parameters of the Hamilton-Thorne Ceros 12.3.

| Parameter | Value | Parameter | Value |
|---|---|---|---|
| Frames Per Sec | 60 | Path Velocity (VAP) | 25 μm/s |
| No. of Frames | 60 | Straightness (STR) | 80 % |
| Minimum Cell Size | 3 pixels | VAP Cutoff | 10 μm/s |
| Default Cell Size | 6 pixels | VSL Cutoff | 0 μm/s |
| Minimum Contrast | 80 | Slow Cells | Motile |
| Default Cell Intensity | 20 | Standard Objective | 10X |
| Chamber Depth | 20 μm | Magnification | 1.87 |

***2.2.6. Whole sperm enzyme-linked immunosorbent assay (ELISA)***. Briefly, half-area polystyrene plates (CLS3690, Corning) were coated with 2 x 105 sperm per well in 50 μL of NaHCO3 buffer (pH 9.6). After overnight incubation at 4°C, the plates were centrifuged at the speed of 300 g for 20 min. The supernatant was discarded, and the plates were air-dried for 1 hr at 45°C. The plates were washed once with 1X PBS. 100 μL of 5% milk was incubated at room temperature for 1 hr to prevent non-specific binding of Abs to the microwells. The serial dilution of mAbs in 1% milk was added to the microwells and incubated overnight at 4°C. Motavizumab, a mAb against the respiratory syncytial virus, was constructed and expressed in the laboratory by accessing the published sequence and used as a negative control for this assay [62]. After primary incubation, the plates were washed three times using 1X PBS. Then, the secondary Ab, goat anti-human IgG F(ab')2 Ab HRP-conjugated (1:10,000 dilutions in 1% milk, 209-1304, Rockland Inc.) was added to the wells and incubated for 1 hr at room temperature. The washing procedure was repeated and 50 μL of the buffer containing substrate (1-Step Ultra TMB ELISA Substrate, Thermo Scientific) was added to develop the colorimetric reaction for 15 min. The reaction was quenched using 50 μL of 2N H2SO4, and the absorbance at 450 nm (signal) and 570 nm (background) was measured using SpectraMax M2 Microplate Reader

(Molecular Devices). Each experiment was done with samples in triplicates and repeated two times as a measure of assay variability.

***2.2.7. Scanning electron microscopy***. Briefly, 20 x $10^6$ washed sperm was centrifuged at 300 g for 10 min and the supernatant was discarded without disturbing the sperm pellet. Then, 200 µL of Abs or 1X PBS was added to the sperm pellet, mixed by pipetting and incubated for 5 mins using an end-over-end rotator. Next, 200 µL of 4% paraformaldehyde was added to the Ab-sperm solution and incubated for 10 min using an end-over-end rotator. 50 µL of fixed sperm sample was filtered and washed through membrane filters (10562, K04CP02500, Osmonics, Minnetonka, MN) using 0.15 M sodium phosphate buffer. The samples were then dehydrated in a graded series of alcohol, transferred to a plate with the transitional solvent, hexamethyldisilazane (Electron Microscopy Sciences, Hatfield, PA), and allowed to dry after one exchange. Next, filters were adhered to aluminum stubs with carbon adhesives and samples were sputter-coated with gold-palladium alloy (Au:Pd 60:40 ratio, 91112, Ted Pella Inc., Redding, CA) to a thickness of 3 nm using Cressington Sputter Coater 208 hr. Six random images were acquired for each sample using a Zeiss Supra 25 FESEM with an SE2 Electron detector at 2500X magnification.

***2.2.8. Sperm escape assay***. Briefly, 40 µL aliquots of purified sperm (10 x $10^6$ PM sperm/mL) were transferred to individual 0.2 mL polymerase chain reaction (PCR) tubes. Sperm count and motility were performed again on each 40 µL aliquot using CASA. This count serves as the original (untreated) concentration of sperm for evaluating the agglutination potencies of respective Ab constructs. Following CASA, 30 µL of purified sperm was mixed into 0.2 mL PCR tubes containing 30 µL of Abs or sperm washing medium control. The tubes were then fixed at 45° angles for 5 min at room temperature. Following this incubation period, 4.4 µL was extracted from the top layer of the mixture with minimal perturbation of the tube and transferred to the CASA instrument to quantify the number of PM sperm. The percentage of the PM sperm that escaped agglutination was computed by dividing the sperm count obtained after treatment with Ab constructs by the original untreated sperm count in each respective tube,

correcting for the 2-fold dilution with Ab. Each experimental condition was evaluated in duplicates on each semen specimen, and the average from the two experiments was used in the analysis. Data represent 6 independent experiments with at least 4 unique semen samples. P values were calculated using a one-way analysis of variance (ANOVA) with Dunnett's multiple comparisons test. 6.25 μg/mL was selected as the starting concentration for the escape assay because it was the lowest working concentration for IgG. Similarly, the assay was continued until 0.095 μg/mL to determine the dose at which tetravalent IgGs fail.

***2.2.9. Agglutination kinetics assay***. Briefly, 4.4 μL of purified sperm (10 x $10^6$ PM sperm/mL) was added to 4.4 μL of Ab constructs in 0.2 mL PCR tubes followed by gentle mixing. Immediately, a timer was started and 4.4 μL of the mixture was transferred to chamber slides. The centerfield of the slides was then imaged and analyzed by CASA instrument every 30 s up to 90 s. The reduction in the percentage of PM sperm at each time point was computed by normalizing the PM sperm count obtained after Ab treatment to the PM sperm count obtained after control treatment with the sperm washing medium. Each experimental condition was evaluated in duplicates on each semen specimen, and the average from the two experiments was used in the analysis. Data represent 6 independent experiments with at least 4 unique semen samples. P values were calculated using a one-way ANOVA with Dunnett's multiple comparisons test. 6.25 μg/mL was selected as the starting concentration for the kinetics assay because it was the lowest working concentration for IgG. Similarly, the assay was continued until 0.39 μg/mL to determine the dose at which tetravalent IgGs fail.

***2.2.10. Fluorescent labeling of sperm***. Purified sperm were fluorescently labeled using Live/Dead Sperm Viability Kit (Invitrogen, Thermofisher Scientific). SYBR 14 dye, a membrane-permeant nucleic acid stain, stained the live sperm while propidium iodide, a membrane impermeant nucleic acid stain, stained the dead sperm. SYBR14 and propidium iodide dye were added to 1 mL of washed sperm resulting in final SYBR 14 and PI concentration of 200 nM and 12 μM respectively and incubated for 10 min at 36

°C. The sperm-dye solution was washed twice using the sperm washing medium to remove unbound fluorophores by centrifuging at 300 g for 10 min. Next, the labeled motile sperm pellet was resuspended in the sperm washing medium, and an aliquot was taken for determination of sperm count and motility using CASA.

***2.2.11. Cervicovaginal mucus (CVM) collection and processing***. CVM was collected as previously described [10]. Briefly, undiluted CVM secretions, averaging 0.5 g per sample, were obtained from women of reproductive age, ranging from 20 to 44 years old, by using a self-sampling menstrual collection device (Instead Softcup). Participants inserted the device into the vagina for at least 30 s, removed it, and placed it into a 50 mL centrifuge tube for collection. Samples were collected at various times throughout the menstrual cycle, and the cycle phase was estimated based on the last menstrual period date normalized to a 28-day cycle. Samples that were non-uniform in color or consistency were discarded. Donors stated they had not used vaginal products nor participated in unprotected intercourse within 3 days before donating. All samples had pH < 4.5.

***2.2.12. Multiple particle tracking of fluorescently labeled sperm in CVM***. Multiple particle tracking was performed as previously described [10]. Briefly, fresh CVM was diluted three-fold using sperm washing medium to mimic the dilution and neutralization of CVM by alkaline seminal fluid in humans and titrated to pH 6.8-7.1 using small volumes of 3 N NaOH. Next, 4 μL of Abs or control (anti-RSV IgG1) was added to 60 μL of diluted and pH-adjusted CVM and mixed well in a CultureWellTM chamber slide (Invitrogen, ThermoFisher Scientific) followed by mixing of 4 μL of 1 x $10^6$ fluorescently labeled PM sperm/mL. Chamber slides were incubated for 5 min at room temperature. Then, translational motions of the fluorescently labeled sperm were recorded using an electron-multiplying charge-coupled-device camera (Evolve 512; Photometrics, Tucson, AZ) mounted on an inverted epifluorescence microscope (AxioObserver D1; Zeiss, Thornwood, NY) equipped with an Alpha Plan-Apo 20/0.4 objective, environmental (temperature and CO2) control chamber, and light-emitting diode (LED) light source

(Lumencor Light Engine DAPI/GFP/543/623/690). 15 videos (512 × 512 pixels, 16-bit image depth) were captured for each Ab condition with MetaMorph imaging software (Molecular Devices, Sunnyvale, CA) at a temporal resolution of 66.7 ms and spatial resolution of 50 nm (nominal pixel resolution, 0.78 μm/pixel) for 10 s. Convolutional neural network-based tracking software, which enables fully automated and high fidelity tracking of the motion of entities captured by high resolution video microscopy, was used to determine x, y location of each sperm from each frame of the video. The x,y coordinates over time were then used to calculate quantitative metrices describing sperm motion, such as VAP, VCL, VSL, and STR [63].Sperm were classified as PM if they exhibited a VAP and VCL of at least 25μm/s and 20 μm/s respectively, as well as a VSL to VAP ratio of at least 0.8 [16,17]. Data represent 6 independent experiments, each using a unique combination of CVM and semen specimens. P values were calculated using a one-tailed t-test. 25μg/mL was selected as the working concentration for the muco-trapping assay because it was the lowest working concentration for IgG.

***2.2.13. Statistical Analysis***. All analyses were performed using GraphPad Prism 8 software. For multiple group comparisons, P values were calculated using a one-way ANOVA with Dunnett's multiple comparisons tests. The comparison between control- and anti-sperm Ab-treated fluorescent PM sperm was performed using a one-tailed t-test. In all analyses, $\alpha=0.05$ for statistical significance. All data are presented as the arithmetic mean ± standard deviation.

## 2.3. Results

### *2.3.1. Expression and characterization of tetravalent IgGs*

Upon transient transfection in mammalian (Expi293F) cells, Fab-IgG and IgG-Fab expressed at comparable levels to the parent IgG (Figure 2.1B). The parent IgG, Fab-IgG and IgG-Fab all exhibited their expected molecular weights of 150 kDa, 250 kDa and 250 kDa, respectively (Figure 2.1C). Surprisingly, while the parent IgG possessed a small fraction of aggregates that is commonly observed

with IgGs in general, the tetravalent IgGs appeared completely homogeneous with no detectable aggregation (Figure 2.1D and E).

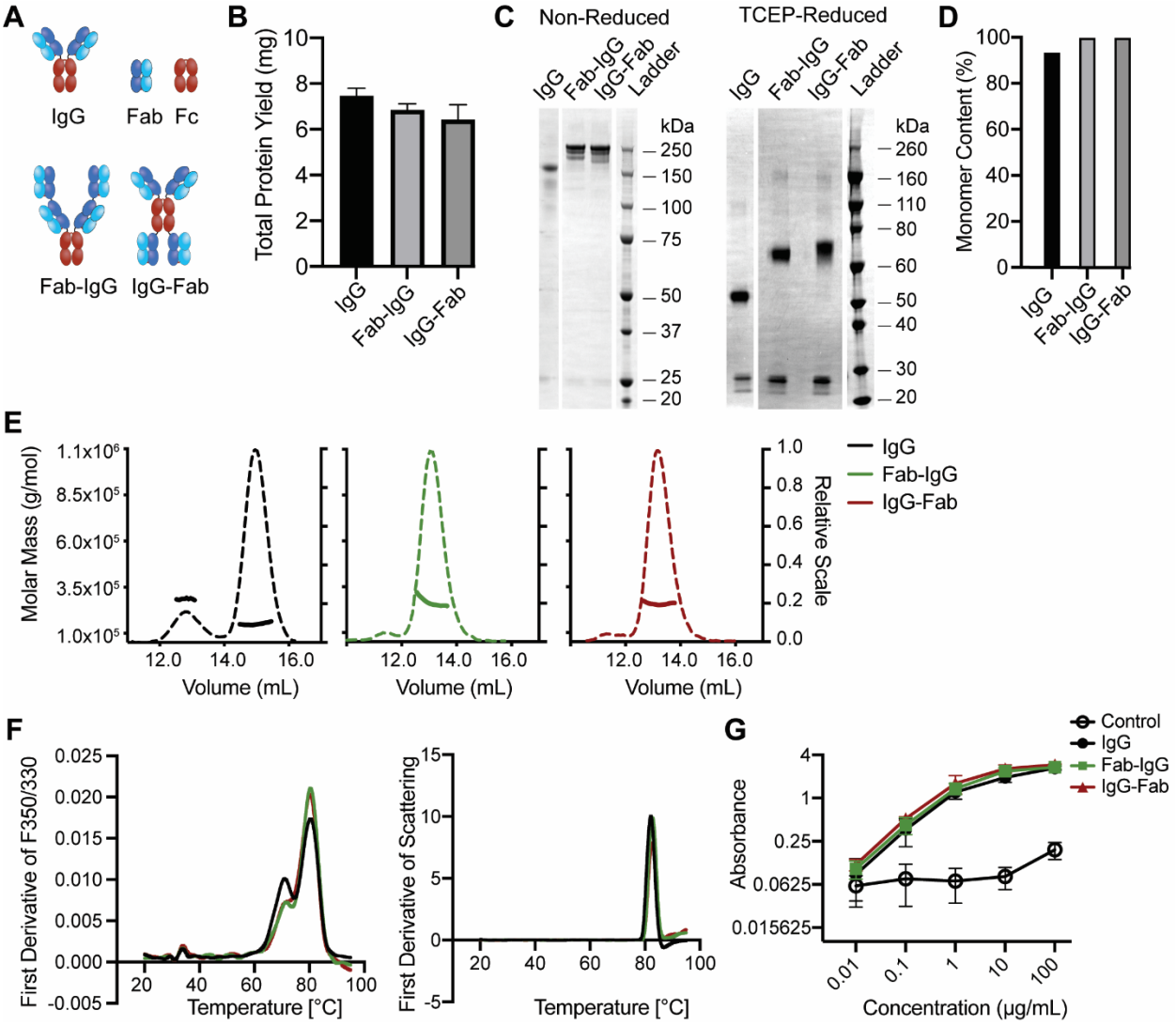


**Figure 2.1: Production and characterization of tetravalent anti-sperm IgG Abs**. (A) Schematic diagrams of anti-sperm IgG, Fab-IgG and IgG-Fab. (B) Purified production yield of IgG, Fab-IgG and IgG-Fab from 90 mL Expi293 cells transfection. Data were obtained from 2 independent transfections. (C) Non-reducing and reducing SDS-PAGE analysis of the indicated Abs (1 µg). (D) Demonstration of the purity and homogeneity of the indicated Abs (50-100 µg) using SEC-MALS analysis. Y-axis indicates the total percentage of Abs representing their theoretical molecular weights. (E) SEC-MALS curves of the indicated Abs. Thick lines indicate the calculated molecular mass (left y-axis) and the dotted lines show the homogenous profile (right y-axis) of the mass for each Ab. (F) The melting temperatures (left) and aggregating temperature (right) of the indicated Abs as determined by the nanoDSF experiment. The experiment was performed in duplicates and averaged. (G) Whole sperm ELISA to assess the binding potency of the indicated Abs to human sperm. Motavizumab (anti-RSV IgG1) was used as the control. Data represent 3 independent experiments with 3 unique semen donors. Each experiment was performed in triplicates and averaged. Lines indicate arithmetic mean values and standard deviation.

We next evaluated the thermostability of the Fab-IgG and IgG-Fab using differential scanning fluorimetry (DSF). Both constructs exhibited exceptional thermal stability, unfolding only at high temperatures of Tm1 (midpoint of unfolding of CH2) ≥ 71.1°C and Tm2 (midpoint of unfolding of Fab and CH3) ≥ 80°C [21,64,65], comparable to those of the parent IgG (Figure 2.1F). We next confirmed the binding of Fab-IgG and IgG-Fab to their sperm antigen using a whole sperm ELISA assay. Both constructs bound comparably to the human sperm as the parent IgG at 0.1 μg/mL (Figure 2.1G).

### *2.3.2. Tetravalent IgGs exhibit stronger agglutination potency than parent IgG*

Species with the greatest active motility are able to most readily penetrate through mucus. Indeed, progressively motile (PM) sperm is the key sperm fraction responsible for fertilization due to their capacity to swim through mucus to reach the egg. We thus assessed the ability of Fab-IgG and IgG-Fab to agglutinate human sperm, using an *in vitro* sperm escape assay that quantified the number of PM sperm that escaped agglutination when treated with the tetravalent IgGs vs the parent IgG as well as sperm washing media control, determined by CASA [60,61]. Upon agglutination in the escape assay, clumps of sperm quickly settle out by gravitation, resulting in reduction of individual PM sperm. The assay was carried out at the final concentration of 5 million PM sperm/mL, reflecting typical amounts of PM sperm in fertile males [59,66]. We found that Fab-IgG and IgG-Fab both exhibited markedly greater sperm agglutination potency than parent IgG. The minimal mAb concentration needed to reduce PM sperm >98% was reduced from 6.25 μg/mL for the parent IgG to 1.56 μg/mL for both Fab-IgG and IgG-Fab (Figure 2.2A). Although both constructs failed to achieve >98% agglutination at 0.39 μg/mL, they were still able to reduce PM sperm by >80% (Figure 2.2B). In comparison, the parent IgG at 0.39 μg/mL offered no detectable reduction in PM sperm populations.

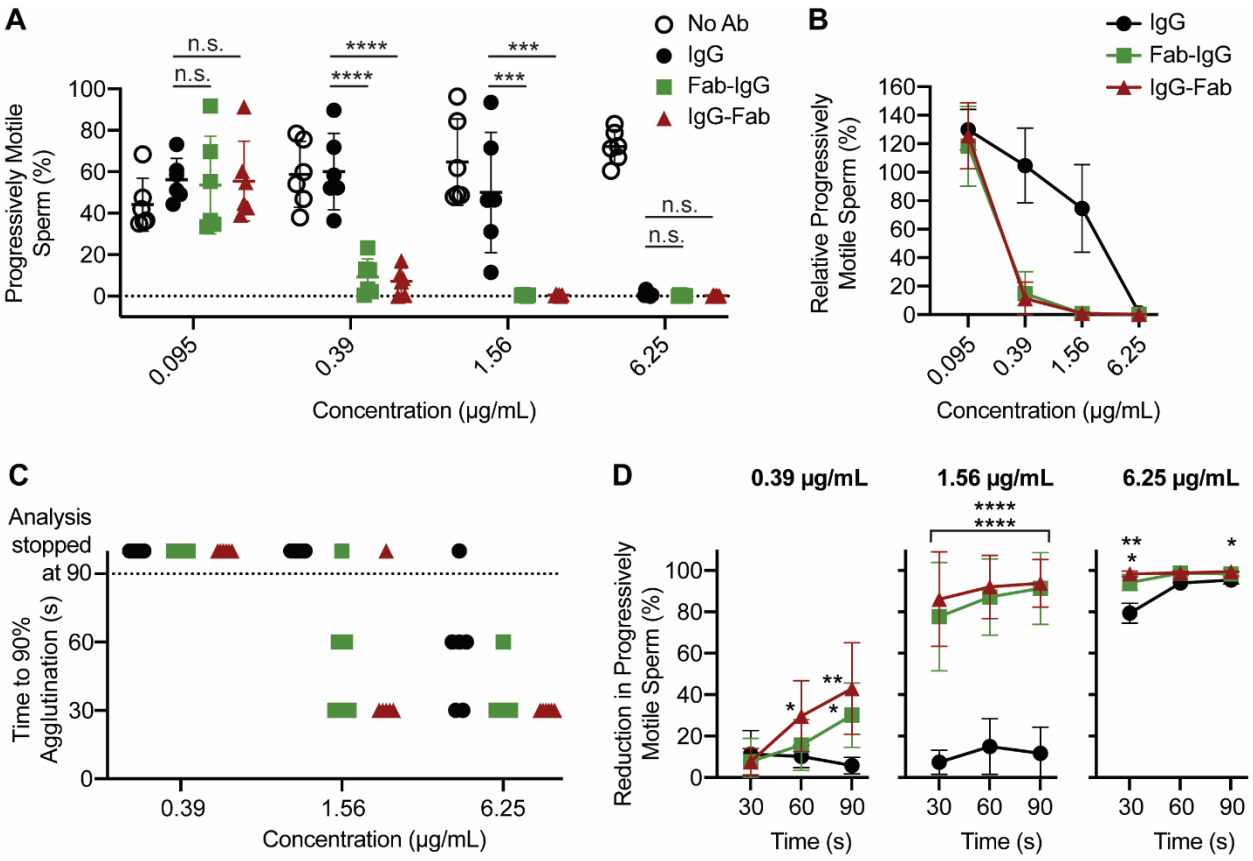


**Figure 2.2: Multimerization markedly enhances the agglutination potency and kinetics of anti-sperm tetravalent IgG Abs.** (A) Sperm agglutination potency of the parent IgG, Fab-IgG and IgG-Fab measured by the CASA-based quantification of the percentage of sperm that remains PM after Ab-treatment compared to pre-treatment condition. (B) The sperm agglutination potency of the Abs normalized to media control. (C) The sperm agglutination kinetics of the indicated Abs measured by the quantification of time required to achieve 90% agglutination of PM sperm compared to the media control. (D) The rate of sperm agglutination determined by the reduction in the percentage of PM sperm count at three timepoints after Ab-treatment compared to the media control. Purified sperm at the final concentration of 5 x $10^6$ PM sperm/mL was used for both agglutination potency and kinetics studies. Data were obtained from N = 6 independent experiments using at least 4 unique semen samples. *P < 0.05, **P < 0.01, ***P < 0.001 and ****P < 0.0001. Lines indicate arithmetic mean values and standard deviation.

### *2.3.3. Tetravalent IgGs exhibit faster agglutination kinetics than parent IgG*

For maximum protection, sufficient number of Ab must bind to the target active species before they permeate through mucus. For instance, sperm must be stopped in mucus before they can swim through the cervix and access the uterus for effective contraception [67]. This suggests Abs that could agglutinate sperm more quickly should provide more effective contraception. Thus, we next quantified the sperm-agglutination kinetics of both tetravalent IgG constructs using CASA, specifically measuring

the fraction of agglutinated and free PM sperm over time immediately after mixing washed sperm with different mAbs. At 6.25 μg/mL, the parent IgG reduced PM sperm by ≥90% within 90s in 5 of 6 semen samples; at 1.56 μg/mL, the parent IgG failed to do so in all 6 of 6 samples (Figure 2.2C). In contrast, Fab-IgG and IgG-Fab achieved ≥90% agglutination within 30s in all 6 of 6 samples at 6.25 μg/mL, and within 60s in 5 of 6 samples at 1.56 μg/mL. Notably, the agglutination kinetics of Fab-IgG and IgG-Fab were both markedly faster and more complete than the parent IgG at each Ab concentrations tested and across all timepoints (Figure 2.2D). We visually confirmed sperm agglutination by the parent IgG vs. tetravalent IgGs at their effective concentrations using scanning electron microscopy (Figure 2.3).

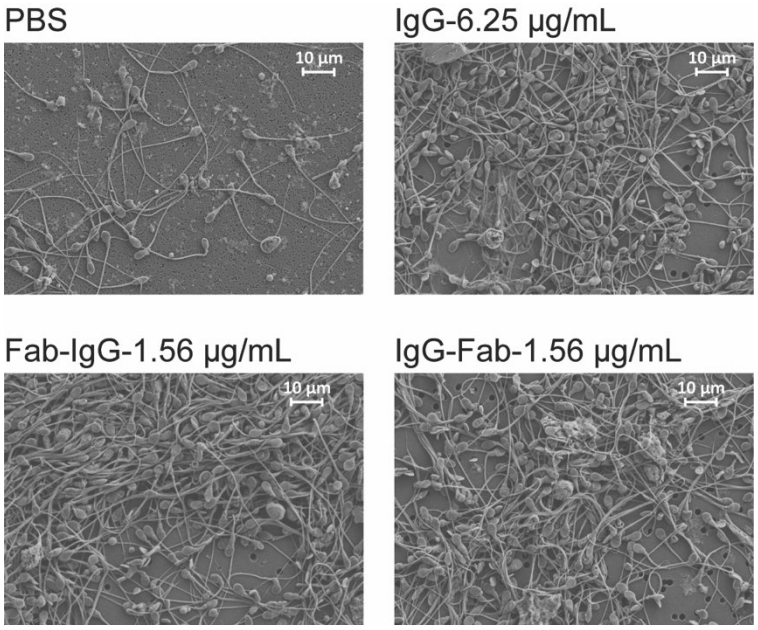


**Figure 2.3: Scanning electron microscopy images of the agglutinated sperm.** 20 million washed sperm were treated with IgG, Fab-IgG and IgG-Fab for 5 min and fixed using 4% paraformaldehyde. Images were obtained at 2500X magnification. Scale bar, 10 μm.

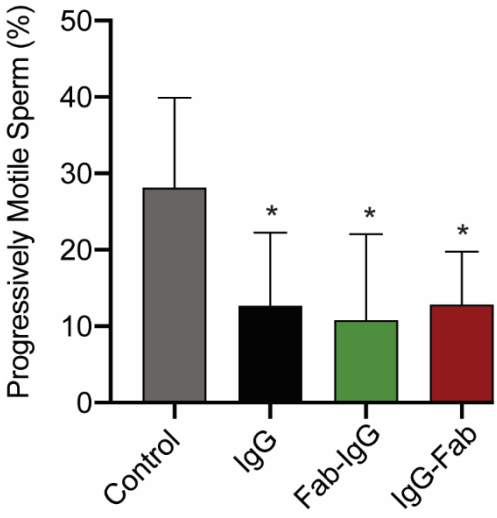


**Figure 2.4: Tetravalent sperm-binding IgG constructs conserve the trapping potency of the parent IgG.** The trapping potency of the indicated Abs measured by quantifying the percentage of fluorescently labeled PM sperm in Ab-treated CVM using neural network tracker analysis software. 25 μg/mL of Abs and purified sperm at the final concentration of 5.8 x 104 PM sperm/mL were used. Motavizumab (anti-RSV IgG) was used as the isotype control. Data were obtained from N =6 independent experiments with 6 unique combinations of semen and CVM specimens. P values were calculated using a one-tailed t-test between control Ab- and anti-sperm Ab-treated sperm samples. *$P < 0.05$. Lines indicate arithmetic mean values and standard deviation.

### *2.3.4. Tetravalent IgGs conserve the muco-trapping potency of parent IgG*

Earlier works have shown that IgA and IgG Abs can completely immobilize individual spermatozoa in the mucus by crosslinking antibody-bound spermatozoa to mucins; this is commonly referred to as the "shaking phenomenon' [2]. We have previously shown that multiple Fc present on Herpes-bound IgGs can effectively immobilize virus in CVM and blocked vaginal Herpes transmission in mice [10]. Since the Fc region was conserved and identical in both tetravalent IgGs and parent IgG, we hypothesized that Fab-IgG and IgG-Fab constructs will trap individual spermatozoa in mucus similar to native IgG. We used multiple particle tracking to analyze the motion of fluorescently labeled sperm in CVM treated with either control, parent IgG or tetravalent IgGs [63]. Both IgG-Fab and Fab-IgG reduced the fraction of PM sperm to a comparable extent as the parent IgG (Figure 2.4), indicating that Fc-mediated crosslinking remained unaffected by the addition of Fabs at both N- and C-terminus.

## 2.4. Discussion

Our finding that both tetravalent sperm-binding IgGs, regardless of the orientation of additional Fab domains, effectively agglutinate sperm at a markedly lower concentration than IgG underscores multimerization as the promising strategy for the development of non-hormonal contraceptives. Many of the current multivalent Abs are bispecific or trispecific in nature and must content with potential mispairing of light and heavy chains. As a result, many such engineered Ab formats, such as single-chain variable fragment (scFv) or camel-derived nanobodies, involve a substantial deviation from natural human Ab structure based on the non-covalent pairing of heavy and light chains. scFv-based multivalent Ab constructs frequently suffer from low stability, heterogeneous expression, and decreased affinity and specificity stemming from the removal of the CH1/CL interface present in a full-length Fab. The introduction of orthogonal mutations to facilitate heavy and light chain pairing can also substantially reduce mAb yield or overall stability. These limitations do not apply when generating monospecific multivalent IgGs like our tetravalent IgGs, which possess identical and full-length human Fabs. Our strategy to covalently link additional Fabs to a parent heavy chain also contrasts from current multimerization strategies based on self-assembly of multiple IgGs based on Fc-mutations [68] or appending an IgM tail-piece, which often suffers poor homogeneity and stability [69,70]. The combination of fully intact human Fabs and covalent linkages likely contributes to the surprising thermal stability, homogeneity and bioprocessing ease of the tetravalent IgGs developed here. We believe the sperm-agglutinating potency of the tetravalent IgGs could be further enhanced by increasing the number of Fab domains up to 10 Fab per molecule, similar to a potent agglutinator IgM, resulting in extremely potent contraceptive mAbs.

Poor sperm motility in mid-cycle cervical mucus and low total sperm count are both strong correlates to low conception rate. Human semen averages ~45-65 million sperm per mL, 15 million sperm per mL marks the lowest 5th percentile in men with proven fertility, and <5 million sperm per mL is considered severe oligospermia with very low fertility [59,66,71]. Additionally, even under ideal circumstances (unprotected intercourse on the cycle day of maximum fertility), the odds of conceiving are

low, only ~10% [72]. These finding, together with contraceptive success with topical ASA against rabbit sperm [20], suggest substantial reduction (even if incomplete, e.g.~98%) of progressive sperm motility in the vagina/cervix by contraceptive mAbs should provide highly effective contraception by limiting the number of fertile motile sperm to reach the egg.

Unlike small molecule contraceptives, contraceptive mAbs should be exceptionally safe due to the specificity of targeting, particularly when binding to unique epitopes present only on sperm and not on expressed in female tissues. Safety is likely to be further enhanced by topical delivery: mAb delivered to mucosal surfaces such as the vagina is poorly absorbed into the systemic circulation [73], and the vagina represents a poor immunization inductive site, with limited immune response even when vaccinating with the aid of highly immunostimulatory adjuvants [74]. Topical delivery also substantially reduces the overall mAb dose needed. Given the limited volume of secretions in the female reproductive tract (FRT), typically ≤1 mL in the vagina [75], a relatively high concentration of mAb locally can be achieved even with very limited total quantities of mAb dosed. In contrast, systemically dosed mAbs must contend with the large blood volume (~5L), distribution to non-target tissues, natural catabolic degradation, and limited distribution into the FRT. The reduced quantities of mAb needed to sustain contraceptive levels in the FRT with vaginal delivery should translate to substantially lower amounts of total mAb needed, and consequently, cost savings.

Given the abundance of endogenous IgGs in the vagina and long half-life of vaginally instilled IgG i.e. ~9 hrs [76,77], locally delivered contraceptive mAbs should remain extremely stable and active in the FRT. Contraceptive mAbs can be delivered using multiple methods. For instance, to enable rapid and transient contraception, mAbs can be formulated into quick-dissolving vaginal film to provide on-demand non-hormonal contraception, effective over a 12-24 hrs period. In addition, contraceptive mAbs can be released from intravaginal rings (IVRs), enable month-long contraception comparable to the Nuvaring®. The ability to stably release antibodies from IVRs was recently demonstrated in rhesus macaques [78].

# CHAPTER 3: ENGINEERING ULTRA-POTENT SPERM-BINDING IGG ANTIBODIES FOR THE DEVELOPMENT OF AN EFFECTIVE NON-HORMONAL FEMALE CONTRACEPTION[2]

## 3.1. Introduction

Nearly half of all pregnancies in the United States are unintended despite the availability of cheap and effective hormonal contraceptives, which creates an enormous cost burden on the healthcare system. Many women avoid hormonal contraception due to real and perceived side effects including increased risks of breast cancer, depression, prolonged menstrual cycle, nausea, and migraines. Many women also have medical contraindications to the use of estrogen-based hormonal contraceptives. Thus, there is a strong unmet need for alternative, non-hormonal contraceptives.

An effective non-hormonal contraceptive mechanism already exists in nature: anti-sperm antibodies (ASAs) in the female reproductive tract (FRT) of infertile women can trap vigorously motile sperm in mucus and prevent them from reaching the egg, via two distinct mechanisms. First, at high sperm concentration, ASA can agglutinate sperm into clusters that are too large to penetrate mucus, a process particularly potent with polymeric antibodies (Abs) such as IgM. Second, at lower sperm concentration, ASA can trap individual spermatozoa in mucus by forming multiple low-affinity Fc-mucin bonds between sperm-bound ASA and mucin fibers. Years ago, these observations motivated the development of contraceptive vaccines. Vaccines eliciting ASA offered considerable contraceptive efficacy, but the approach stalled due to unresolved variability in the intensity and duration of the vaccine responses in humans, as well as concerns that active vaccination might lead to irreversible infertility. In contrast, sustained delivery of ASA at pharmacologically active doses locally in the vagina can overcome many of the key drawbacks of contraceptive vaccines, making possible both consistently effective

[2] This chapter is based on an article that was resubmitted by Shrestha B. et al to Science Translational Medicine in 2021.

contraception and rapid reversibility. Indeed, vaginal delivery of sperm agglutinating IgM in the highly fertile rabbit model reduced embryo formation by 95%.

Unfortunately, this topical passive immunocontraception approach has never been tried in humans, due in part to manufacturing and stability challenges with IgM and the limited potencies with IgG Abs. To overcome these challenges, we engineered a panel of stable and potently agglutinating ASA for non-hormonal contraception by linking multiple Fabs to a parent IgG, creating highly multivalent IgGs (HM-IgGs) with precisely tunable valencies. Our panel of ASAs target a unique glycoform of CD52 (hereafter referred to as CD52g) that is produced and secreted by epithelial cells lining the lumen of the epididymis, and present only on sperm, semen white blood cells, and the epithelium of the vas deferens and seminal vesicles. The CD52g antigen appears to be universally present on all human sperm (Table 3.1 and 3.2) while absent in all other tissues, and absent in women. Here, we report the development and characterization of three mAbs within this panel: Fab-IgG-Fab (FIF;6-Fabs), Fab-IgG-Fab-Fab (FIFF; 8-Fabs), and Fab-Fab-IgG-Fab-Fab (FFIFF; 10-Fabs) (Figure 3.1A). These constructs all exhibited superior (>10-fold) agglutination potency than the parent IgG, and effectively reduced progressively motile (PM) sperm in the sheep vaginal model.

**Table 3.1:** The demographics of the 100 semen samples agglutinated with parent IgM.

| Race | Composition (%) |
|---|---|
| Caucasian | 73 |
| African-American | 26 |
| Asian | 1 |

**Table 3.2:** The demographics of the 20 male donors used in agglutination studies with HM-IgGs.

| Race | Composition (%) |
|---|---|
| Caucasian | 60 |
| Hispanic | 15 |
| Asian | 20 |
| Black | 5 |

**3.2. Materials and Methods:**

***3.2.1. Study design and ethics***. Ex vivo studies with human semen as well as human CVM utilized specimens obtained following a protocol approved by the Institutional Review Board (IRB) of the University of North Carolina at Chapel Hill (IRB-101817). Informed written consent was obtained from all male and female subjects before the collection of any material. Subjects were recruited from the Chapel Hill and Carrboro, NC area in response to mass student emails and ads in print media. For the CD52g presence study in human semen samples, the protocol was approved by the IRB of the Union Memorial Hospital, Baltimore, MD. For the sheep surrogate post-coital test performed at the University of Texas Medical Branch (UTMB), UTMB IRB approval (IRB-180254) and written consent allowed for the collection of fresh semen from pre-screened male volunteers on the day of each sheep study. Sheep studies were approved by the UTMB Institutional Animal Care and Use Committee (IACUC; 0608038D) and utilized 5 female Merino crossbred sheep.

***3.2.2. Construction of the parent IgG and HM-IgGs plasmids***. The variable heavy (VH) and variable light (VL) DNA sequences for anti-sperm IgG1 Ab were obtained from the published sequence of H6-3C4 mAb. For the construction of expression plasmid encoding the light chain (LC), the gene fragment consisting of VL and CL (Cλ) DNA sequences was synthesized using a custom gene-synthesis service (Integrated DNA Technologies) and cloned in-house into a customized empty mammalian expression vector (pAH, ThermoFisher Scientific) using KpnI (5') and EcoRI (3') restriction sites.

For the construction of expression plasmids encoding heavy chains (HC) for parent and HM-IgG Abs, four cloning vectors comprising of VH/CH1-(G4S)6 Linker-VH, VH/CH1-(G4S)6 Linker-VH/CH1-(G4S)6 Linker-VH, (G4S)6 Linker-VH/CH1 and (G4S)6 Linker-VH/CH1-(G4S)6 Linker-VH/CH1 sequences were synthesized using GeneArt® gene synthesis service (ThermoFisher Scientific).

For the construction of expression plasmid encoding HC for IgG, VH fragment was amplified from the cloning vector comprising of VH/CH1-(G4S)6 Linker-VH using forward primer, 5' TAAGCAGGTACCGCCACCATGAAGTG 3', and reverse primer, 5'

TGCTTAGCTAGCTGGAGAAACTGTC 3', and then cloned into a mammalian IgG1 expression vector (pAH comprising CH1-CH2-CH3 DNA sequence) using KpnI (5') and NheI (3') restriction sites.

For the construction of expression plasmid encoding HC for FIF, VH/CH1-(G4S)6 Linker-VH fragment was first cloned into a mammalian IgG1 expression vector using KpnI (5') and NheI (3') restriction sites followed by the cloning of (G4S)6 Linker-VH/CH1 fragment using BamHI (5') and MluI (3') restriction sites.

For the construction of expression plasmid encoding HC for FIFF, VH/CH1-(G4S)6 Linker-VH fragment was first cloned into the mammalian IgG1 expression vector using KpnI (5') and NheI (3') restriction sites followed by the cloning of (G4S)6 Linker-VH/CH1-(G4S)6 Linker-VH/CH1 fragment using BamHI (5') and MluI (3') restriction sites.

For the construction of expression plasmid encoding HC for FFIFF, VH/CH1-(G4S)6 Linker-VH/CH1-(G4S)6 Linker-VH fragment was first cloned into the same mammalian expression vector using KpnI (5') and NheI (3') restriction sites followed by the cloning of (G4S)6 Linker-VH/CH1-(G4S)6 Linker-VH/CH1 using BamHI (5') and MluI (3') restriction sites.

For the ligation of all HCs as well as the LC into mammalian expression vectors, a quick ligation kit (New England Biolabs) was used. All ligated DNA constructs were chemically transformed into TOP10 E. coli cells (Life Technologies) and plated on ampicillin plates for selection. Several bacterial colonies were picked from each plate and cultured, followed by plasmid miniprep (Qiagen MiniPrep Kit). Correct assembly of the HC and LC sequences into expression vectors were confirmed by sanger sequencing of the purified plasmids (Eurofins Genomics).

***3.2.3. Expression and purification of the parent IgG and HM-IgGs***. The sequencing-confirmed expression plasmids encoding the HC and LC sequences of parent and HM-IgG Abs were chemically transformed and cultured in a 100 mL Terrific broth media overnight. Midi-prep plasmid purifications were done using NucleoBond® Xtra Midi EF Kits (Macherey-Nagel), according to the manufacturer's protocols. Purified HC and LC plasmids were transfected into Expi293F cells using ExpiFectamine™ 293

Transfection reagents, according to the manufacturer's protocols (Gibco). For IgG, HC and LC plasmid were co-transfected using a 1:1 ratio at 1 μg total DNA per 1 mL of culture. For FIF, HC and LC plasmid were co-transfected using a 1:3 ratio at 1 μg total DNA per 1 mL culture. For FIFF, HC and LC plasmid were co-transfected using a 1:4 ratio at 1 μg total DNA per 1 mL culture. For FFIFF, HC and LC plasmid were co-transfected using a 1:5 ratio at 1 μg total DNA per 1 mL culture. Transfected Expi293F cells were grown at 37°C in a 5% CO2 incubator and shaken at 125 r.p.m. for 3-5 days. Supernatants were harvested by centrifugation at 12,800 g for 10 min, passed through 0.22 μm filters, and purified using the standard protein A/G chromatography method. Purified Abs were quantified using absorbance at 280 nm along with corresponding protein extinction coefficients.

***3.2.4. Antibody characterization***. SDS-PAGE experiments were performed using 4-12% NuPage Bis-Tris gels (Invitrogen) in 1x NuPage MOPS buffer under both reducing and non-reducing conditions to confirm the molecular weight and assembly of all Ab constructs. For each sample, 1 μg of protein was diluted in 3.75 μL LDS sample buffer followed by the addition of 11.25 μL nuclease-free water. Proteins were then denatured at 70°C for 10 min. Next, 0.3 μL of 0.5 M tris (2-carboxyethyl) phosphine (TCEP) was added as a reducing agent to the denatured protein for reduced samples and incubated at room temperature (RT) for 5 min. Bio-Rad Precision Protein Plus Unstained Standard and Novex™ Sharp Pre-stained Protein Standard were used as ladders. After loading the samples, the gel was run for 50 min at a constant voltage of 200 V. The protein bands were visualized by staining with Imperial Protein Stain (Thermo Scientific) for 1 hr followed by overnight de-staining with Milli-Q water. Image J software (Fiji) was used to adjust the brightness and contrasts of the SDS-PAGE gel for visual purposes.

SEC-MALS experiments were performed at room temperature using a GE Superdex 200 10/300 column connected to an Agilent FPLC system, a Wyatt DAWN HELEOS II multi-angle light-scattering instrument, and a Wyatt T-rEX refractometer. The flow rate was maintained at 0.5 mL/min. The column was equilibrated with 1X PBS, pH 7.4 containing 200 mg/L of NaN3 before sample loading. 50-100 μg of

each sample was injected onto the column, and data were collected for 50 min. The MALS data were collected and analyzed using Wyatt ASTRA software (Ver. 6).

NanoDSF experiments were performed using a Nanotemper Prometheus NT.48 system. Samples were diluted to 0.5 mg/mL in 1X PBS at pH 7.4 and loaded into Prometheus NT.48 capillaries. Thermal denaturation experiments were performed from 25°C to 95°C at the rate of 1°C/min, measuring the intrinsic tryptophan fluorescence at 330 nm and 350 nm. The melting temperature for each experiment was calculated automatically by Nanotemper PR. Thermcontrol software by plotting the ratiometric measurement of the fluorescent signal against increasing temperature. The aggregation temperature for each experiment was also calculated automatically by Nanotemper PR. Thermcontrol software via the detection of the back-reflection intensity of a light beam that passes the sample.

***3.2.5. Whole sperm ELISA***. Briefly, half-area polystyrene plates (CLS3690, Corning) were coated with 2 x 105 sperm per well in 50 µL of NaHCO3 buffer (pH 9.6). After overnight incubation at 4°C, the plates were centrifuged at the speed of 300 g for 20 min. The supernatant was discarded, and the plates were air-dried for 1 hr at 45°C. The plates were washed once with 1X PBS. 100 µL of 5% milk was incubated at RT for 1 hr to prevent non-specific binding of Abs to the microwells. The serial dilution of mAbs in 1% milk was added to the microwells and incubated overnight at 4°C. Motavizumab, a mAb against the respiratory syncytial virus, was constructed and expressed in the laboratory by accessing the published sequence and used as a negative control for this assay (75). After primary incubation, the plates were washed three times using 1X PBS. Then, the secondary Ab, goat anti-human IgG F(ab')2 Ab HRP-conjugated (1:10,000 dilutions in 1% milk, 209-1304, Rockland Inc.) was added to the wells and incubated for 1 hr at RT. The washing procedure was repeated and 50 µL of the buffer containing substrate (1-Step Ultra TMB ELISA Substrate, Thermo Scientific) was added to develop the colorimetric reaction for 15 min. The reaction was quenched using 50 µL of 2N H2SO4, and the absorbance at 450 nm (signal) and 570 nm (background) was measured using SpectraMax M2 Microplate Reader (Molecular

Devices). Each experiment was done with samples in triplicates and repeated two times as a measure of assay variability.

***3.2.6. Stability assay***. Briefly, 1.2 mL of Expi293 produced IgG, FIF, FIFF and FFIFF at the 1 mg/mL concentration were prepared using PBS as the solvent. The 1.2 mL of mAbs was split into 6 tubes with 0.2 mL aliquots. Three tubes with 0.2 mL aliquots were stored in 4°C as controls. Another three tubes with 0.2 mL aliquots were stored in 40°C bead bath for 14 days. On each time point: Day 0, Day 7, Day 14, one aliquot was taken out from both 4°C and 40°C for the characterization using SEC-MALS, SDS-PAGE, DSF and whole sperm ELISA.

***3.2.7. Semen collection and isolation of motile sperm***. Healthy male subjects were asked to refrain from sexual activity for at least 24 hr prior to semen collection. Semen was collected by masturbation into sterile 50 mL sample cups and incubated for a minimum of 15 min post-ejaculation at room temperature to allow liquefaction. Semen volume was measured, and the density gradient sperm separation procedure (Irvine Scientific) was used to extract motile sperm from liquefied ejaculates. Briefly, 1.5 mL of liquified semen was carefully layered over 1.5 mL of Isolate® (90% density gradient medium, Irvine Scientific) at room temperature, and centrifuged at 300 g for 20 min. Following centrifugation, the upper layer containing dead cells and seminal plasma was carefully removed without disturbing the motile sperm pellet in the lower layer. The sperm pellet was then washed twice with the sperm washing medium (Irvine Scientific) by centrifugation at 300 g for 10 min. Finally, the purified sperm pellet was resuspended in the sperm washing medium, and an aliquot was taken for determination of sperm count and motility using CASA. All semen samples used in the functional assays exceeded lower reference limits for sperm count ($15 \times 10^6$ total sperm/mL) and total motility (40%) as indicated by WHO guidelines.

***3.2.8. Assessment of CD52g presence in human semen samples***. The presence of the CD52g target antigen on the sperm of human semen donors was assessed on de-identified residual aliquots of semen

samples from 100 donors presenting to an andrology clinic for semen quality evaluation (see Table 3.3 for ethnic background). Aliquots of semen were placed on glass slides and an equal volume of H6-3C4 IgM mAb directed against the CD52g antigen (tissue culture supernatant, a gift of S. Isojima ), was added and mixed briefly with a pipette tip. A coverslip was applied, and agglutination was assessed microscopically 3 minutes after Ab addition via a 20X objective. Strong agglutination was observed in all samples.

***3.2.9. Sperm count and motility using CASA***. The Hamilton-Thorne computer-assisted sperm analyzer, 12.3 version, was used for the sperm count and motility analysis in all experiments unless stated otherwise. This device consists of a phase-contrast microscope (Olympus CX41), a camera, an image digitizer, and a computer with Hamilton-Thorne Ceros 12.3 software to save and analyze the acquired data. For each analysis, 4.4 µL of the semen sample was inserted into MicroTool counting chamber slides (Cytonix). Then, six randomly selected microscopic fields, near the center of the slide, were imaged and analyzed for progressively motile (PM) and non-progressively motile (NPM) sperm count. The parameters that were assessed by CASA for motility analysis were as follows: average pathway velocity (VAP: the average velocity of a smoothed cell path in µm/s), the straight-line velocity (VSL: the average velocity measured in a straight line from the beginning to the end of a track in µm/s), the curvilinear velocity (VCL: the average velocity measured over the actual point-to-point track of the cell in µm/s), the lateral head amplitude (ALH: amplitude of lateral head displacement in µm), the beat cross-frequency (BCF: frequency of sperm head crossing the sperm average path in Hz), the straightness (STR: the average value of the ratio VSL/VAP in %), and the linearity (LIN: the average value of the ratio VSL/VCL in %). PM sperm were defined as having a minimum of 25 µm/s VAP and 80% STR. The complete parameters are listed in Table 2.1.

***3.2.10. Scanning electron microscopy***. Briefly, 20 x $10^6$ washed sperm was centrifuged at 300 g for 10 min. The supernatant was discarded without disturbing the sperm pellet. Next, 200 µL of anti-sperm IgG constructs or 1X PBS was added to the sperm pellet. The Ab-sperm solution was mixed by pipetting and

incubated for 5 mins using an end-over-end rotator. 200 µL of 4% PFA prepared in 0.15 M Sodium Phosphate buffer was added to the Ab-sperm solution and incubated for 10 min using an end-over-end rotator. 50 µL of fixed sperm samples was filtered through membrane filters (10562, K04CP02500, Osmonics) with 5 mL of 0.15 M Sodium Phosphate buffer. The filter was washed one more time with 0.15 M Sodium Phosphate buffer. Next, the samples were dehydrated in a graded series of alcohol (30% ethanol, 50% ethanol, 70% ethanol, 90% ethanol, 100% ethanol x 3) for 10 minutes each. Filters were transferred to a plate with the transitional solvent, Hexamethyldisilazane (Electron Microscopy Sciences) and allowed to dry after one exchange. Filters were adhered to aluminum stubs with carbon adhesives and samples were sputter-coated with gold-palladium alloy (Au:Pd 60:40 ratio, 91112, Ted Pella Inc.) to a thickness of 3 nm using Cressington Sputter Coater 208 hr. Six random images were acquired for each sample using a Zeiss Supra 25 FESEM with an SE2 Electron detector at 2500X magnification.

***3.2.11. Sperm escape assay***. This assay was conducted using purified sperm at the final concentration of 5 x $10^6$ PM sperm/mL and whole semen. Briefly, 40 µL aliquots of purified sperm or whole semen were transferred to individual 0.2 mL PCR tubes. As a conservative measure, an aliquot of 4.4 µL was sampled from each aliquot for the sperm count and motility using CASA to serve as the baseline concentration for each aliquot. (This baseline untreated count was performed for each 40 µL aliquot, only for escape assay, because sperm count was slightly varied for each aliquot despite frequent mixing while aliquoting.) Next, 30 µL of purified sperm or native semen from 40 µL aliquot was added to 0.2 mL PCR tubes containing 30 µL of Ab constructs or media control, and gently mixed by pipetting. The tubes were then held fixed at 45° angles in a custom 3D printed tube holder for 5 min at room temperature. Following this incubation period, 4.4 µL was pipetted from the top layer of the mixture with minimal perturbation of the tube and transferred to the CASA instrument to quantify the number of PM sperm. Sperm present in the top layer of the tube were characterized as escaped sperm, since agglutinated sperm settle to the bottom of the tube. The percentage of the PM sperm that escaped agglutination was computed by dividing the sperm count obtained after mAb-treatment with Ab constructs by the adjusted baseline sperm count in each respective

tube: the baseline sperm count was adjusted by dividing the count by 2 to balance the 2-fold dilution of treated samples with Ab or media control. Each experimental condition was evaluated in duplicates on each semen specimen, and the average from the two experiments was used in the analysis. Six independent experiments were done with at least 4 unique semen samples.

***3.2.12. Agglutination kinetics assay***. This assay was conducted using purified sperm at the final concentration of 5 x $10^6$ PM sperm/mL, 1 x $10^6$ PM sperm/mL and 25 x $10^6$ PM sperm/mL and whole semen. Briefly, 4.4 µL of purified sperm or whole semen was added to 4.4 µL of Ab constructs in 0.2 mL PCR tubes, and mixed by gently pipetting up and down three times over 3 s. A timer was started immediately while 4.4 µL of the mixture was transferred to chamber slides with a depth of 20 µm (Cytonix). At 30s, 60s, and 90s time points, CASA measurements were taken focusing on the center of chamber slides. The reduction in the percentage of the PM sperm at each time point was computed by subtracting the PM sperm count obtained after mAb-treatment from the PM sperm count obtained after treatment with media control followed by the division by the same PM sperm count obtained after treatment with media control. The experiment was evaluated in duplicates on each semen specimen, except for the experiment involving 2 x $10^6$ PM sperm/mL, and the average from the two experiments was used in the analysis. Six independent experiments were performed with 6 unique semen samples.

***3.2.13. Induction of capacitation in washed sperm***. Briefly, motile sperm was isolated using the density gradient sperm separation procedure as described above. 2 mL of sperm preparation medium (Origio, Denmark) that was pre-equilibrated under 37°C and 5% CO2 for 2 hr was used to wash the isolated sperm by centrifuging at 300 g for 10 min. The sperm washing was repeated. The purified sperm pellet was suspended in pre-equilibrated sperm preparation medium and an aliquot was taken for determination of sperm count and motility using CASA. Next, purified sperm at the concentration of 20 million motile sperm/mL was prepared using pre-equilibrated medium. Then, the purified sperm was incubated under 37°C and 5% CO2 for at least 1 hr to induce capacitation. To confirm capacitation, an aliquot was taken

for CASA measurement and CASA's DBT file was further analyzed using CASANOVA software (https://csbio.unc.edu/CASAnova/index.py) [83] to quantify hyperactivated sperm. CASANOVA was used for additional analysis because of the limitation of our Hamilton-Thorne CASA (12.3 version) in quantifying hyperactivated sperm.

***3.2.14. Agglutination assay using capacitated sperm***. Briefly, purified sperm at the concentration of 20 million motile sperm/mL incubated under 37°C and 5% CO2 for 1 hr to induce capacitation. Capacitated sperm were used within an hour of capacitation for the agglutination assay. Briefly, 5 µL of capacitated sperm was mixed with 5 µL of mAbs or media control and incubated for 3 mins at RT. Next, 5 µL of mAb-capacitated sperm was loaded into the chamber slides and CASA measurements were taken to quantify the number of PM sperm. The DBT file from CASA analysis was then uploaded to CASANOVA software (https://csbio.unc.edu/CASAnova/index.py) to quantify the number of hyperactivated sperm. Five independent experiments were performed using 3 unique semen donors.

***3.2.15. Stability of sperm-mAb agglutinates upon vortexing***. Briefly, purified sperm at the concentration of 10 million PM sperm/mL was prepared. 40 µL of purified sperm was mixed with 40 µL of mAbs or media control, and incubated for 5 min at RT. CASA measurements were taken to quantify the number of PM sperm after treatment. Next, the mAb- or control- treated sperm was vortexed for 1 min at full speed using vortex mixer (#S0200, Labnet International). CASA measurements were taken again after vortexing. The reduction in percentage of the PM sperm was computed for both non-vortex and vortex conditions by normalizing the PM sperm count obtained after mAb-treatment to the PM sperm count obtained after media-control treatment. Lastly, to confirm the reduction of PM sperm by mAbs under vortex condition was not a mere vortex artifact, the number of PM sperm present in control-treated samples after vortexing was normalized to the PM sperm count present in non-vortex control-treated samples. Five independent experiments were done with at least 3 unique semen samples.

***3.2.16. Stability of sperm-mAb agglutinates over time***. Briefly, purified sperm at the concentration of 10 million PM sperm/mL was prepared. 40 µL of purified sperm was mixed with 40 µL of mAbs or media control, and incubated for 5 min at RT. CASA measurements were taken to quantify the number of PM sperm after treatment. Next, the mAb- or control- treated sperm were incubated for 24 hr at RT. At three different time points: 2 hr, 4 hr, 24 hr, the sperm-mAb mixtures was gently mixed followed by CASA measurements. The reduction in percentage of the PM sperm was computed for each time point by normalizing the PM sperm count obtained after Ab-treatment to the PM sperm count obtained after media-control treatment. Lastly, to illustrate the decrease in PM sperm count over time in control samples, the number of PM sperm present in control-treated samples of each time point was normalized to the PM sperm count in control-treated samples of initial 5 min incubation. Four independent experiments were done with at least 3 unique semen samples.

***3.2.17. CVM collection and processing***. CVM was collected as previously described. Briefly, undiluted CVM secretions, averaging 0.5 g per sample, were obtained from women of reproductive age, ranging from 20 to 44 years old, by using a self-sampling menstrual collection device (Instead Softcup). Participants inserted the device into the vagina for at least 30 s, removed it, and placed it into a 50 mL centrifuge tube. Samples were centrifuged at 230 g for 5 min to collect the secretions. Samples were collected at various times throughout the menstrual cycle, and the cycle phase was estimated based on the last menstrual period date normalized to a 28-day cycle. No samples were ovulatory based on visual observation (none exhibited spinnbarkeit). Samples that were non-uniform in color or consistency were discarded. Donors stated they had not used vaginal products nor participated in unprotected intercourse within 3 days before donating in their donation forms. All samples had pH < 4.5.

***3.2.18. Fluorescent labeling of sperm***. Purified sperm were fluorescently labeled using Live/Dead Sperm Viability Kit (Invitrogen Molecular Probes), which stains live sperm with SYBR 14 dye, a membrane-permeant nucleic acid stain, and dead sperm with propidium iodide (PI), a membrane impermeant nucleic

acid stain. Briefly, SYBR 14 stock solution was diluted 50-fold in sperm washing media. Next, 5 µL of diluted SYBR 14 and PI dye were added to 1 mL of washed sperm resulting in final SYBR 14 and PI concentration of 200 nM and 12 µM respectively. The sperm-dye solution was incubated for 10 min at 36°C. Then, the solution was washed twice using the sperm washing medium to remove unbound fluorophores by centrifuging at 300 g for 10 min. Next, the labeled motile sperm pellet was resuspended in the sperm washing medium, and an aliquot was taken for determination of sperm count and motility using CASA.

***3.2.19. Multiple particle tracking studies***. To mimic the dilution and neutralization of CVM by alkaline seminal fluid, CVM was first diluted three-fold using sperm washing medium and titrated to pH 6.8-7.1 using small volumes of 3 N NaOH. The pH was confirmed using pH test strips. Next, 4 µL of Ab constructs or control (anti-RSV IgG1) was added to 60 µL of diluted and pH-adjusted CVM and mixed well in a CultureWellTM chamber slide (Invitrogen). Next, 4 µL of 1 x $10^6$ PM sperm/mL of fluorescently labeled sperm was mixed into the chamber slides comprising of Ab and CVM, and incubated for 5 min at room temperature. Then, translational motions of the fluorescent sperm were recorded using an electron-multiplying charge-coupled-device camera (Evolve 512; Photometrics) mounted on an inverted epifluorescence microscope (AxioObserver D1; Zeiss) equipped with an Alpha Plan-Apo 20/0.4 objective, environmental (temperature and CO2) control chamber, and light-emitting diode (LED) light source (Lumencor Light Engine DAPI/GFP/543/623/690) [10]. Total 15 videos (512 × 512 pixels, 16-bit image depth) were captured for each mAb condition with MetaMorph imaging software (Molecular Devices) at a temporal resolution of 66.7 ms and spatial resolution of 50 nm (nominal pixel resolution, 0.78 µm/pixel) for 10 s. Next, the acquired videos were analyzed using a neural network tracking software to determine the percentage of PM sperm present in each condition. The neural network tracking software was modified with standard sperm motility parameters (Table 2.1) to quantify PM sperm. Six independent experiments were performed, each using a unique combination of CVM and semen specimens.

***3.2.20. Bovine cervical mucus (BCM) capillary tube assay***. Briefly, mucus penetration test was performed as previously described (77) with some modifications. Estrus bovine cervical mucus (BioIVT, New York) was diluted 2-fold using sperm washing media (Irvine Scientific) prior to loading into the flat rectangular capillary tubes (#2540, VitroCom, New Jersey) of 0.4 mm depth and 5 mm length. The capillary tubes were sealed at one end using critoseal (Ward's Microhematocrit set). The capillary tubes were marked at 1 cm, 3 cm and 4.5 cm from the unsealed end. Next, 150 µL of whole semen was mixed with 150 µL of mAbs or media control in 0.5 mL microcentrifuge tubes. Then, the capillary tubes were immediately inserted into the mAb-semen solution. The capillary tube and the mAb-semen solution were next adjusted to horizontal set up and incubated for 2 hr at RT. The capillary tubes were examined for sperm at the 1 cm, 3 cm and 4.5 cm mark using 20X objective of phase-contrast microscope (Olympus CX41). Manual counting of sperm was performed with sperm categorized as i. Actively motile if forward motility was observed and ii. Shaking/Immotile if sperm appeared trapped in the same location. Total number of sperm present at 1 cm mark in control-treatment conditions was not counted due to the limitation of manual counting against high concentration of sperm. Four independent experiments were performed using 3 different semen donors. Experiment was evaluated in duplicates on each semen specimen, and the average from the two experiments was used in the analysis.

***3.2.21. In vivo surrogate efficacy studies***. On the test day, each sheep received a randomized Ab treatment and all sheep were dosed with the same semen mixture that was pooled from 3-5 donors. Briefly, 1 mL of anti-sperm Abs or PBS control, provided under blind to the animal facility, were instilled into sheep's vagina and thoroughly mixed using a vaginal dilator for 15 strokes. Next, 1 mL of pooled whole semen was pipetted into the sheep's vagina, followed by simulated intercourse with a vaginal dilator for 5 strokes. Two minutes after the introduction of semen, fluids from the sheep vagina were recovered and assessed for the PM sperm count in a hemocytometer (Bright-Line™ Hemacytometer) under a light microscope (Olympus IX71) using a 20X objective and recorded with a Thorlabs camera.

Each Ab condition was repeated two more times in the same group of sheep (n = 5) with at least 7 days interval in between experiments. Treatments and quantifications were performed in a blinded fashion.

***3.2.22. Statistical analysis***. All analyses were performed using GraphPad Prism 8 software. For multiple group comparisons, P values were calculated using a one-way ANOVA with Dunnett's multiple comparisons tests. To compare the percent reduction of PM sperm by IgG vs. FFIFF in sperm escape and agglutination kinetics assays, one-tailed t-tests were performed. Similarly, the comparison between control- and anti-sperm Ab-treated fluorescent PM sperm in CVM was performed using a one-tailed t-test. In all analyses, $\alpha$=0.05 for statistical significance. All data are presented as the mean ± standard deviation.

## 3.3. Results

### *3.3.1. Generation of FIF, FIFF and FFIFF mAbs*

We engineered different HM-IgG molecules with a Fab domain previously isolated from a healthy but immune infertile woman; this Fab rapidly bound sperm in 100 out of 100 semen specimens (Table 3.1 and 3.2), with Fab domains interspersed by flexible glycine-serine linkers. Anti-CD52g FIF, FIFF, and FFIFF all expressed at levels similar, if not exceeding those of the parent IgG when produced via transient expression in Expi293F cells (Figure 3.1B). All 3 constructs properly assembled at their theoretical molecular weights (Figure 3.1C) and were highly homogenous (Figure 3.1D and E), with even greater homogeneity than the parent IgG, which possesses a small fraction of aggregates. All 3 constructs were highly stable, with comparable melting temperatures (Tm) and aggregating temperatures (Tagg) to the parent IgG. All mAbs unfolded (denatured) at similar high temperatures of Tm1 ≥ 71.1°C and Tm2 ≥ 80°C, while aggregation began only at ≥ 80°C (Figure 3.1F), with slightly increased Tm and Tagg for the 3 HM-IgG constructs. All constructs bound to human sperm in a whole-sperm ELISA assay, with apparent greater avidity of the FIFF and FFIFF multivalent constructs than the parent IgG at lower mAb

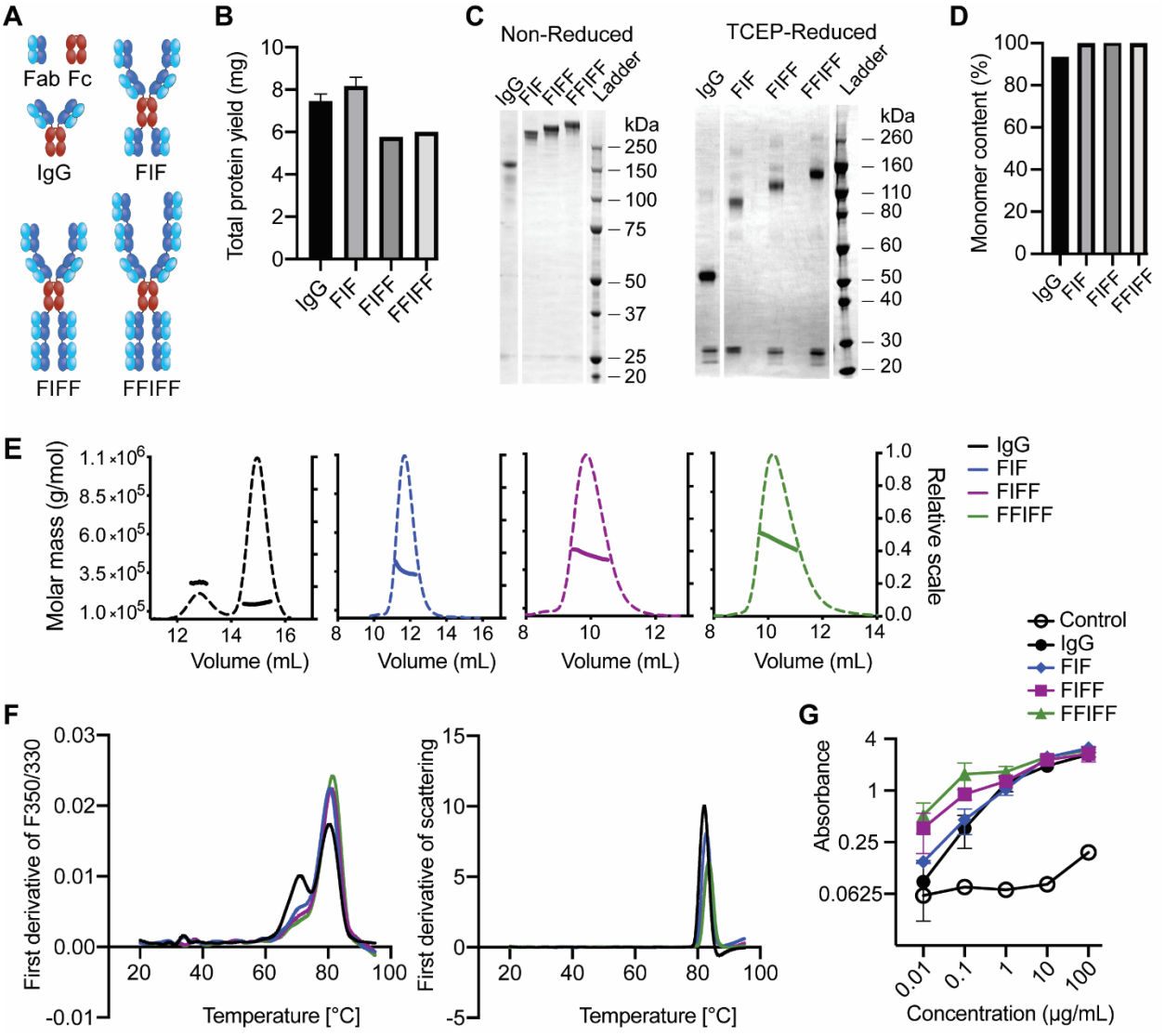


**Figure 3.1: Production and characterization of highly multivalent anti-sperm IgG antibodies.** (A) Schematic diagrams of anti-sperm IgG, Fab-IgG-Fab (FIF), Fab-IgG-Fab-Fab (FIFF), and Fab-Fab-IgG-Fab-Fab (FFIFF). (B) Production yield of the indicated mAbs, purified from 90 mL Expi293 transfection. Data were obtained from N =2 independent transfection for IgG and FIF, and one transfection for FIFF and FFIFF. (C) Non-reducing and reducing SDS-PAGE analysis of the indicated Abs (1 µg). (D) Demonstration of the purity and homogeneity of the indicated anti-sperm Abs (50-100 µg) using SEC-MALS analysis. Y-axis indicates the total percentage of Abs representing their theoretical molecular weights. (E) SEC-MALS curves of the parent IgG, FIF, FIFF and FFIFF. Thick lines indicate the calculated molecular mass (left y-axis) and the dotted lines show the homogenous profile (right y-axis) of each antibody. (F) The melting temperatures (left) and aggregating temperature (right) of the indicated antibodies as determined by nanoDSF. (G) Whole sperm ELISA to assess the binding potency of the indicated antibodies to human sperm. Motavizumab (anti-RSV IgG) was used as the control. Data were obtained from N =3 independent experiments using 3 unique semen donors. Each experiment was performed in triplicates and averaged. Lines indicate arithmetic mean values and standard deviation.

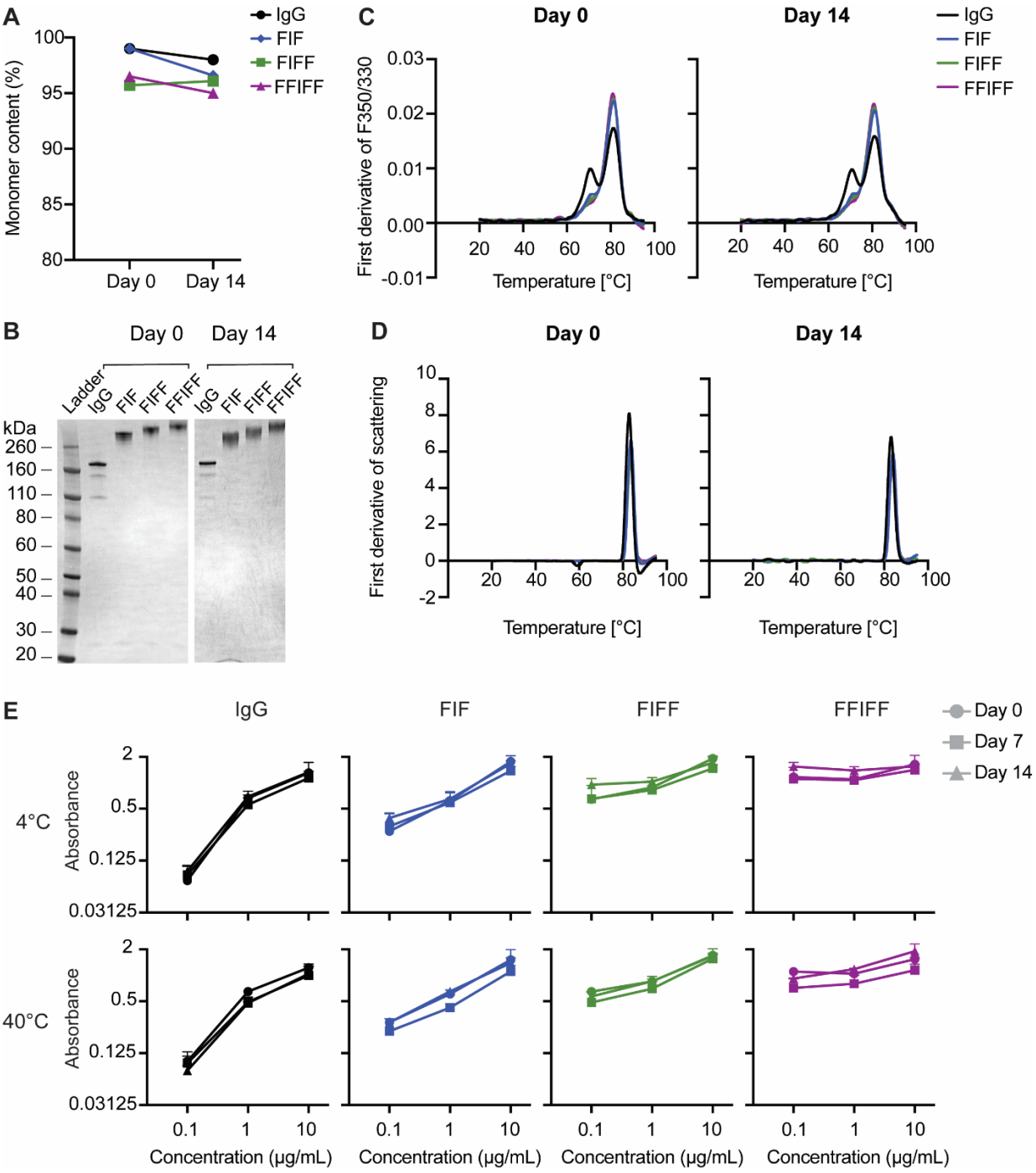


**Figure 3.2: HM-IgGs exhibit excellent stability at 40°C.** (A) Demonstration of the purity and homogeneity of the indicated anti-sperm Abs (100 µg) after storage at 40°C for 14 days using SEC-MALS analysis. (B) Non-reducing SDS-PAGE analysis of the indicated Abs (1 µg) after storage at 40°C for 14 days. (C) The melting temperatures and (D) aggregating temperature (right) of the indicated antibodies after storage at 40°C for 14 days determined by nanoDSF. The experiment was performed in triplicates and averaged. (E) Whole sperm ELISA to assess the sperm-binding potency of the indicated Abs after storage at 40°C for 14 days. ELISA was performed using Abs stored at 4°C for 14 days for reference. Data were obtained from N=2 independent experiments using 2 unique semen donors. Each experiment was performed in triplicates and averaged. Lines indicate arithmetic mean values and standard deviation.

concentration (Figure 3.1G). We further assessed the shelf-life and storage conditions for the 3 HM-IgGs by characterizing the mAbs after storage at 40°C for 14 days. All mAbs stored at 40°C were highly homogeneous (Figure 3.2A), correctly assembled (Figure 3.2B), thermostable (Figure 3.2C and D) and potent at binding sperm similar to respective mAbs stored at 4°C (Figure 3.2E).

### *3.3.2. HM-IgGs exhibit greater agglutination potency than IgG*

Progressively motility is crucial for sperm, both to enable sperm to swim through mucus to reach the egg as well as to penetrate the zona pellucida to fertilize the egg. We first assessed the agglutination potencies of all mAbs using a sperm escape assay, which quantifies, using Computer Assister Sperm Analysis (CASA), the number of PM sperm that escaped agglutination over 5 mins when mixed with specific mAbs or sperm washing media control. At the final concentration of 5 million PM sperm/mL reflecting typical concentrations of PM sperm in fertile males, all 3 HM-IgG constructs exhibited at least 16-fold greater agglutination potency than IgG, defined as the minimal mAb concentrations at which PM sperm are reduced by >98%. The minimum concentration of IgG needed was ~6.25 μg/mL, whereas all 3 HM-IgG constructs were able to do so down to 0.39 μg/mL (Figure 3.3A and B). To ensure efficient agglutination occurs not just with the washed sperm but also with native semen, we further assessed the agglutination of the most potent construct (FFIFF) vs IgG. Both FFIFF and the parent IgG required higher mAb concentration to reduce PM sperm quantities by >98% in whole semen, likely due to the greater amounts of CD52g in whole semen due to its additional presence on non-motile sperm and exosomes in the seminal plasma. Nevertheless, FFIFF remained approximately 16-fold more potent than IgG (Figure 3.3C and D). The greater agglutination potency of HM-IgG constructs was visually confirmed using scanning electron microscopy (SEM) on the mAb-treated washed sperm (Figure 3.4).

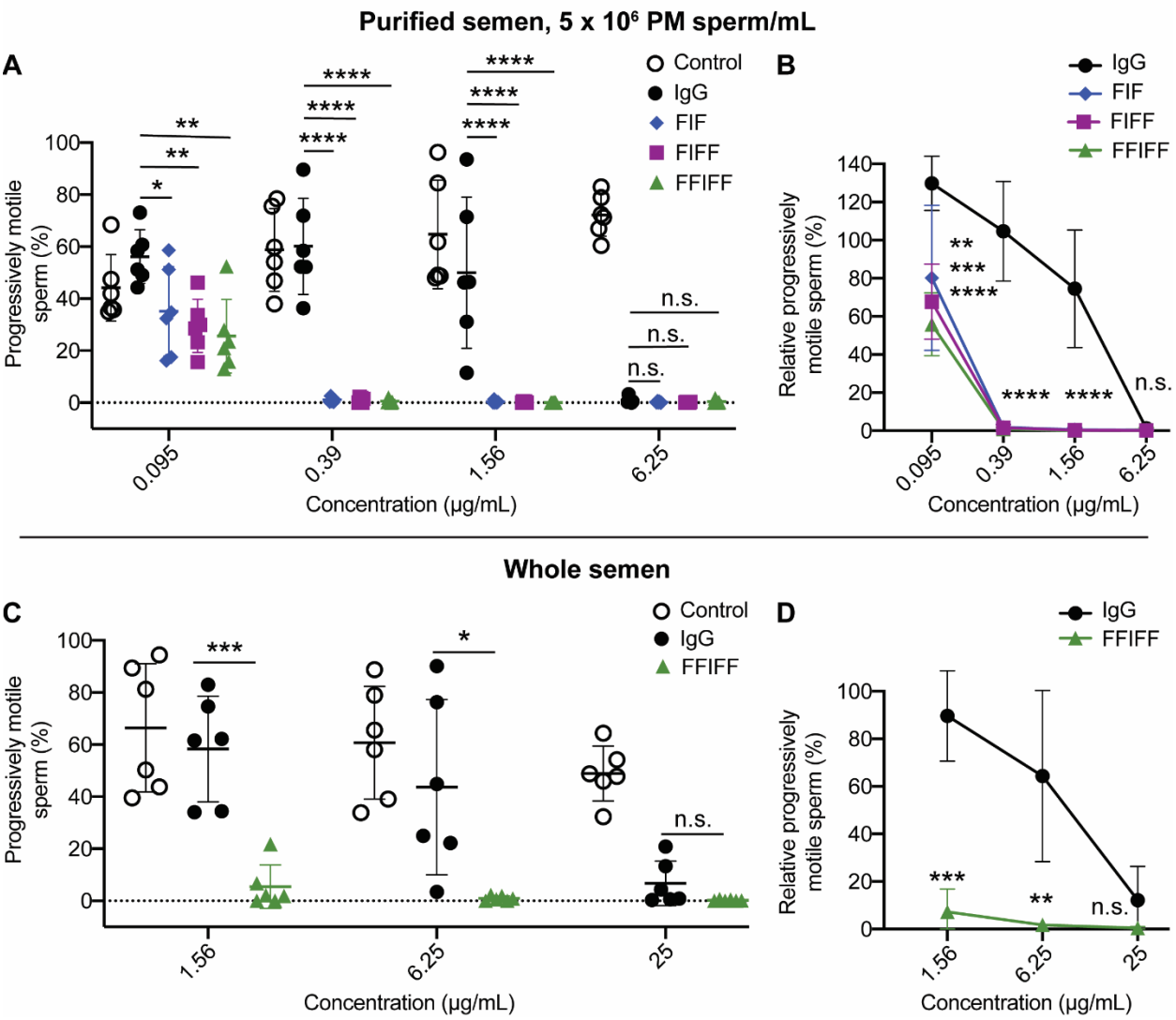


**Figure 3.3: Multimerization markedly enhances the agglutination potency of anti-sperm IgG antibodies**. (A) Sperm agglutination potency of the parent IgG, FIF, FIFF, and FFIFF measured by the CASA-based quantification of the percentage of sperm that remains progressively motile (PM) after Ab-treatment compared to pre-treatment condition. Purified sperm at the final concentration of 5 x $10^6$ PM sperm/mL was used. (B) The sperm agglutination potency of the Abs against 5 x $10^6$ PM sperm/mL normalized to the sperm washing media control. (C) Further assessment of sperm agglutination potency of the parent IgG and FFIFF using whole semen. (D) The sperm agglutination potency of the parent IgG and FFIFF against whole semen normalized to the sperm washing media control. Data were obtained from N=6 independent experiments using at least 4 unique semen donors. Each experiment was performed in duplicates and averaged. P values were calculated using a one-way ANOVA with Dunnett's multiple comparisons test. *P < 0.05, **P < 0.01, ***P < 0.001 and ****P < 0.0001. Lines indicate arithmetic mean values and standard deviation.

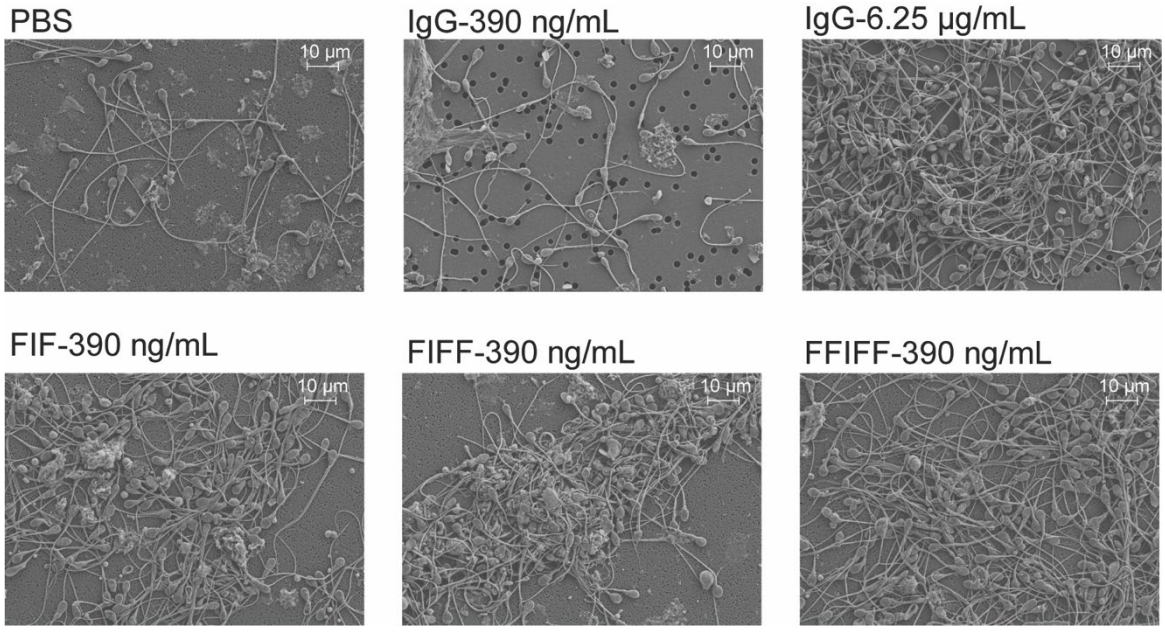


**Figure 3.4: Scanning electron microscopy images of the agglutinated sperm.** 20 million washed sperm were treated with anti-sperm IgGs for 5 min and fixed using 4% PFA. Images were obtained at 2500X magnification. Scale bar, 10 µm.

### *3.3.3. HM-IgGs induce faster agglutination kinetics than IgG*

For effective vaginal immunocontraception, mAbs must agglutinate/immobilize sperm before they reach the upper reproductive tract; thus, the speed with which PM sperm become agglutinated will likely correlate with contraceptive efficacy. We, therefore, quantified the kinetics of sperm agglutination immediately following mixing of sperm and mAb using CASA with washed sperm at a standard concentration of 5 million PM sperm/mL. The parent IgG reduced PM sperm by ≥90% within 90 s in 5 of 6 semen samples at 6.25 µg/mL but failed to do so in 6 of 6 samples at 1.56 µg/mL (Figure 3.5A). In contrast, all 3 HM-IgG constructs agglutinated ≥90% of PM sperm within 60 s in all cases at both 1.56 µg/mL and 6.25 µg/mL concentrations, and only began to fail to do so at 0.39 µg/mL (Figure 3.5A). Notably, the agglutination kinetics of all HM-IgGs were markedly faster and more complete than the parent IgG at each Ab concentration and across all time points (Figure 3.5B).

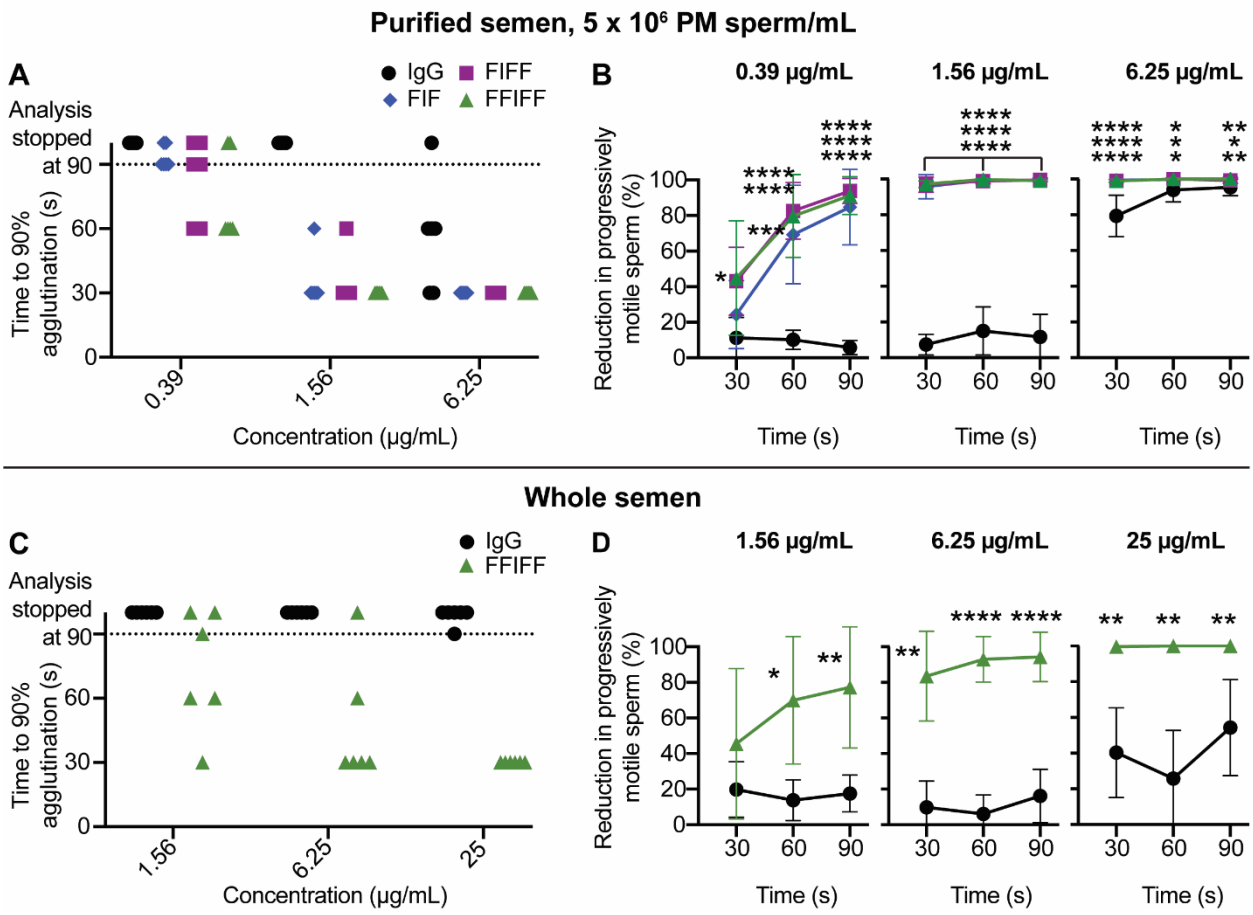


**Figure 3.5: Multimerization markedly accelerates the agglutination kinetics of anti-sperm IgG antibodies**. (A) Sperm agglutination kinetics of the parent IgG, FIF, FIFF, and FFIFF measured by the quantification of time required to achieve 90% agglutination of PM sperm compared to sperm washing media control using the final concentration of 5 x $10^6$ PM sperm/mL. (B) The rate of sperm agglutination for IgG, FIF, FIFF, and FFIFF determined by the reduction in the percentage of PM sperm at three different time points after Ab-treatment compared to sperm washing media control using 5 x $10^6$ PM sperm/mL. (C) Sperm agglutination kinetics and (D) The rate of sperm agglutination for IgG and FFIFF evaluated using whole semen. Data were obtained from N=6 independent experiments using at least 4 unique semen donors. Each experiment was performed in duplicates and averaged. P values were calculated using a one-way ANOVA with Dunnett's multiple comparisons test for Figure 3B and a one-tailed t-test for Figure 3D. *P < 0.05, **P < 0.01, ***P < 0.001 and ****P < 0.0001. Lines indicate arithmetic mean values and standard deviation.

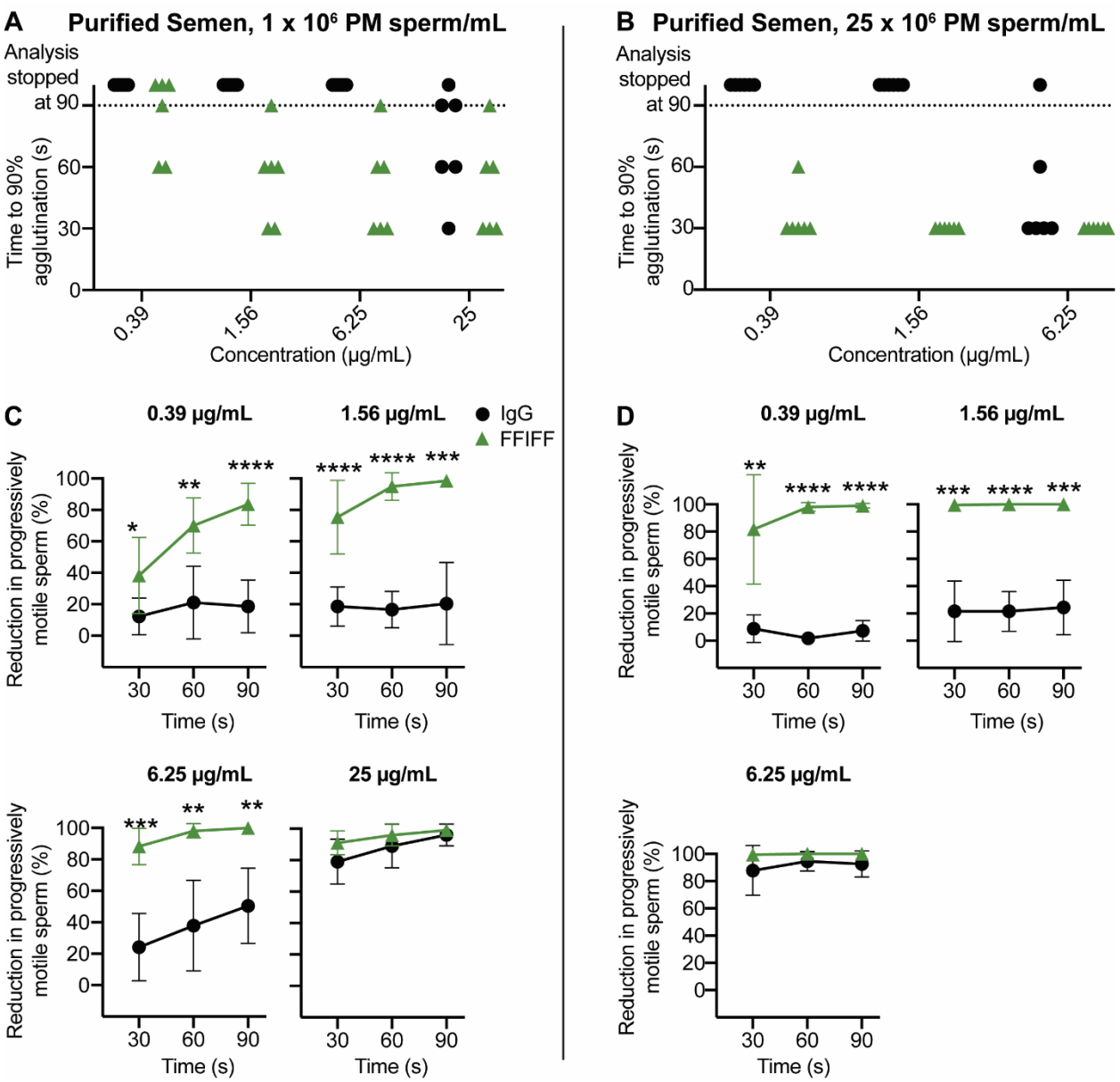


**Figure 3.6: FFIFF demonstrates faster agglutination kinetics than the parent IgG at both low and high sperm concentration.** (A) Sperm agglutination kinetics of the parent IgG and FFIFF measured by the quantification of time required to achieve 90% agglutination of PM sperm compared to sperm washing media control using the final concentration of 1 x $10^6$ PM sperm/mL and (B) 25 x $10^6$ PM sperm/mL. (C) The rate of sperm agglutination for the parent IgG and FFIFF measured by the reduction in percentage of PM sperm at three different timepoints after Ab-treatment compared to sperm washing media control using 1 x $10^6$ PM sperm/mL and (D) 25 x $10^6$ PM sperm/mL. Data were obtained from N=6 independent experiments using 6 different semen donors. Experiment involving 1 x $10^6$ PM sperm/mL was performed in duplicates and averaged. P values were calculated using a one-tailed t-test. *P < 0.05, **P < 0.01, ***P < 0.001 and ****P < 0.0001. Lines indicate arithmetic mean values and standard deviation.

We again assessed agglutination kinetics of FFIFF vs. IgG using whole semen. Similar to the PM sperm escape assay, substantially more FFIFF and the parent IgG were required to agglutinate sperm in native semen with comparable kinetics as washed sperm. FFIFF again exhibited markedly faster and more complete sperm agglutination kinetics than IgG at all mAb concentrations and all time points in whole semen (Figure 3.5D). Indeed, FFIFF agglutinated ≥90% of PM sperm within 30 s in 6 of 6 semen samples at 25 μg/mL, while IgG agglutinated ≥90% of PM sperm in 90 s in only one of six specimens at the same concentration (Figure 3.5C). Since lower sperm concentration (as found in semen from oligospermia, sub-fertile individuals) may limit agglutination potency due to reduced likelihood of a sperm-sperm collision, and higher quantities of sperm may saturate the agglutination potential, we further assessed whether FFIFF can effectively reduce PM sperm at 1 million PM sperm/mL and 25 million PM sperm/mL. FFIFF maintained similar superior agglutination kinetics than IgG across both conditions (Figure 3.6). These results underscore the increased potency for FFIFF compared to the parent IgG across diverse conditions.

### *3.3.4. HM-IgGs maintain robust agglutination activity against the capacitated sperm*

Sperm capacitation leads to greater motility and changes in certain surface proteins. Thus, we sought to test whether FIF and FFIFF can effectively agglutinate capacitated sperm. We induced capacitation following well-established protocols, and confirmed sperm capacitation. Both FIF and FFIFF exhibited excellent agglutinating activity against capacitated sperm with zero hyperactivated and progressively motile sperm present even at low mAb concentrations (1.56 μg/mL; Figure 3.7).

### *3.3.5. Sperm-agglutinates induced by HM-IgGs are highly stable over time and shear*

Sperm is exposed to agitation and mechanical stress in the vagina. We assessed the stability of mAb-sperm agglutinates by exposing the agglutinates to high-speed vortexing, and quantified the number of PM sperm post-vortexing by CASA. Sperm agglutinates with FFIFF were highly stable even at just

0.39 µg/mL of FFIFF (Figure 3.8). We further assessed the stability of sperm-agglutinates over time, and found that sperm was comparably agglutinated at 2 hr, 4 hr, and 24 hr post-HM-IgG addition (Figure 3.9).

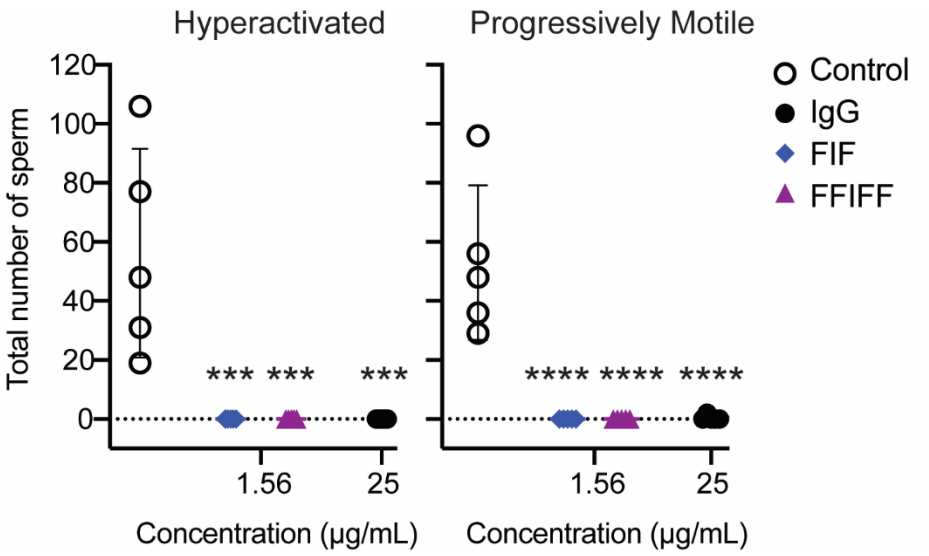


**Figure 3.7: HM-IgGs exhibit robust agglutination against capacitated sperm.** Sperm agglutination activity of the indicated Abs measured by the CASANOVA-based quantification of the number of sperm that remains Capacitated/Hyperactivated and CASA-based quantification of the number of sperm that remains PM after control- or Ab- treatment. Washed semen at the final concentration of 10 x $10^6$ motile sperm/mL that was capacitated for 1 hr at 37°C and 5% CO2 was used. Data were obtained from N=5 independent experiments using 3 unique semen donors. P values were calculated using a one-way ANOVA with Dunnett's multiple comparisons test. *P < 0.05, **P < 0.01, ***P < 0.001 and ****P < 0.0001. Lines indicate arithmetic mean values and standard deviation.

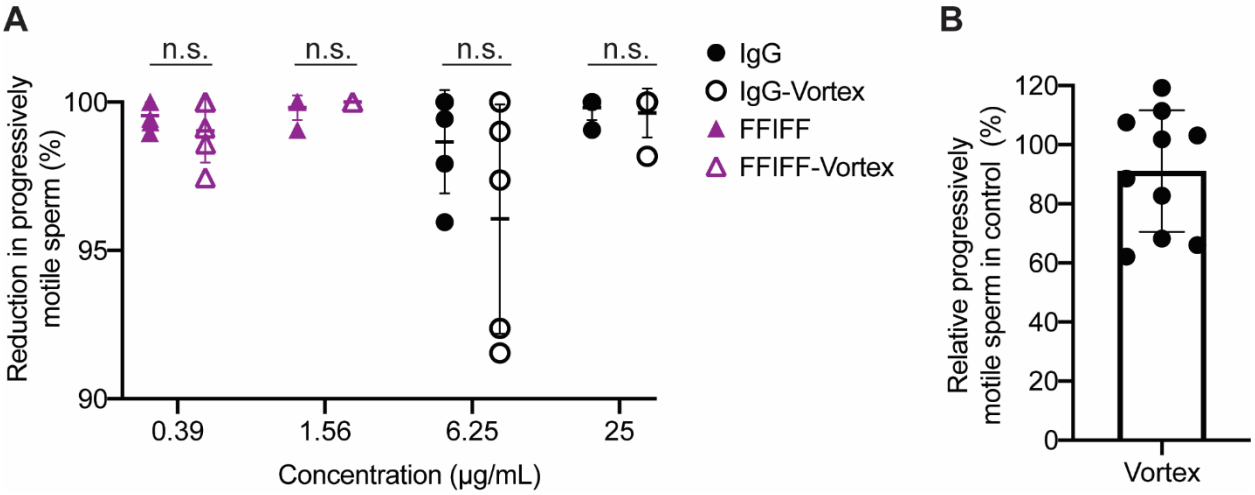


**Figure 3.8: FFIFF conserves the sperm-agglutination upon mechanical stress**. (A) The stability of mAb-agglutinated sperm upon vortexing measured by the reduction in percentage of PM sperm after Ab-treatment compared to control-treatment. Agglutination was first performed in non-vortex condition as the reference. (B) The number of PM sperm in control-treated sample of post-vortexing condition normalized

to the number of PM sperm in control-treated sample of non-vortexing condition. Purified sperm at the final concentration of 5 x $10^6$ PM sperm/mL was used. Data were obtained from N=5 independent experiments using 3 different semen donors. P values were calculated using paired two-tailed t-tests between vortex and non-vortex conditions. *P < 0.05, **P < 0.01, ***P < 0.001 and ****P < 0.0001. Lines indicate arithmetic mean values and standard deviation.

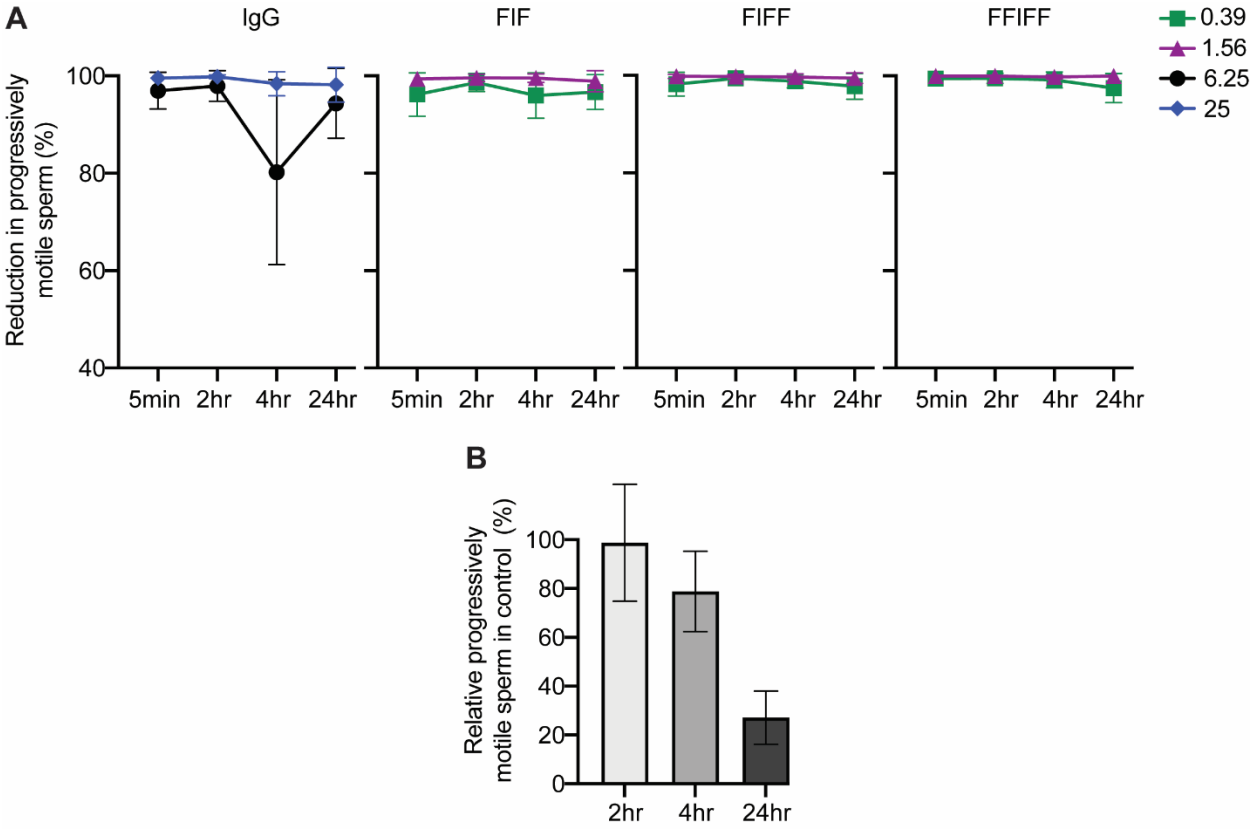


**Figure 3.9: HM-IgGs conserve the sperm-agglutination for at least 24 hrs.** (A) The stability of mAb-agglutinated sperm over time measured by the reduction in percentage of PM sperm after Ab-treatment compared to control-treatment over three different timepoints. Agglutination activity observed initially at 5 min timepoint is used as the reference. (B) The number of PM sperm in control-treated samples of three different timepoints normalized to the number of PM sperm in control-treated sample of initial 5 min timepoint. Purified sperm at the final concentration of 5 x $10^6$ PM sperm/mL was used. Data were obtained from N=4 independent experiments using 3 different semen donors. No significant difference was observed for the agglutination activity of all mAbs at different timepoints. For each mAb concentration, P values were calculated using paired one-way ANOVA with Dunnett's multiple comparisons test. *P < 0.05, **P < 0.01, ***P < 0.001 and ****P < 0.0001. Lines indicate arithmetic mean values and standard deviation.

### *3.3.6. HM-IgGs preserve Fc-mucin crosslinking and block sperm from penetrating bovine cervical mucus*

Previous work has shown that IgG and IgM Abs can trap individual spermatozoa in mucus despite the continued vigorously beating action of the flagellum; clinically, this is referred to as the "shaking phenomenon". This muco-trapping function is similar to our recent observations with Herpes Simplex Virus (HSV) that multiple HSV-bound IgGs can form polyvalent adhesive interactions between their Fc domains and mucin fibers in cervicovaginal mucus (CVM), resulting in effective trapping of individual viral particles in CVM and blocking the vaginal transmission of HSV in mice. Therefore, we next assessed whether the HM-IgGs can reduce progressive motility in the relatively thin (low viscosity) human cervicovaginal mucus (CVM). We fluorescently labeled human sperm and quantified their motion in CVM treated with different mAbs using multiple particle tracking. All 3 constructs were able to reduce progressive motility of individual spermatozoa to the same extent as the parent IgG, indicating that the addition of Fabs to both the N- and C-terminus of the IgG did not interfere with Fc-mucin crosslinking (Figure 3.10). We further assessed the ability of HM-IgGs to block sperm penetration using the well-established bovine cervical mucus model. With control mAb, there were too many actively motile sperm to count at 1 cm distance into the capillary tube, and substantial numbers at 3 cm distance. In contrast, with FFIFF, there were very few actively motile sperm even at just 1 cm distance, and zero actively motile sperm at 3 cm (Figure 3.11). These results demonstrate the ability of HM-IgGs to effectively limit sperm permeation through mucus.

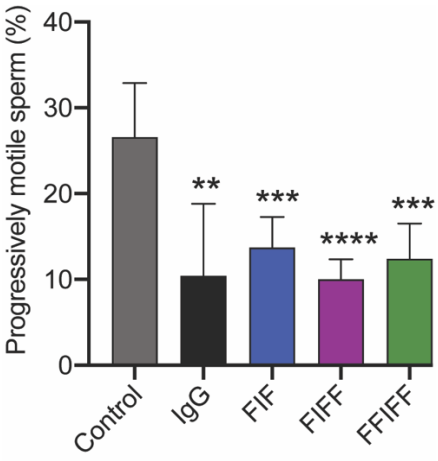


**Figure 3.10: Highly multivalent anti-sperm IgG constructs conserve the trapping potency of the parent IgG.** The trapping potency of the indicated Abs measured by quantifying the percentage of fluorescently labeled PM sperm in Ab-treated CVM using neural network tracker analysis software. 25 µg/mL of multivalent Abs and purified sperm at the final concentration of 5.8 x 104 PM sperm/mL were used. Motavizumab (anti-RSV IgG) was used as the control. Data were obtained from N=6 independent experiments with 6 unique combinations of semen and CVM specimens. P values were calculated using a one-tailed t-test. *P < 0.05, **P < 0.01, ***P < 0.001 and ****P < 0.0001. Lines indicate arithmetic mean values and standard deviation.

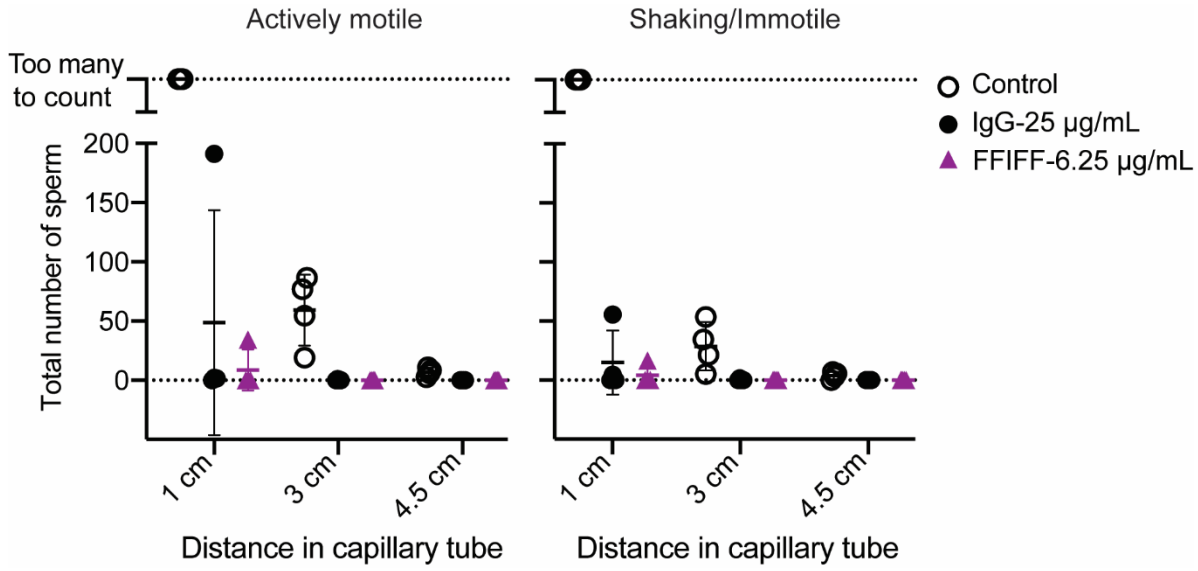


**Figure 3.11: FFIFF prevent the penetration of vanguard human sperm in bovine cervical mucus.** The total number of actively motile and immotile sperm present at three different distances marked on 5 mm BCM-capillary tubes after incubation into semen-mAb mixture for 2 hrs. 25 µg/mL of IgG, 6.25 µg/mL of FFIFF and whole semen was used for the experiment. Data were obtained from N=4 independent experiments using 3 different semen donors. Experiment was evaluated in duplicates on each semen specimen, and the average from the two experiments was used in the analysis. Lines indicate arithmetic mean values and standard deviation.

### *3.3.7. FIF and FFIFF effectively reduce PM sperm in sheep vagina*

Since the unique glycoform of CD52g is only found in human and chimpanzee sperm, there is no practical animal model to perform mating-based contraceptive efficacy studies. Instead, we designed a sheep study that parallels the human post-coital test (PCT), which assesses the reduction of PM sperm in the FRT given that PM sperm is required for fertilization. Clinical PCT studies have proven to be highly predictive of contraceptive efficacy in contraceptive effectiveness clinical trials. The sheep vagina is physiologically and anatomically very similar to the human vagina, making it the gold standard for assessing vaginal products. We instilled PBS, IgG, FIF, or FFIFF into the sheep vagina, followed by brief simulated intercourse with a vaginal dilator (15 strokes), vaginal instillation of whole human semen, brief simulated intercourse (5 strokes), and finally, recovery of the semen mixture from the sheep vagina 2 mins post semen instillation for immediate assessment of sperm motility. The parent IgG, FIF, and FFIFF all effectively reduced PM sperm at 333 µg dose (Figure 3.12). At 10-fold lower concentrations i.e. 33 µg dose per sheep, FIF and FFIFF were still able to reduce PM sperm by 97% and >99%, respectively, whereas the parent IgG failed to substantially reduce PM sperm at the same concentration (Figure 3.12).

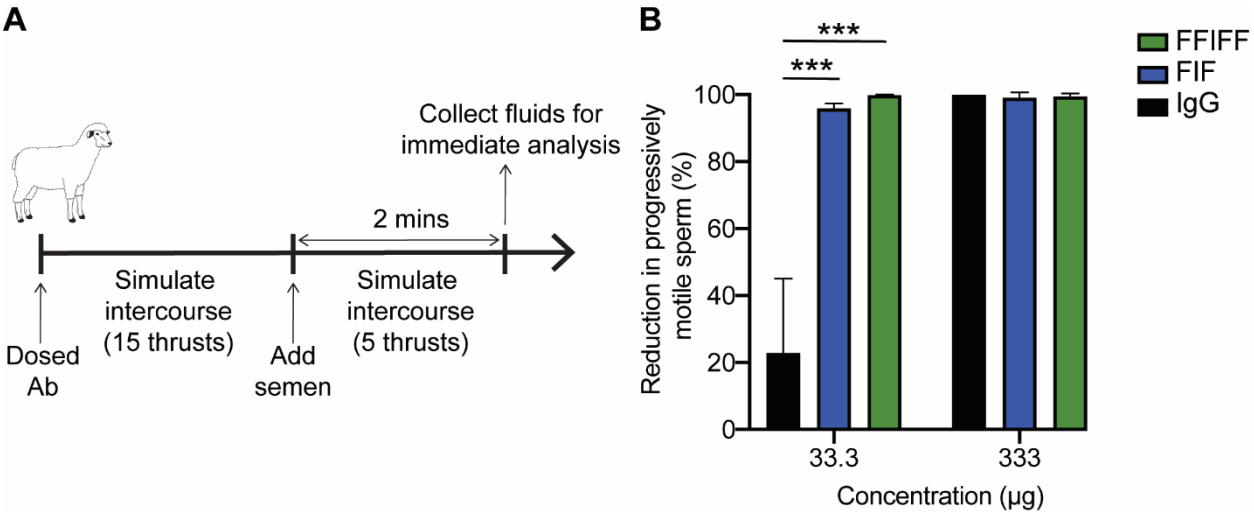


**Figure 3.12: Highly multivalent anti-sperm IgG constructs demonstrate stronger agglutination potency than the parent IgG in surrogate sheep studies.** (A) Schematic of the study design. (B) The potency of IgG, FIF, and FFIFF measured by the reduction in the percentage of PM sperm in sheep's vaginal fluid after Ab-treatment compared to PBS-treatment. Data were obtained from N=3 independent experiments. Treatment administration was blinded, and quantifications were manually performed in a

blinded fashion. P values were calculated using a one-way ANOVA with Dunnett's multiple comparisons test. *P < 0.05, **P < 0.01, and ***P < 0.001. Lines indicate arithmetic mean values and standard deviation.

### 3.4. Discussion

The exceptional potencies we observed in sheep despite the low total dose of mAb are a direct consequence of topical vaginal delivery. Since sperm is restricted to the FRT, topical delivery confines the contraceptive mAb directly at the site of action. Given the limited volume of secretions in the FRT (≤ ~1 mL in the human vagina, a relatively high concentration of mAb locally can be achieved even with a very limited total dose of mAb. In contrast, systemically delivered mAbs must dilute into a large blood volume (~5L), distribution to non-target tissues, natural catabolic degradation, and limited distribution into the FRT, including the vagina. The markedly lower doses of mAb needed to sustain contraceptive levels in the FRT with vaginal delivery should translate to substantially less mAb needed, and consequently, cost savings. Furthermore, by simply reinforcing the mucus barrier that is continuously secreted and cleared, rather than altering physiological mechanisms underpinning fertility (e.g. hormones), topical immunocontraception most likely affords rapid return to fertility, unlike the many months of delay experienced by some women even after they discontinued the use of long-acting hormonal contraceptives.

Unlike small-molecule contraceptives, contraceptive mAbs are likely to be exceptionally safe due to the specificity of targeting, particularly when targeted to unique epitopes present only on sperm and not on expressed in female tissues. Safety is likely to be further enhanced by topical delivery: mAb delivered to mucosal surfaces such as the vagina is poorly absorbed into the systemic circulation, and the vagina represents a poor immunization inductive site, with limited immune response even when vaccinating with the aid of highly immunostimulatory adjuvants. Finally, vaginal secretions already contain much higher levels of endogenous IgG (i.e. 1-2 mg/mL), making it unlikely that vaginal delivery of HM-IgGs comprised of fully human Fabs and Fc would trigger local toxicities.

Sperm must swim through mucus and ascend to the upper tract to reach and fertilize the egg. Typically, only ~1% of the ejaculated sperm enter the cervix, even fewer arrive at the uterus, and only

dozens of sperm (out of the ~200 million in the ejaculate) reach the neighborhood of the egg. Indeed, even under ideal circumstances of unprotected intercourse on the cycle day of maximum fertility, the odds of conceiving are only about ~10%. This indicates that only a very small (i.e. limiting) number of motile sperm could reach the egg per intercourse; thus, reducing progressive sperm motility in the vagina and cervical canal should proportionally reduce the likelihood of conceiving. While low sperm count alone is not predictive of the fertility status of an individual, both poor sperm motility in mid-cycle cervical mucus and modestly reduced total sperm count increases the odds ratio for infertility. Human semen averages between 45-65 million sperm/mL, 15 million sperm/mL marks the lowest 5th percentile in men with proven fertility, and <5 million sperm/mL is often considered severe oligozoospermia and is associated with low fertility. Likewise, testosterone-induced azoospermia and oligospermia in males, which did not affect the morphology or impair *in vitro* fertilizing capacity of the sperm, have very low fertility rates (0.8 conceptions per 100 women-years at a concentration of <1 million sperm/mL). These findings, together with the contraceptive success with topical ASA against rabbit sperm, suggest a marked reduction of progressive sperm motility, even if incomplete, may provide effective contraception. Due to the absence of a readily available contraceptive efficacy animal model for our antibody, actual contraceptive efficacy in humans must be determined through rigorous clinical studies.

Advances in vaginal drug delivery technologies have made available multiple methods for delivering contraceptive mAbs. For instance, a rapidly dissolving vaginal film could provide on-demand non-hormonal contraception. For a non-coitally associated method, HM-IgGs can be released from intravaginal rings (IVRs) that afford nearly constant, the zero-order release kinetics of mAbs. The fertility window in women typically starts a few days after the end of menses, and ends ~12-14 days before the start of the next menses. Thus, for a 35-day menstrual cycle, an IVR would only need to release contraceptive mAbs for ~18 days if the IVR is inserted at the end of menses (~Day 5 of a typical cycle). A hypothetical 20 mg of FFIFF loaded per IVR could sustain >33 μg/mL concentrations in FRT secretions. With the cost of large-scale mAb manufacturing at ~$95-200/g in 2020, and a continued

decrease in mAb manufacturing costs, we speculate the FFIFF Ab quantity required to provide month-long non-hormonal contraception may cost no more than $2-4/month to produce.

Many of the current multivalent Abs are bispecific or tri-specific in nature and must contend with potential mispairing of light and heavy chains. As a result, many such engineered Ab formats, such as single-chain variable fragment (scFv) or camel-derived nanobodies, involve a substantial deviation from natural human Ab structure. scFv-based multivalent Ab constructs frequently suffer from low stability, heterogeneous expression, and decreased affinity and specificity stemming from the removal of the CH1/CL interface present in a full-length Fab. The introduction of orthogonal mutations to facilitate heavy and light chain pairing can also substantially reduce mAb yield or overall stability. These limitations do not apply when generating monospecific HM-IgGs, which possess identical and full-length human Fabs. Our strategy to covalently link additional Fabs to a parent heavy chain also contrasts with current multimerization strategies based on self-assembly of multiple IgGs based on Fc-mutations or appending an IgM tail-piece, which often suffers poor homogeneity and stability. The combination of fully intact human Fabs and covalent linkages likely contributes to the surprising thermal stability, homogeneity, and bioprocessing ease of the HM-IgGs developed here. We believe the IgG multimerization strategy presented here is likely a promising platform for developing mAbs where agglutination is a critical effector function.

There are a number of limitations to our current study. First, we did not directly demonstrate efficacy by preventing pregnancies. We are unable to do so due to the unique antigen (CD52g) that our antibody targets: prior work has shown that only chimpanzees possess CD52g, and it is not possible to conduct chimpanzee studies in the U.S. Instead, we were forced to demonstrate *in vivo* proof-of-concept using a sheep study designed to closely mimic the human post-coital test that is routinely used to assess the efficacy of sperm-targeted contraceptives in early phase clinical studies, which has shown to correlate well with eventual efficacy in preventing pregnancies. However, the parent anti-CD52g IgG is currently being evaluated (ClinicalTrials.gov Identifier: NCT04731818) via the human post-coital test in surgically sterilized women, which allows an early assessment of contraceptive promise without risk of pregnancy.

Second, the precise dose of antibodies needed to ensure highly effective sperm agglutination remains not well understood. In the current study, we administer our mAb shortly before prior to the introduction of sperm into the sheep vagina. While this design is far more realistic than pre-mixing the mAb and the semen prior to vaginal delivery, it does not address how much mAb must be delivered via an intravaginal ring in order to sustain effective contraceptive levels in the vagina. We are actively pursuing the development of an intravaginal ring that can release our mAbs and anticipate those insights to emerge in the years ahead.

# CHAPTER 4: HEXAVALENT SPERM-BINDING IGG ANTIBODY RELEASED FROM SELF-DISSOLVING VAGINAL FILM ENABLES POTENT, ON-DEMAND NON-HORMONAL FEMALE CONTRACEPTION[3]

## 4.1. Introduction

Despite the availability of potent and low-cost, long-acting, reversible contraceptives (LARCs), many women continue to use on-demand contraceptives due to infrequent sexual activity. In addition, many women strongly prefer non-hormonal contraceptives because of the real and/or perceived side-effects associated with existing hormonal methods [46,47,116]. Indeed, the FDA-approved Vaginal Contraceptive Film (VCF) meets the contraceptive needs of many women as it provides a contraceptive method that is women-controlled, inexpensive, non-hormonal, discrete, and readily available over the counter. Unfortunately, VCF and most other spermicides use nonoxynol-9 (N9) as an active ingredient. N9 can damage the mucosal surfaces by disrupting the vulvar, vaginal, and cervical epithelium, and substantially increases the risks of sexually transmitted infections [117–119]. We believe there is a substantial unmet need for alternatives that can offer effective on-demand contraception, and are free of exogenous hormones or detergents.

Anti-sperm antibodies (ASA) to surface antigens on sperm [120] represent a promising class of molecules that could enable safe, on-demand, non-hormonal contraception. ASAs found in the vaginal secretions of some immune infertile women could prevent fertilization by stopping sperm from reaching the egg via two distinct mechanisms [9]. First, ASAs can agglutinate multiple motile sperm into clumps that stop forward progression [14,121]. This mechanism is most effective at high sperm concentrations, and is more potent with polyvalent antibodies (Abs) such as IgM. Second, ASAs can trap individual

[3] This chapter is based on an article that was submitted by Shrestha B., et al. to Proceedings of the National Academy of Sciences of the United States of America in 2021.

spermatozoa in mucus by forming multiple low-affinity Fc-mucin bonds between sperm-bound ASA and mucin fibers [2], resulting in individual sperm that simply shake in place, unable to assume progressive motility needed to reach the upper reproductive tract. Over time, sperm that are agglutinated or immobilized in mucus either die or are eliminated from the female reproductive tract by natural mucus clearance mechanisms.

Years ago, the discovery of the contraceptive potential of ASAs motivated the development of contraceptive vaccines. ASAs elicited by vaccination with sperm antigens offered considerable contraceptive efficacy, but this approach stalled due to unresolved variability in the intensity and duration of the vaccine responses in humans, as well as concerns that active vaccination might lead to irreversible infertility [1,80,81]. In contrast, topical delivery of pharmacologically active doses of ASA in the vagina can overcome many of the key drawbacks of contraceptive vaccines by providing consistent amounts of antibodies needed without risks of inducing immunity to sperm, thus making possible both consistently effective contraception and rapid reversibility. In good agreement with this concept, vaginal delivery of a highly multivalent anti-sperm IgM reduced embryo formation by 95% in a highly fertile rabbit model [20].

This approach of topical passive immunocontraception has not been reported in humans, due in part to manufacturing and purification challenges with polyvalent Abs such as sIgA and IgM, and the lower agglutinating potencies of IgG. To overcome these challenges, we report here a highly multivalent IgG that possesses 6 Fabs per IgG molecule, with Fab domains interspersed by flexible glycine-serine linkers arranged in a Fab-IgG-Fab orientation; we term this molecule FIF (Figure 4.1A). To determine whether FIF may be useful for on-demand contraception, we produced FIF using a cGMP-compliant *Nicotiana benthamiana* manufacturing platform, and formulated the FIF into a dissolvable vaginal film comprised of polyvinyl alcohol. We report here the *in vitro* characterization and *in vivo* potency of this novel FIF Film.

**4.2. Materials and Methods**:

***4.2.1. Experimental design and ethics***. The objective was to assess the sperm- agglutinating and:trapping potency of PVA film formulated with *Nicotiana*-produced FIF Ab *in vitro* and *in vivo*. The *in vitro* studies using human semen and human cervicovaginal mucus samples were approved by the Institutional Review Board (IRB) of the University of North Carolina at Chapel Hill (IRB-101817). Prior to the collection of semen and mucus samples, informed written consents were obtained from all male and female subjects. Mass student emails and printed posters were utilized to recruit subjects for the UNC-Chapel Hill studies. The sheep surrogate post-coital test using human semen samples was approved by the IRB of the University of Texas Medical Branch (UTMB; IRB-180254). Informed written consent was obtained from the pre-screened male volunteers. Sheep studies were approved by the UTMB Institutional Animal Care and Use Committee (IACUC; 0608038D) and utilized 5 female Merino crossbred sheep. IgG-N-Film and FIF-N-Film were dissolved in ultra-pure water before all *in vitro* experiments.

***4.2.2. Construction of N. benthamiana expression vectors***. The variable light (VL) and variable heavy (VH) DNA sequences for anti-sperm IgG antibody were obtained from the published sequence of H6-3C4 mAb(18, 19). For the construction of expression vector encoding light chain (LC), a gene fragment consisting of VL and CL DNA sequences was codon-optimized and synthesized using GeneArt® gene synthesis services (ThermoFisher Scientific) and cloned into PVX viral backbone (Icon Genetics)(20). For the construction of an expression vector containing IgG1 heavy chain (HC), a gene fragment consisting of VH and CH1-CH2-CH3 DNA sequences was codon-optimized and synthesized using GeneArt® gene synthesis services (ThermoFisher Scientific) and cloned into TMV viral backbone (Icon Genetics)(20). For the construction of expression vector containing FIF HC, a gene fragment consisting of VH/CH1-(G4S)6 Linker-VH/CH1-CH2-CH3-(G4S)6 Linker-VH/CH1 DNA sequences was synthesized using GeneArt® gene synthesis services (ThermoFisher Scientific) and cloned into TMV viral backbone (Icon Genetics).

***4.2.3. Production of mAbs in Nb7KOΔXylT/FucT N. benthamiana***. Briefly, IgG and FIF mAbs were expressed in *N. benthamiana* plants using "magnifection" procedure(23). Cloned expression vectors i.e. PVX-LC, TMV-IgG-HC, and TMV-FIF-HC were transformed into Agrobacterium tumefaciens strain ICF320 (Icon Genetics) and grown overnight at 28.0 ºC followed by 1:000 dilution in infiltration buffer [10 mM MES (pH 5.5) and 10 mM MgSO4]. The combinations of diluted bacterial cultures (TMV-IgG-HC + PVX-LC and TMV-FIF-HC + PVX-LC) were used to transfect 4 wks old *N. benthamiana* plants (ΔXTFT glycosylation mutants) using vacuum infiltration. Using a custom-built vacuum chamber (Kentucky Bioprocessing), the aerial parts of entire plants were dipped upside down into the bacterial/buffer solution and a vacuum of 24'' mercury was applied for 2 mins. Infiltrated plants were allowed to recover and left in the growth room for transient expression of antibodies. 7 days after infiltration, plants were harvested and homogenized in extraction buffer containing 100 mM Glycine, 40mM Ascorbic Acid, 1mM EDTA (pH 9.5) in a 0.5:1 buffer (L) to harvested plants (kg) ratio. The resulting green juice was clarified by filtration through four layers of cheesecloth followed by centrifugation at 10,000 g for 20 mins. Next, mAbs were captured from the clarified green juice using MabSelect SuRe Protein A columns (GE Healthcare). Protein A Columns were equilibrated and washed with buffer containing 50 mM Tris, pH 7.4, and bound protein were eluted with buffer containing 100 mM Acetic acid, pH 3. The eluates were immediately neutralized using 1 M Tris, pH 8.0. The eluted mAbs were further purified using equilibrated Capto Q columns (GE Healthcare) and flow-through fractions, which contain mAbs, were collected. The mAb-containing fractions were finally polished with CHT chromatography with type II resin (Bio-Rad). The CHT columns were equilibrated and washed with phosphate running buffer and eluted with running buffer containing NaCl.

***4.2.4. Biophysical characterization of mAbs***. SDS-PAGE at reducing and non-reducing conditions was performed to determine the molecular weight of FIF-N. Briefly, 1 μg of mAb was denatured at 70°C for 10 min. Next, 0.3 μL of 0.5 M tris (2-carboxyethyl) phosphine (TCEP) was added as a reducing agent to the denatured protein for a reduced sample and incubated at room temperature for 5 min. After the

incubation, samples were loaded, and the gel was run for 40 min at a constant voltage of 200 V. Bio-Rad Precision Protein Plus Unstained Standard was used as a protein ladder. Imperial Protein Stain (Thermo Scientific) was used to visualize the protein bands. The brightness and contrasts of the SDS-PAGE image were linearly adjusted using Image J software (Fiji).

HPLC-SEC was performed to determine the purity of IgG-N and FIF-N mAbs. The HPLC-SEC system consisted of a TSK Gel Super SW3000 column (Tosoh Biosciences) connected to Agilent 1260 HPLC system and a UV detector. The flow rate was maintained at 0.2 mL/min. The column was equilibrated with 0.1M sodium phosphate, 0.15 M NaCl buffer, pH 7.2 before loading the samples. 100 µg of each mAbs (50uL) were injected onto the column, and data were collected and analyzed using the ChemStation chromatography data system and software (Agilent). The proportion of monomers, aggregates, and fragments present in each mAb sample were calculated using ChemStation software (Agilent).

Endotoxin levels in mAbs were measured with Endosafe PTS (Charles River), which detects by measuring color-intensity related to endotoxin concentration.

Bioburden was determined for IgG-N and FIF-N by counting the number of colony-forming units that formed after mAbs were incubated overnight on the bacterial agar plate at 37°C.

***4.2.5. Production of IgG-N and FIF-N films***. Films were manufactured using the solvent casting method (55). Briefly, PVA 8-88 (67 kDa; 25%, w/w) was dissolved in MilliQ water. Next, IgG and FIF mAbs suspended in 10 mM Histidine + 0.005% Polysorbate 20, pH 6.5 were slowly added into the PVA solution followed by 200 mg/mL maltitol. The solution was stirred over 15 minutes to ensure uniform distribution of mAbs and to remove the entrapped air bubbles. The final uniform polymer solution was cast onto a polyester substrate attached to a glass plate using a 2’’x2’’x0.020’’ die press. The film sheet was allowed to dry for 20 min before it was removed from the substrate, and then cut into 2”x1.8” individual unit doses using a scalpel. Placebo film was prepared using the same method as described

above except without drug substances in the polymer solution. IgG-N-Film and FIF-N-Film were dissolved in ultra-pure water prior to *in vitro* experiments.

***4.2.6. Semen collection and isolation of purified motile sperm***. Healthy male subjects were asked to refrain from sexual activity for at least 24 hr prior to semen collection. Semen was collected by masturbation into sterile 50 mL sample cups and incubated for a minimum of 15 min post-ejaculation at RT to allow liquefaction. Semen volume was measured, and the density gradient sperm separation procedure (Irvine Scientific) was used to extract motile sperm from liquefied ejaculates. Briefly, 1.5 mL of liquified semen was carefully layered over 1.5 mL of Isolate® (90% density gradient medium, Irvine Scientific) at RT, and centrifuged at 300 g for 20 min. Following centrifugation, the upper layer containing dead cells and seminal plasma was carefully removed without disturbing the motile sperm pellet in the lower layer. The sperm pellet was then washed twice with the sperm washing medium (Irvine Scientific) by centrifugation at 300 g for 10 min. Finally, the purified motile sperm pellet was resuspended in the sperm washing medium, and an aliquot was taken for determination of sperm count and motility using CASA. All semen samples used in the functional assays exceeded lower reference limits for sperm count ($15 \times 10^6$ total sperm/mL) and total motility (40%) as indicated by WHO guidelines.

***4.2.7. Sperm count and motility using CASA***. The Hamilton-Thorne computer-assisted sperm analyzer, 12.3 version, was used for the sperm count and motility analysis in all experiments unless stated otherwise. This device consists of a phase-contrast microscope (Olympus CX41), a camera, an image digitizer, and a computer with Hamilton-Thorne Ceros 12.3 software to save and analyze the acquired data. For each analysis, 4.4 µL of the semen sample was inserted into MicroTool counting chamber slides (Cytonix). Then, six randomly selected microscopic fields, near the center of the slide, were imaged and analyzed for progressively motile and non-progressively motile sperm count. The parameters that were assessed by CASA for motility analysis were as follows: average pathway velocity (VAP: the average

velocity of a smoothed cell path in μm/s), the straight-line velocity (VSL: the average velocity measured in a straight line from the beginning to the end of the track in μm/s), the curvilinear velocity (VCL: the average velocity measured over the actual point-to-point track of the cell in μm/s), the lateral head amplitude (ALH: amplitude of lateral head displacement in μm), the beat cross-frequency (BCF: frequency of sperm head crossing the sperm average path in Hz), the straightness (STR: the average value of the ratio VSL/VAP in %), and the linearity (LIN: the average value of the ratio VSL/VCL in %). PM sperm were defined as having a minimum of 25 μm/s VAP and 80% STR [61]. The complete parameters of the Hamilton-Thorne Ceros 12.3 software are listed in Table 2.1.

***4.2.8. Sperm escape assay***. This assay was conducted using whole semen and purified motile sperm at the starting concentration of 10 x $10^6$ PM sperm/mL. Briefly, 40 μL aliquots of purified motile sperm or whole semen were transferred to individual 0.2 mL PCR tubes. Sperm count and motility were performed again on each 40 μL aliquot using CASA. This count serves as the original (untreated) concentration of sperm for evaluating the agglutination potencies of respective Ab constructs. Following CASA, 30 μL of purified motile sperm or native semen was added to 0.2 mL PCR tubes containing 30 μL of Ab constructs, and gently mixed by pipetting. The tubes were then held fixed at 45° angles in a custom 3D printed tube holder for 5 min at RT. Following this incubation period, 4.4 μL was pipetted from the top layer of the mixture with minimal perturbation of the tube and transferred to the CASA instrument to quantify the number of PM sperm. The percentage of the PM sperm that escaped agglutination was computed by dividing the sperm count obtained after treatment with Ab constructs by the original (untreated) sperm count in each respective tub followed by multiplication with 2 to correct for the 2-fold dilution that occurs upon Ab-treatment. Each experimental condition was evaluated in duplicates on each semen specimen, and the average from the two experiments was used in the analysis. At least 6 independent experiments were done with at least 6 unique semen samples.

***4.2.9. Agglutination kinetics assay***.

*FIF-N-Film vs IgG-N-Film:* This assay was conducted using both whole semen and purified motile sperm at the starting concentration of 2 x $10^6$ PM sperm/mL, 10 x $10^6$ PM sperm/mL, and 50 x $10^6$ PM sperm/mL. Briefly, 4.4 µL of purified motile sperm or whole semen was added to 4.4 µL of Ab constructs in 0.2 mL PCR tubes, and mixed by gently pipetting up and down three times over 3 s. A timer was started immediately while 4.4 µL of the mixture was transferred to chamber slides with a depth of 20 µm (Cytonix), and video microscopy (Olympus CKX41) using a 10x objective lens focused on the center of the chamber slide was captured up to 90 s at 60 frames/s. PM sperm count was measured by CASA every 30 s up to 90 s. The reduction in the percentage of the PM sperm at each time point was computed by normalizing the PM sperm count obtained after Ab-treatment to the PM sperm count obtained after treatment with sperm washing medium. Each experimental condition, except for 50 x $10^6$ PM sperm/mL, was evaluated in duplicates on each semen specimen, and the average from the two experiments was used in the analysis. At least 6 independent experiments were done with at least 6 unique semen samples.

*FIF-N vs FIF-Expi293:* This experiment was conducted using the starting concentration of 10 x $10^6$ PM sperm/mL. Briefly, 4.4 µL of purified motile sperm was added to 4.4 µL of Ab constructs in 0.2 mL PCR tubes, and mixed by gently pipetting up and down three times over 3 s. A timer was started immediately while 4.4 µL of the mixture was transferred to chamber slides with a depth of 20 µm (Cytonix), and video microscopy (Olympus CKX41) using a 10x objective lens focused on the center of the chamber slide was captured up to 90 s at 60 frames/s. PM sperm count was measured by CASA every 30 s up to 90 s. The reduction in the percentage of the PM sperm at each time point was computed by normalizing the PM sperm count obtained after Ab-treatment to the PM sperm count obtained after treatment with sperm washing medium. At least 3 independent experiments were done with at least 3 unique semen samples.

***4.2.10. CVM collection and processing***. CVM was collected as previously described. Briefly, undiluted CVM secretions, averaging 0.5 g per sample, were obtained from women of reproductive age, ranging

from 20 to 44 years old, by using a self-sampling menstrual collection device (Instead Softcup). Participants inserted the device into the vagina for at least 30 s, removed it, and placed it into a 50 mL centrifuge tube. Samples were centrifuged at 230 g for 5 min to collect the secretions. Samples were collected at various times throughout the menstrual cycle, and the cycle phase was estimated based on the last menstrual period date normalized to a 28-day cycle. Samples that were non-uniform in color or consistency were discarded. Donors stated they had not used vaginal products nor participated in unprotected intercourse within 3 days before donating. All samples had pH < 4.5.

***4.2.11. Fluorescent labeling of purified sperm***. Purified motile sperm were fluorescently labeled using Live/Dead Sperm Viability Kit (Invitrogen Molecular Probes), which stains live sperm with SYBR 14 dye, a membrane-permeant nucleic acid stain, and dead sperm with propidium iodide (PI), a membrane impermeant nucleic acid stain. Briefly, SYBR 14 stock solution was diluted 50-fold in sperm washing media. Next, 5 µL of diluted SYBR 14 and PI dye were added to 1 mL of purified sperm resulting in final SYBR 14 and PI concentration of 200 nM and 12 µM respectively. The sperm-dye solution was incubated for 10 min at 36ºC. Then, the solution was washed twice using the sperm washing medium to remove unbound fluorophores by centrifuging at 300 g for 10 min. Next, the labeled motile sperm pellet was resuspended in the sperm washing medium, and an aliquot was taken for determination of sperm count and motility using CASA.

***4.2.12. Multiple particle tracking studies***. To mimic the dilution and neutralization of CVM by alkaline seminal fluid, CVM was first diluted three-fold using sperm washing medium and titrated to pH 6.8-7.1 using small volumes of 3 N NaOH. The pH was confirmed using pH test strips. Next, 4 µL of Ab constructs or control (anti-RSV IgG1) was added to 60 µL of diluted and pH-adjusted CVM and mixed well in a CultureWellTM chamber slide (Invitrogen) followed by the addition of 4 µL of 1 x $10^6$ PM sperm/mL of fluorescently labeled sperm. Once mixed, sperm, Ab, and CVM were incubated for 5 min at RT. Then, translational motions of the sperm were recorded using an electron-multiplying charge-

coupled-device camera (Evolve 512; Photometrics, Tucson, AZ) mounted on an inverted epifluorescence microscope (AxioObserver D1; Zeiss) equipped with an Alpha Plan-Apo 20/0.4 objective, environmental (temperature and CO2) control chamber, and light-emitting diode (LED) light source (Lumencor Light Engine DAPI/GFP/543/623/690). 15 videos (512 × 512 pixels, 16-bit image depth) were captured for each Ab condition with MetaMorph imaging software (Molecular Devices) at a temporal resolution of 66.7 ms and spatial resolution of 50 nm (nominal pixel resolution, 0.78 μm/pixel) for 10 s. Next, the acquired videos were analyzed via a neural network tracking software [63] modified with standard sperm motility parameters (Table 2.1) to determine the percentage of PM sperm. At least 6 independent experiments were performed, each using a unique combination of CVM and semen specimens.

***4.2.13. In vivo surrogate efficacy studies***. On the test day, each sheep received a randomized unique Ab treatment and all sheep were dosed with the same semen mixture that was pooled from 3-5 donors. Briefly, placebo film or FIF-N-film (provided under blind to the animal facility) or saline were instilled into sheep's vagina and incubated for 30 mins, followed by thorough mixing using a vaginal dilator for 15 strokes. Next, 1 mL of pooled whole semen was pipetted into the sheep's vagina, followed by simulated intercourse with a vaginal dilator for 5 strokes. Two minutes after the introduction of semen, fluids from the sheep vagina were recovered and assessed for the PM sperm count in a hemocytometer (Bright-Line™ Hemacytometer) under a light microscope (Olympus IX71) using a 20x objective with Thorlabs camera. Each Ab condition was repeated one more time in the same group of sheep (n = 5) with at least 7 days interval in between experiments. Treatments and quantifications were performed in a blinded fashion.

***4.2.14. Statistical analysis***. All analyses were performed using GraphPad Prism 8 software. For multiple group comparisons, P values were calculated using a one-way ANOVA with Dunnett's multiple comparisons tests. To compare the percent reduction of PM sperm *in vitro* by IgG-N-Film vs FIF-N-Film, using whole semen as well as purified semen at the final concentration of 1 x $10^6$ PM sperm/mL, 5 x $10^6$

PM sperm/mL, and 25 x $10^6$ PM sperm/mL, one-tailed t-test was performed. Similarly, the comparison between control- and anti-sperm Ab-treated fluorescent PM sperm was performed using a one-tailed t-test. Lastly, to compare the percent reduction of PM sperm *in vivo* by Placebo-Film vs FIF-N-Film one-tailed t-test was performed. In all analyses, $\alpha$=0.05 for statistical significance. The values for N, P, and the specific statistical test performed for each experiment are included in the appropriate figure legends. All data are presented as the mean ± standard deviation.

## 4.3. Results

### *4.3.1. cGMP production of FIF in N. benthamiana*

Efficient agglutination requires ASA to bind a ubiquitous antigen that is highly expressed on the surface of human sperm. For these reasons, we chose to engineer a monoclonal antibody (mAb) targeting a unique glycoform of CD52 (hereafter referred to as CD52g) that was previously shown to be produced and secreted by epithelial cells lining the lumen of the epididymis, and present on sperm, white blood cells in semen, and the epithelium of the vas deferens and seminal vesicles [19,24]. The CD52g glycan-based antigen appears to be universally present on all human sperm while absent in most other tissues [19]. Using a Fab-domain isolated from a healthy but immune infertile woman [8,52], we designed a 6 Fab antibody construct, cloned the sequences into the magnICON® vector system, and transfected *Nicotiana* benthamiana using agrobacterial-infiltration process [122–124]. This system allows for rapid and scalable production of full-length mAbs in two weeks; the same system has been used to produce various cGMP-compliant mAbs for clinical studies [125]. To generate mAbs with homogeneous mammalian glycans, we used a transgenic strain, Nb7KOΔXylT/FucT of *N. benthamiana* which yields mAb with predominantly G0 N-glycans. Without optimization, the production yields of the *Nicotiana*-produced FIF (FIF-N) post-protein A chromatography were approximately 29 mg/kg of plant tissue (Figure 4.1B). The mAbs were further purified using ceramic hydroxyapatite chromatography prior to further biophysical characterization. SDS-PAGE analysis demonstrated the correct assembly of FIF-N at its theoretical molecular weight, ~350 kDa (Figure 4.1C). Purified FIF contained >99% monomeric form

as determined by high performance liquid size exclusion chromatography analysis (Figure 4.1D and Figure 4.1E). FIF-N demonstrated excellent stability, with no appreciable aggregation or degradation upon storage at room temperature for 3 weeks and freezing at 70°C (Figure 4.1E and F).

### *4.3.2 Production of FIF-N-Film*

Polyvinyl alcohol (PVA) is a polymer routinely used in biomedical applications. Low molecular weight PVA is widely used in female reproductive health products suitable for intravaginal administration, with no appreciable vaginal toxicity or irritation. Similar to prior work in formulating a vaginal film releasing both an anti-HIV (VRC01) and anti-HSV (HSV8) mAb [126] evaluated in a Phase 1 trial, we prepared water-soluble PVA films comprised of PVA 8-88 (67 kDa) together with 10 mg of FIF-N, using an aqueous casting method. As a control, an IgG-N-Film with 20 mg of anti-CD52g IgG was also prepared. Both films were fabricated to 2”x2” in dimensions, clear in visual appearance with few bubbles present, homogeneous, and resistant to tear (Figure 4.1G). Both films showed no significant levels of endotoxin, and no detectable bioburden (CFU/mL), indicating efficient and aseptic removal of potential contaminants (Table 4.1).

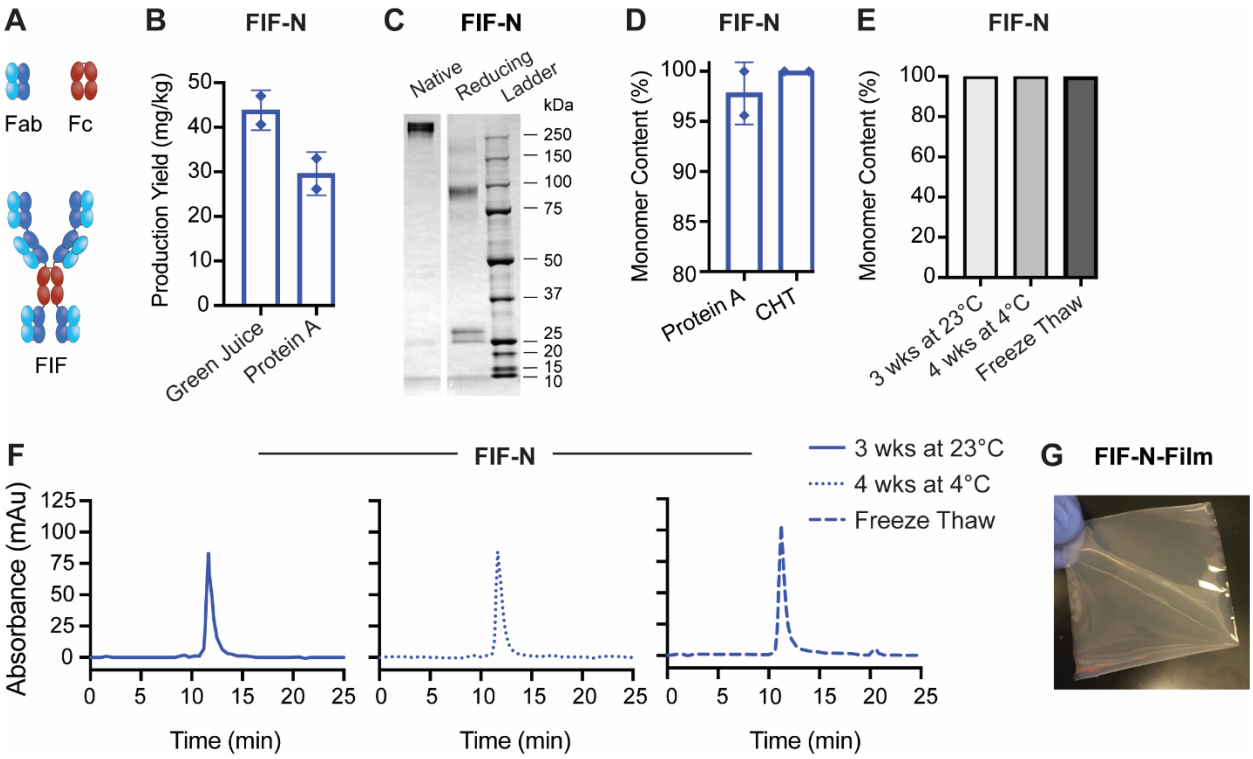


**Figure 4.1: Production of FIF-N-Film.** (A) Schematic diagrams of anti-sperm Fab-IgG-Fab (FIF). The additional Fab is linked to the N-terminal and C-terminal of parent IgG using flexible glycine-serine linkers to assemble FIF. (B) The production yield of IgG and FIF from *Nicotiana* benthamiana expression (Green Juice) followed by purification using protein A chromatography. Data were obtained from 2 independent transfections. (C) SDS-PAGE analysis of FIF-N in native (non-reducing) and reducing conditions. (D) Demonstration of the homogeneity of FIF-N after protein A and ceramic hydroxyapatite (CHT) chromatography using high performance liquid size exclusion chromatography (HPLC-SEC) analysis. (E) Demonstration of the homogeneity of the FIF-N under different storage conditions using size exclusion chromatography (SEC) analysis. Y-axis indicates the total percentage of Abs representing their theoretical molecular weights. (F) SEC curves of the FIF-N stored under different conditions. (G) Image of water-soluble polyvinyl alcohol (PVA) film comprising of *Nicotiana*-produced FIF Ab. Lines indicate arithmetic mean values and standard deviation.

**Table 4.1**: Safety parameter results for IgG-N-Film and FIF-N-Film.

| Test Method | IgG-N-Film | FIF-N-Film |
|---|---|---|
| Endotoxin | Film1: <0.958 | Film1: 1.505 |
| | Film3: <26.1 | Film3: <0.953 |
| Bioburden | Film1: 0 | Film1: 2 |
| | Film3: <1 | Film3: 0 |

### *4.3.3. FIF-N-Film possesses superior agglutination potency*

We next assessed the sperm-agglutinating potencies of dissolved IgG-N and FIF-N films. We focused on assessing the reduction in progressive motile (PM) fraction of sperm, since it is the PM sperm

fractions that reach the uterus and penetrate the zona pellucida to fertilize the egg. We first assessed the agglutination potencies of FIF-N-Film vs. IgG-N-Film using a sperm escape assay with purified sperm. The sperm escape assay uses Computer Assisted Sperm Analysis (CASA) to quantify the number of PM sperm that escapes agglutination over 5 mins when mixed with specific mAbs at different mAb and sperm concentrations. We elected to first assess agglutination at a low concentration of 5 million PM sperm/mL, the minimal PM sperm concentration in semen associated with fertility, which limits sperm collision frequency and making it more challenging to achieve rapid and complete agglutination. FIF-N-Film exhibited at least 16-fold greater agglutination potency than IgG-N-Film, defined here as the minimal mAb concentration at which PM sperm are reduced by >98%. The minimum concentration of IgG-N-Film needed was ~6.25 μg/mL, whereas just 0.39 μg/mL of FIF-N-Film was sufficient (Figure 4.2A and B).

To confirm efficient agglutination also occur with native semen, we further assessed the agglutination potency of the FIF-N-Film vs IgG-N-Film using whole semen. FIF-N-Film again exhibited at least 10-fold greater agglutination potency than IgG-N-Film (Figure 4.2C and D). Both FIF-N-Film and IgG-N-Film required ~16-fold more mAb to achieve >98% agglutination of PM sperm in whole semen compared to in purified motile sperm, likely due to CD52g present on other components in whole semen, including non-PM sperm, seminal leukocytes, as well as on exosomes from the epithelium of the vas deferens and seminal plasma [85].

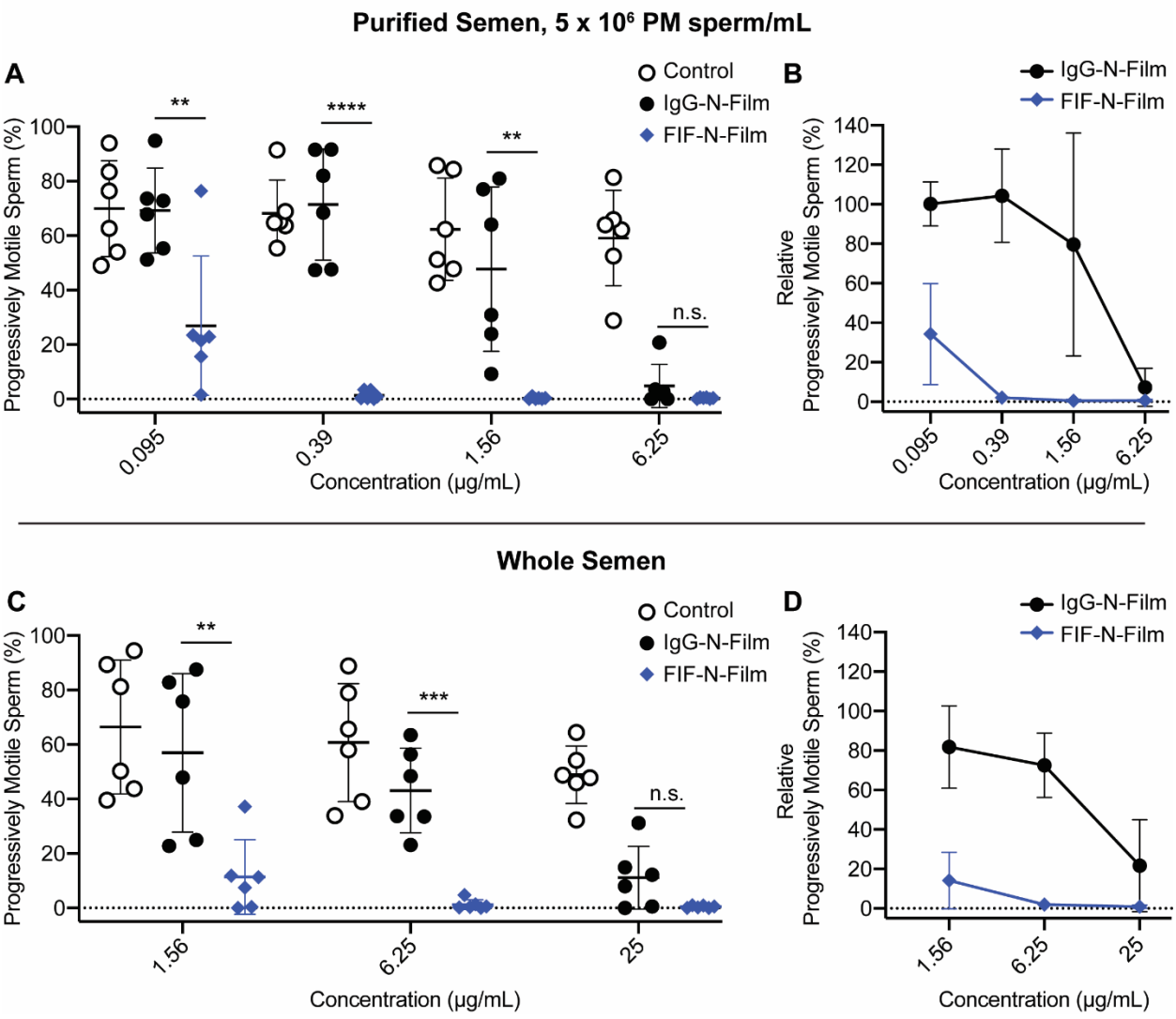


**Figure 4.2: FIF-N-Film possesses markedly greater agglutination potency than IgG-N-Film.** (A) Sperm agglutination potency of the IgG-N-Film and FIF-N-Film determined by quantifying PM sperm that escaped agglutination after Ab-treatment compared to pre-treatment condition using CASA. Purified sperm at the final concentration of 5 x $10^6$ PM sperm/mL was used. (B) Sperm agglutination potency of the Abs normalized to the media control. (C) Further assessment of sperm-agglutination potency of the IgG-N-Film and FIF-N-Film using whole semen. (D) Sperm-agglutination potency of the IgG-N-Film and FIF-N-Film against whole semen normalized to the sperm washing media control. Data were obtained from N=6 independent experiments using 6 unique semen specimens. Each experiment was performed in duplicates and averaged. P values were calculated using a one-way ANOVA with Dunnett's multiple comparisons test. *P < 0.05, **P < 0.01, ***P < 0.001 and ****P < 0.0001. Data represent mean ± standard deviation.

### *4.3.4. FIF-N-Film exhibits faster sperm agglutination kinetics*

For effective vaginal immunocontraception based on limiting sperm motility in mucus, mAbs must agglutinate/immobilize sperm before they reach the upper reproductive tract; thus, rapid reduction of

PM sperm is likely an important factor in contraceptive efficacy. Thus, we next quantified the kinetics of sperm agglutination by quantifying the number of PM motile sperm present at 30 s intervals following treatment of purified sperm (5 million PM sperm/mL) with IgG-N-Film and FIF-N-Film. IgG-N-Film reduced PM sperm by ≥90% within 90 s in 5 of 6 semen samples at 6.25 μg/mL, but failed to do so in 6 of 6 samples at 1.56 μg/mL (Figure 4.3A). In contrast, FIF-N-Film agglutinated ≥90% of PM sperm within 30 s in all cases at both 6.25 μg/mL and 1.56 μg/mL concentrations (Figure 4.3A). Even at 0.39 μg/mL, FIF-N-Film still agglutinated ≥90% of PM sperm within 90 s in 5 of 6 samples. Notably, the agglutination kinetics of FIF-N-Film was markedly faster and more complete than the parent IgG at all mAb concentrations and across all time points (Figure 4.3B).

Similar to the sperm escape assay, we also assessed agglutination kinetics of FIF-N-Film vs. IgG-N-Film using whole semen. Again, a higher concentration of FIF-N-Film and IgG-N-Film was required to obtain comparable agglutination kinetics vs. purified sperm. Nonetheless, FIF-N-Film exhibited markedly faster and more complete sperm agglutination kinetics than IgG-N-Film at all mAb concentrations and all time points in whole semen (Figure 4.3D). At 25 μg/mL, FIF-N-Film agglutinated ≥90% of PM sperm within 30 s in 6 of 6 whole semen samples while IgG-N-Film agglutinated ≥90% of PM sperm in 90 s in only 2 of 6 specimens at the same concentration (Figure 4.3C). Lower sperm concentration (as found in semen from oligospermia, sub-fertile individuals) may limit sperm agglutination due to reduced likelihood of a sperm-sperm collision, whereas higher sperm amounts may saturate the agglutination potential. We thus further assessed whether FIF-N-Film can effectively reduce PM sperm at 1 million PM sperm/mL and 25 million PM sperm/mL. FIF-N-Film maintained similar superior agglutination kinetics over IgG-N-Film across both lower and higher sperm concentrations (Figure 4.4). These results underscore the increased potency for FIF-N-Film compared to the IgG-N-Film across diverse conditions.

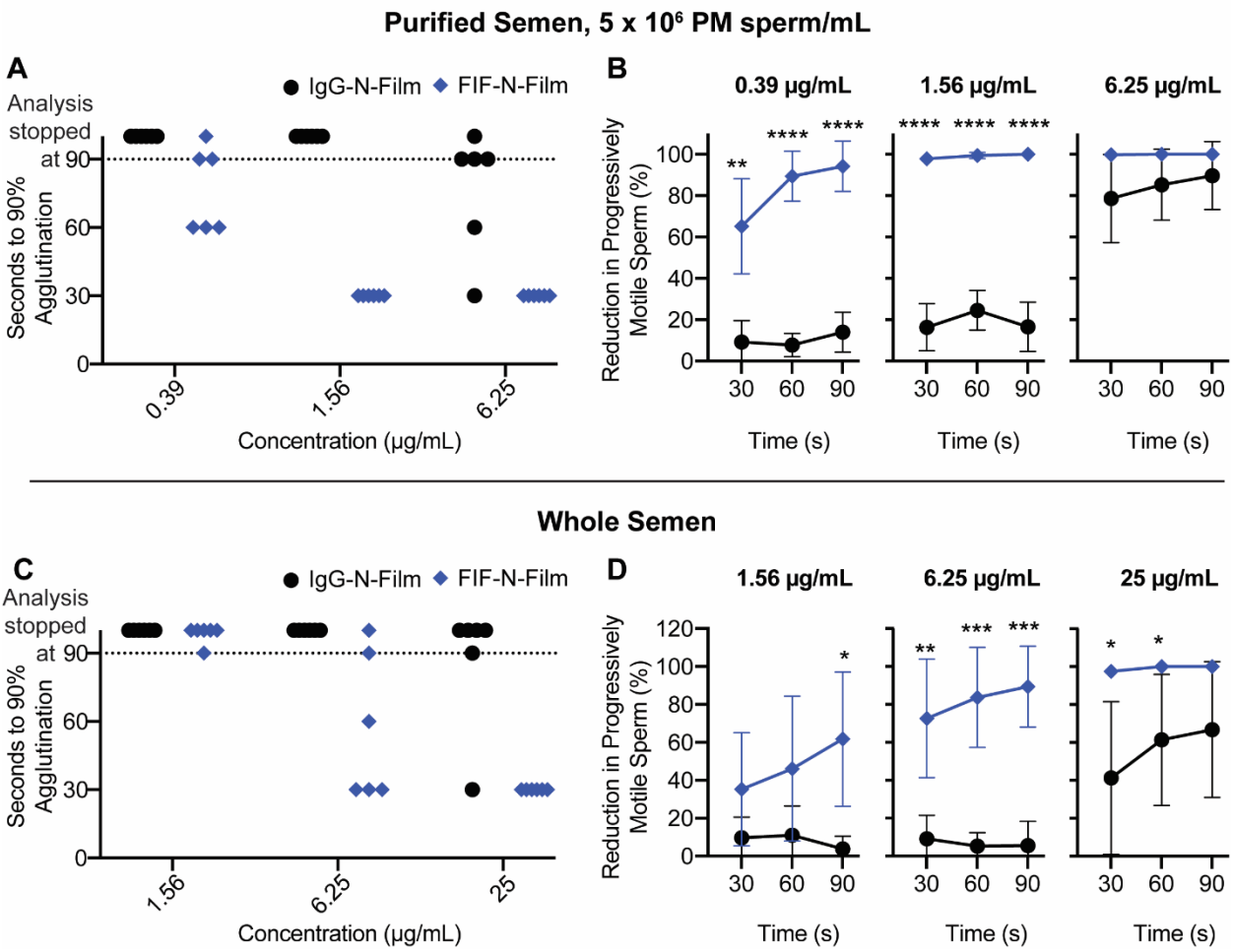


**Figure 4.3: FIF-N-Film exhibits markedly faster agglutination kinetics than IgG-N-Film.** (A) Sperm agglutination kinetics of IgG-N-Film and FIF-N-Film measured by quantifying the time required to achieve 90% agglutination of PM sperm compared to sperm washing media control. (B) The rate of sperm agglutination determined by measuring the reduction in the percentage of PM sperm at three timepoints after Ab-treatment compared to sperm washing media control. Purified sperm at the final concentration of 5 x $10^6$ PM sperm/mL was used. (C) Sperm agglutination kinetics and (D) The rate of sperm agglutination assessed for IgG-N-Film and FIF-N-Film using whole semen. Data were obtained from N=6 independent experiments using 6 unique semen specimens. Each experiment was performed in duplicates and averaged. P values were calculated using a one-tailed t-test. *P < 0.05, **P < 0.01, ***P < 0.001 and ****P < 0.0001. Data represent mean ± standard deviation.

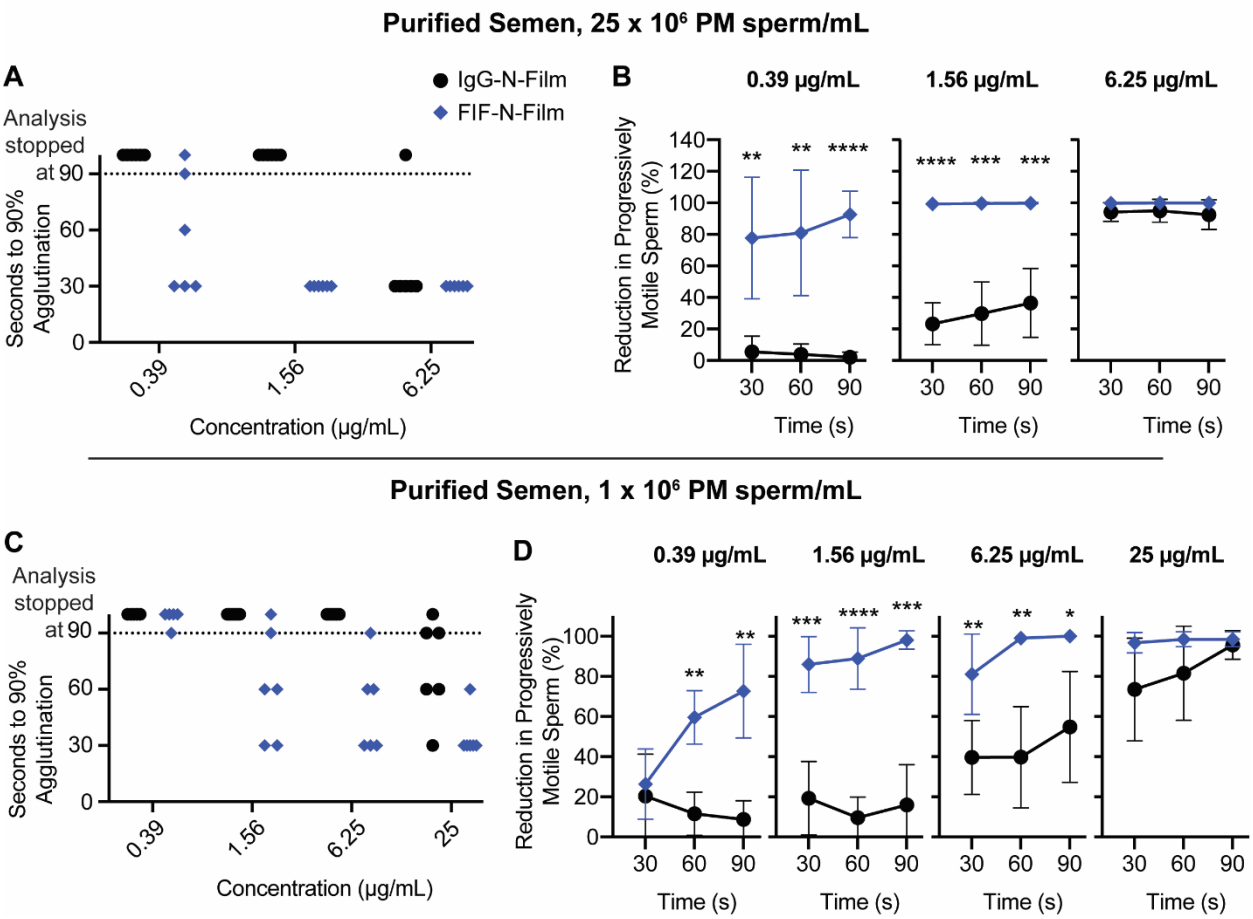


**Figure 4.4: FIF-N-Film demonstrates faster agglutination kinetics than IgG-N-Film at both low and high sperm concentration.** (A) Sperm agglutination kinetics of the IgG-N-Film and FIF-N-Film measured by quantifying time required to achieve 90% agglutination of PM sperm compared to media control using a final concentration of 25 x $10^6$ PM sperm/mL. (B) The rate of sperm agglutination of the IgG-N-Film and FIF-N-Film measured by measuring the reduction in the percentage of PM sperm at three different time points after Ab-treatment compared to negative control using a final concentration of 25 x $10^6$ PM sperm/mL. (C) Sperm agglutination kinetics and (D) The rate of sperm agglutination of the IgG-N-Film and FIF-N-Film measured using a final concentration of 1 x $10^6$ PM sperm/mL. Data were obtained from N=6 independent experiments with using 6 different semen donors. The experiment involving 1 x $10^6$ PM sperm/mL was performed in duplicates and averaged. P values were calculated using a one-tailed t-test. *P < 0.05, **P < 0.01, ***P < 0.001 and ****P < 0.0001. Data represent mean ± standard deviation.

### *4.3.5. FIF-N and FIF-Expi293 exhibits equivalent agglutination*

To confirm that the production of FIF in *N. benthamiana* and their subsequent formulation into PVA films did not reduce their agglutination activity, we further compared the sperm agglutination potencies of FIF-N, before and after film formulation, to Expi293-produced FIF. At 0.39 µg/mL, FIF-Expi293, FIF-N, and FIF-N from four dissolved FIF-N-Films all demonstrated comparable sperm

agglutination potencies (Figure 4.5A). Similarly, FIF-Expi293, FIF-N, and FIF-N from dissolved FIF-N-Films all agglutinated all sperm within 60 s in 3 of 3 samples at 1.56 µg/mL (Figure 4.5B). The agglutination kinetics profile of Expi293- and *Nicotiana*- produced FIF, pre- and post- film formulation, were also virtually identical (Figure 4.5C). These results underscore that neither production of FIF in *Nicotiana* nor formulation of FIF-N into films had any significant impact on the actual agglutination potencies of FIF.

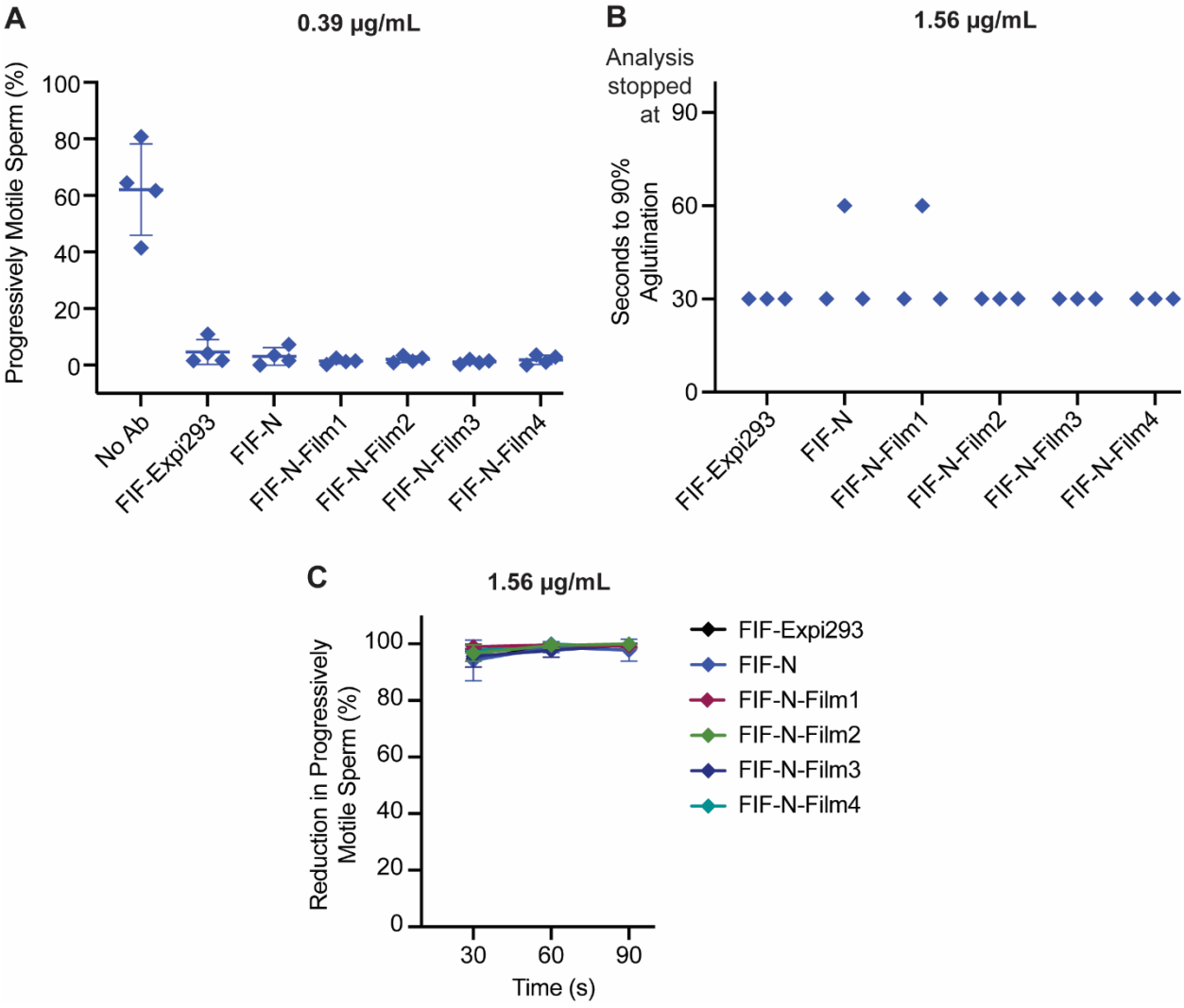


**Figure 4.5: Nicotiana-produced FIF exhibit agglutination comparable to Expi293-produced FIF.** (A) Sperm agglutination potency of the indicated mAbs determined by quantifying PM sperm that escaped agglutination after Ab-treatment compared to pre-treatment condition using CASA. FIF-N-Film1 and FIF-N-Film2 are the film duplicates from one batch whereas FIF-N-Film3 and FIF-N-Film4 are the duplicates

from a separate batch. (B) Sperm agglutination kinetics of the indicated mAbs measured by quantifying the time required to achieve 90% agglutination of PM sperm compared to media control. (C) The rate of sperm agglutination of the indicated mAbs measured by measuring the reduction in the percentage of PM sperm at three different time points after Ab-treatment compared to the negative control. Purified sperm at the final concentration of 5 x $10^6$ PM sperm/mL was used for all experiments. A significant difference was not observed between the agglutination potency and kinetics of Expi293- and *Nicotiana*- produced mAbs upon one-way ANOVA with Dunnett's multiple comparisons tests. Agglutination potency data were obtained from N=4 independent experiments using 3 unique semen specimens. Agglutination kinetics data were obtained from N=3 independent experiments with using 3 unique semen specimens. Data represent mean ± standard deviation.

### *4.3.6. FIF-N-Film traps individual spermatozoa in vaginal mucus*

Previous work has shown that IgG and IgM Abs can retard the active motility of individual spermatozoa in mucus despite continued vigorous beating action of the sperm flagellum; clinically, this is referred to as the "shaking phenomenon" [2]. This muco-trapping function is similar to recent observations with Herpes Simplex Virus (HSV) [10,11], whereby multiple HSV-bound IgGs formed polyvalent adhesive interactions between their Fc domains and mucin fibers in cervicovaginal mucus (CVM). Anti-HSV IgG-mediated effective trapping of individual viral particles in CVM, and blocked vaginal Herpes transmission in mice [10]. We thus assessed whether FIF-N-Film can reduce progressive motility of fluorescently labeled spermatozoa in the relatively thin (low viscosity) CVM using multiple particle tracking. FIF-N-Film reduced progressively motile spermatozoa to the same extent as the IgG-N-Film, indicating that the addition of Fabs to both the N- and C-terminus of the IgG did not interfere with Fc-mucin crosslinking (Figure 4.6).

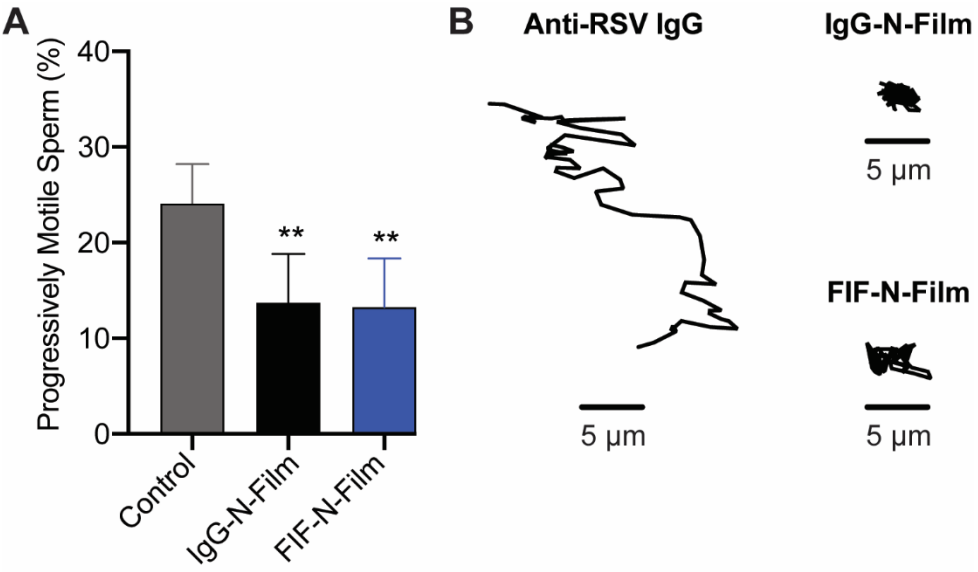


**Figure 4.6: FIF-N-Film maintains the trapping potency of IgG-N-Film.** (A) The trapping potency of the indicated Abs (25 µg/mL) measured by quantifying fluorescently labeled PM sperm in Ab-treated CVM using neural network tracker analysis software. Purified sperm at the final concentration of 5.8 x 104 PM sperm/mL was used. Data were obtained from N=6 independent experiments with 6 unique combinations of semen and CVM specimens. P values were calculated using a one-tailed t-test. *P < 0.05 and **P < 0.01. Data represent mean ± standard deviation. (B) Representative 4 s traces of sperm within one standard error mean of average path velocity at a timescale τ of 1 s in CVM treated with control (anti-RSV IgG), IgG-N-Film, and FIF-N-Film.

### *4.3.7. FIF-N-Film rapidly eliminates PM sperm in sheep vagina*

Since the unique glycoform of CD52g is only found in human and chimpanzee sperm [26], there is no practical animal model to perform mating-based contraceptive efficacy studies. Instead, we designed a sheep study that parallels the human post-coital test (PCT) [90–94], which assesses the reduction of PM sperm in the female reproductive tract (FRT) given that PM sperm are required for fertilization. Clinical PCT studies have proven to be highly predictive of contraceptive efficacy in clinical trials [37,94–98,127]. The sheep vagina is physiologically and anatomically very similar to the human vagina [99,100], making it the gold standard for assessing vaginal products. We instilled either Placebo-Film (no mAb) or FIF-N-Film into the sheep vagina, allowed 30 mins for the film to dissolve, followed by brief simulated intercourse with a vaginal dilator (15 strokes), vaginal instillation of fresh whole human semen, brief simulated intercourse (5 strokes), and finally, recovery of the semen mixture from the sheep vagina 2 mins post semen instillation for immediate visual assessment of sperm motility via quantifying

progressively motile sperm. Despite this exceptionally stringent criteria, FIF-N-Film reduced 100% of PM sperm in all four of the animals studied over two independent studies, with no observable PM sperm (Figure 4.7; $p<0.0001$). In contrast, there were high PM sperm fractions recovered from all four sheep receiving the placebo film, with a few to several hundred PM sperm counts in the microscopy field, comparable to those from sheep treated with saline control.

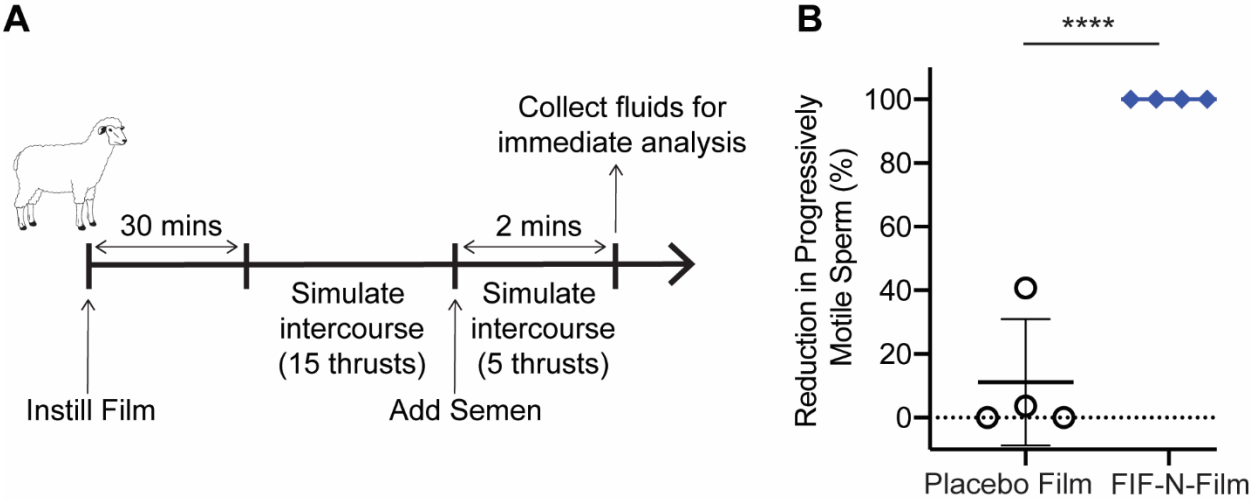


**Figure 4.7: FIF-N-Film exhibits complete agglutination in surrogate sheep studies**. (A) Schematic of the study design. (B) The potency of Placebo-Film and FIF-N-Film measured by quantifying PM sperm in sheep's vaginal fluid after Ab- or Placebo- treatment compared to saline-treatment. Treatment administration was blinded, and quantifications were performed using a neural network tracker coded with sperm motility parameters. Data were obtained from N=2 independent experiments. P values were calculated using a one-tailed t-test. *P < 0.05, **P < 0.01, ***P < 0.001 and ****P < 0.0001. Data represent mean ± standard deviation.

### 4.4. Discussion

The sperm agglutination potency of FIF-N-Film in sheep reported here is likely attributed in large part to the additional Fab arms of the FIF molecule. By delivering FIF directly to where it is needed i.e. the vagina, the fraction of FIF available to bind sperm is maximized, thereby enabling complete agglutination and immobilization of progressively motile sperm within just two minutes of semen exposure. In contrast, only a tiny fraction of systemically delivered mAb will be available to bind sperm because of the large blood volume (~5L), distribution to non-target tissues, natural catabolic degradation,

and finally limited and delayed distribution into the FRT, including the vagina. As a result, markedly lower total amount of FIF is needed with vaginal delivery to achieve contraceptive levels in the FRT compared to delivering the same mAb systemically. An added advantage of vaginal delivery is that the entire dose of FIF delivered is quickly available, without any delays in reaching Cmax in the vagina from delayed extravasation from the systemic circulation. Vaginal IgG has a half-life of ~9 hrs [77]; thus, even after 24 hrs, there will likely be sufficient quantities of FIF from the original 10 mg film to maintain effective sperm agglutination, given *in vitro* measurements that showed highly effective sperm agglutination even at FIF concentrations as low as ~390 ng/mL.

Decades ago, the high costs of mAb production and emphasis on systemic administration critically limited the feasibility of passive immunization with ASA as a strategy for non-hormonal contraception. However, the cost of mAb production has declined over the years due to advances in CHO cell production. It reportedly costs between $95–$200/gram to produce currently marketed mAbs [114]. If a CHO facility uses a continuous bioprocess system integrated with single-use bioreactors it has been predicted to reduce mAb manufacturing costs per gram to less than $15 per gram, or $3 for an average 200 mg dose of most systemic mAbs. Based on 10 mg of FIF per film that resulted in exceptional sperm agglutination potency in the sheep vagina, the costs to produce the needed amount of FIF per film in CHO is likely much less than $1. Since FIF exhibits considerable agglutination potencies down to 390 ng/mL, additional dose optimization may further reduce the amount of FIF needed per film, thus further decreasing costs and improving scale.

mAbs based topical contraceptives, such as the FIF-N-film reported here, are likely to be safe due to their binding specificity, particularly when targeted to epitopes present primarily on sperm. Vaginally dosed mAbs are poorly absorbed into the systemic circulation [73,101], and the vaginal immune response is limited even when vaginally vaccinating with the aid of highly immunostimulatory adjuvants [74]. Vaginal secretions naturally contain high levels of endogenous IgG (i.e. 1-2 mg/mL [128,129], making it unlikely that vaginal delivery of FIF, which is comprised of fully human Fabs and Fc, would trigger inflammation, sensitization, or other local toxicities. Finally, PVA (67 kDa) film, which is widely used in

pharmaceutical applications as well as in contraceptive products such as VCF, has been found to be safe and non-immunogenic to use. Altogether, these features make PVA film delivering mAb vaginally for immunocontraception likely to be exceptionally safe.

Typically, only ~1% of the ejaculated sperm enter the cervix, even fewer reaching the uterus, and only dozens of sperm (out of the ~200 million in the ejaculate) reach the neighborhood of the egg [102]. Accordingly, poor sperm motility in mid-cycle cervical mucus and low total sperm count are considered good correlates to low conception rates. Human semen averages between 45-65 million sperm/mL [66], 15 million sperm/mL marks the lowest 5th percentile in men with proven fertility [59], and <5 million sperm/mL is often considered severe oligospermia that correlates with very low fertility37. These observations suggest a marked reduction of progressive sperm motility, even if incomplete (e.g. 10-fold reduction in PM sperm fractions), may likely provide substantial contraceptive efficacy. This expectation is also consistent with the observations that even under ideal circumstances, with unprotected intercourse on the cycle day of maximum fertility, the odds of conceiving are only about ~10% [72]. This indicates that only a small (i.e. limiting) number of motile sperm would reach the egg per intercourse; thus, reducing progressive sperm motility in the vagina and cervical canal should proportionally reduce the likelihood of conceiving. These findings, together with the contraceptive success with topical ASA against rabbit sperm [20], suggest arresting progressive sperm motility in mucus using mAb (which can reduce PM sperm by >99.9%) should provide an effective form of contraception.

One potentially important mechanism of vaginal HIV transmission is cell-associated HIV transmission, whereby HIV in immune cells of HIV+ semen facilitates direct cell-to-cell spread of the virus to target cells in the female reproductive tract [130]. Cell-associated HIV transmission may be more efficient than cell-free HIV transmission, since intracellular viruses are not exposed to the same host restriction factors and innate immune molecules the FRT. Since CD52g is adsorbed on the surface of immune cells originating from the male reproductive tract, it is possible that FIF can also agglutinate such immune cells and limit their access to target cells in the FRT, thereby limiting cell-associated vaginal HIV transmission. Combining contraception with the prevention of sexually transmitted infections is also

an attractive public health strategy. With further reduction in manufacturing costs and greater availability of multi-metric ton manufacturing capacity for mAbs, it may be possible to create a cost-effective, on-demand multi-purpose technology product based on a cocktail of antiviral and anti-sperm mAbs that can simultaneously afford potent contraception and effective protection against STI transmission.

Polymeric vaginal films are advantageous for delivering active pharmaceutical ingredients (API) and preferred over other delivery methods due to enhanced bio-adhesive properties, ease of use, compact size and negligible vaginal leakage [131–135]. Currently, multiple vaginal films with anti-retroviral microbicides are under development and evaluation [136–139]. In a recent Phase I study, a vaginal film formulated with the microbicide drug candidate, dapivirine, was found to be safe and acceptable with uniform vaginal distribution while exhibiting considerable efficacy against ex vivo HIV-1 challenge model [133]. Similarly, vaginal films could be formulated with contraceptive mAbs and microbicides or anti-fungal agents to achieve multipurpose prevention. Finally, it may be possible to formulate vaginal films to provide sustained release in the vagina spanning days to weeks [140,141].

There are a number of limitations to our current study. First, we did not directly demonstrate efficacy by preventing pregnancies. We are unable to do so due to the unique antigen (CD52g) that our antibody targets: prior work has shown that, besides humans, only chimpanzees possess CD52g [26], and it is not possible to conduct chimpanzee studies in the U.S. Instead, for our *in vivo* proof-of-concept study, we were forced to adopt a sheep model designed to closely mimic the human post-coital test that is routinely used to assess the efficacy of sperm-targeted contraceptives in early phase clinical studies. Fortunately, the human cost-coital test has shown to correlate well with eventual efficacy in preventing pregnancies. Second, the precise dose of antibodies needed to ensure highly effective sperm agglutination remains not well understood. In the current study, to ensure success, we incorporated a relatively large dose of mAb (10 mg) into the vaginal film formulation. Although we expect this dose of mAb to be commercially viable (~$1/film based on bulk manufacturing costs of mAb at $100/g), it is likely we can achieve effective agglutination of sperm with even lower quantities of mAb released from the film, which would translate to even lower costs. We are also pursuing the development of other vaginal delivery

formats, such as an intravaginal ring that can afford sustained release of our mAbs across the potential fertility window, which may further reduce the dose needed.

# CHAPTER 5: CONCLUSIONS AND FUTURE DIRECTIONS

In this dissertation, I engineered a panel of multivalent sperm-binding IgGs possessing 4-10 Fab per molecule and selected appropriate multivalent IgG for the development of the intravaginal film to provide on-demand non-hormonal contraception. All multivalent IgGs are easy to produce with yields similar to the conventional IgG. Multivalent IgGs are highly stable and homogeneous at 4ºC, room temperature, as well as the physiological temperature of ≥37ºC. All multivalent IgGs, possess markedly superior agglutination potency and faster agglutination kinetics than the parent IgG. The degree of multivalency seems to be the determining factor for the increase in agglutination potency and kinetics because HM-IgGs possessing 6-10 Fabs exhibited stronger agglutination activity than the tetravalent IgGs meanwhile 10Fab IgG (FFIFF) emerged as the strongest agglutinator amongst all HM-IgG constructs. Additionally, the addition of Fabs at both N- and C-terminus of the IgG does not affect the Fc-mediated muco-trapping potency as all multivalent IgGs exhibited similar muco-trapping potency as the parent IgG. The multivalent IgGs are amenable to large-scale production and purification in the cGMP-compliant system, and maintain their exceptional potency upon formulation into the water-soluble vaginal film. Lastly, the immediate sperm-agglutination (>95%) by mere 33 μg of 10Fab IgG or a 6Fab IgG (FIF)-film in the sheep's vagina substantiates the benefit of local delivery of multivalent mAbs for effective contraception.

Overall, I demonstrated the utility of multivalent sperm-binding monoclonal antibodies as topical biologics to achieve effective non-hormonal contraception in women. Additionally, the findings from the ongoing clinical trial assessing the efficacy of parent anti-CD52g IgG (ClinicalTrials.gov Identifier: NCT04731818) in surgically sterilized women via human post-coital test could demonstrate the practicality of mAb-based contraception. However, to advance our engineered multivalent anti-sperm

antibodies into clinical development, additional stability, safety and potency studies must be performed. FFIFF was recently lyophilized and formulated into the intravaginal ring (IVR) format to enable month-long contraception in women. The *in vitro* mAb release studies showed that the FFIFF was stably released from IVR for 30 days at 37°C. However, IVR mAb-release studies using human cervicovaginal and cervical mucus *in vitro* and/or non-human primate model could be performed to properly determine the stability and release kinetics of FFIFF. In ongoing pilot sheep studies, FFIFF was sufficiently stable when released from the IVR over 21 days to ensure complete sperm agglutination in the sheep across the entire duration. To confirm the observed stability and potency of FFIFF-IVR at physiological temperature over 21 days, the sheep-IVR studies is currently being repeated with an additional objective to assess the local and systemic toxicity of FFIFF in sheep. FIF and FFIFF are also currently being tested for safety *in vitro* using a human vaginal epithelial model. While additional studies still remain to be performed prior to the advancement of multivalent IgGs to the human clinical trial, the preliminary sheep-IVR studies point to a promising potential for multivalent ASA-based contraception.

The potential for ASA-based contraception could be further strengthened by increasing the binding affinity of the CD52g-binding Fab domain via affinity maturation, facilitating effective sperm trapping and agglutination at even lower ASA concentrations. The contraceptive potency of multivalent ASAs could also be enhanced by engineering bispecific multivalent mAb that binds to two different sperm-specific antigens, preferably that are critical to sperm's fertilization potential. Bispecific multivalent ASAs targeting CD52g and a sperm surface protein, EPPIN, are currently being engineered using the OrthoMab platform to facilitate both sperm-agglutination and the inhibition of capacitation or hyperactivation to prevent fertilization in women. The bispecific mAb platform could also be adopted to develop antibody-based multipurpose prevention technology (MPT) that not only acts as an effective contraceptive method but also prevents from sexually transmitted infections. Currently, bispecific FIF possessing Fab domains against CD52g and CD4-binding-site (CD4bs) is being engineered as the MPT product for contraception and the protection against HIV-1. Additionally, the multivalent IgG platform could be readily employed to develop potent mAbs against different pathogens where agglutination is the

main effector function. Currently, the multivalent IgG platform is being employed to generate a panel of multivalent IgGs targeting lipooligosaccharides of Neisseria gonorrhoeae and CD4bs of HIV for the development of potent anti-gonorrhea and anti-HIV therapeutics.

Lastly, due to the presence of single Fc region in the multivalent IgGs, the multivalent mAbs could activate effector functions such as complement-dependent cytotoxicity and antibody-dependent cellular cytotoxicity, which could be advantageous for anti-bacterial and anti-viral therapeutics but unfavorable for anti-sperm antibodies. Thus, depending on the pathogen of interest, the effector function of the multivalent mAbs could be easily modified by introducing either effector-enhancing or effector attenuating mutations in the Fc region resulting in the development of potent, yet versatile therapeutics.

## REFERENCES


[1] M.J. Baskin, Temporary sterilization by the injection of human spermatozoa. A preliminary report, Am. J. Obstet. Gynecol. 24 (1932) 892–97.

[2] G.N. Clarke, Induction of the Shaking Phenomenon by IgA Class Antispermatozoal Antibodies From Serum, Am. J. Reprod. Immunol. Microbiol. 9 (1985) 12–14. https://doi.org/10.1111/j.1600-0897.1985.tb00333.x.

[3] S. Isojima, K. Tsuchiya, K. Koyama, C. Tanaka, O. Naka, H. Adachi, Further studies on sperm-immobilizing antibody found in sera of unexplained cases of sterility in women, Am. J. Obstet. Gynecol. 112 (1972) 199–207. https://doi.org/10.1016/0002-9378(72)90116-0.

[4] A.B. Diekman, E.J. Norton, V.A. Westbrook, K.L. Klotz, S. Naaby-Hansen, J.C. Herr, Anti-Sperm Antibodies from Infertile Patients and their Cognate Sperm Antigens : A Review. Identity Between SAGA-1 , the H6-3C4 Antigen , Am. J. Reprod. Immunol. 43 (2000) 134–143.

[5] A.A. Cantuária, Sperm Immobilizing Antibodies in the Serum and Cervicovaginal Secretions of Infertile and Normal Women, BJOG An Int. J. Obstet. Gynaecol. 84 (1977) 865–868. https://doi.org/10.1111/j.1471-0528.1977.tb12510.x.

[6] P.B. Marshburn, W.H. Kutteh, The role of antisperm antibodies in infertility, Fertil. Steril. 61 (1994) 799–811. https://doi.org/10.1016/S0015-0282(16)56687-4.

[7] A.C. Menge, N.E. Medley, C.M. Mangione, J.W. Dietrich, The incidence and influence of antisperm antibodies in infertile human couples on sperm-cervical mucus interactions and subsequent fertility, Fertil. Steril. 38 (1982) 439–446. https://doi.org/10.1016/S0015-0282(16)46578-7.

[8] S. Isojima, K. Kameda, Y. Tsuji, M. Shigeta, Y. Ikeda, K. Koyama, Establishment and characterization of a human hybridoma secreting monoclonal antibody with high titers of sperm immobilizing and agglutinating activities against human seminal plasma, J. Reprod. Immunol. 10 (1987) 67–78. https://doi.org/10.1016/0165-0378(87)90051-9.

[9] T. Hjort, H. Meinertz, Anti-sperm antibodies and immune subfertility, Hum. Reprod. 3 (1988) 59–62. https://doi.org/10.1093/oxfordjournals.humrep.a136652.

[10] Y.Y. Wang, A. Kannan, K.L. Nunn, M.A. Murphy, D.B. Subramani, T. Moench, R. Cone, S.K. Lai, IgG in cervicovaginal mucus traps HSV and prevents vaginal Herpes infections, Mucosal Immunol. 7 (2014) 1036–1044. https://doi.org/10.1038/mi.2013.120.

[11] H.A. Schroeder, K.L. Nunn, A. Schaefer, C.E. Henry, F. Lam, M.H. Pauly, K.J. Whaley, L. Zeitlin, M.S. Humphrys, J. Ravel, S.K. Lai, Herpes simplex virus-binding IgG traps HSV in human cervicovaginal mucus across the menstrual cycle and diverse vaginal microbial composition, Mucosal Immunol. 11 (2018) 1477–1486. https://doi.org/10.1038/s41385-018-0054-z.

[12] C.E. Henry, Y.Y. Wang, Q. Yang, T. Hoang, S. Chattopadhyay, T. Hoen, L.M. Ensign, K.L. Nunn, H. Schroeder, J. McCallen, T. Moench, R. Cone, S.R. Roffler, S.K. Lai, Anti-PEG antibodies alter the mobility and biodistribution of densely PEGylated nanoparticles in mucus,

Acta Biomater. 43 (2016) 61–70. https://doi.org/10.1016/j.actbio.2016.07.019.

[13] S. Isojima, T.S. Li, Y. Ashitaka, Immunologic analysis of sperm-immobilizing factor found in sera of women with unexplained sterility, Am. J. Obstet. Gynecol. 101 (1968) 677–683. https://doi.org/10.1016/0002-9378(68)90307-4.

[14] R.A. Cone, Mucus, in: Handb. Mucosal Immunol., 2005: pp. 49–72.

[15] G.F.B. Schumacher, Immunology of spermatozoa and cervical mucus, Hum. Reprod. 3 (1988) 289–300. https://doi.org/10.1093/oxfordjournals.humrep.a136698.

[16] R.K. Naz, Vaccine for contraception targeting sperm, Immunol. Rev. 171 (1999) 193–202. https://doi.org/10.1111/j.1600-065X.1999.tb01349.x.

[17] L.E. Kerr, Sperm antigens and immunocontraception, Reprod. Fertil. Dev. 7 (1995) 825–830. https://doi.org/10.1071/RD9950825.

[18] R.K. Naz, Immunocontraceptive Effect of Izumo and Enhancement by Combination Vaccination, Mol. Reprod. Dev. 344 (2008) 336–344. https://doi.org/10.1002/mrd.

[19] E.J. Norton, A.B. Diekman, V.A. Westbrook, D.W. Mullins, K.L. Klotz, L.L. Gilmer, T.S. Thomas, D.C. Wright, J. Brisker, V.H. Engelhard, C.J. Flickinger, J.C. Herr, A male genital tract-specific carbohydrate epitope on human CD52: Implications for immunocontraception, Tissue Antigens. 60 (2002) 354–364. https://doi.org/10.1034/j.1399-0039.2002.600502.x.

[20] P.E. Castle, K.J. Whaley, T.E. Hoen, T.R. Moench, R.A. Cone, Contraceptive Effect of Sperm-Agglutinating Monoclonal Antibodies in Rabbits, Biol. Reprod. 56 (1997) 153–159. https://doi.org/10.1095/biolreprod56.1.153.

[21] X. Wu, A.J. Sereno, F. Huang, S.M. Lewis, R.L. Lieu, C. Weldon, C. Torres, C. Fine, M.A. Batt, J.R. Fitchett, A.L. Glasebrook, B. Kuhlman, S.J. Demarest, Fab-based bispecific antibody formats with robust biophysical properties and biological activity, MAbs. 7 (2015) 470–482. https://doi.org/10.1080/19420862.2015.1022694.

[22] S.J. Demarest, S.M. Glaser, Antibody therapeutics, antibody engineering, and the merits of protein stability, Curr. Opin. Drug Discov. & Dev. 11 (2008) 675—687. http://europepmc.org/abstract/MED/18729019.

[23] D.J. Anderson, P.M. Johnson, N.J. Alexander, W.R. Jones, P.D. Griffin, Monoclonal antibodies to human trophoblast and sperm antigens: Report of two WHO-sponsored workshops, June 30, 1986-Toronto, Canada, J. Reprod. Immunol. 10 (1987) 231–257. https://doi.org/10.1016/0165-0378(87)90089-1.

[24] A.B. Diekman, E.J. Norton, K.L. Klotz, V.A. Westbrook, H. Shibahara, S. Naaby-Hansen, C.J. Flickinger, J.C. Herr, N-linked glycan of a sperm CD52 glycoform associated with human infertility, FASEB J. 13 (1999) 1303–1313. https://doi.org/10.1096/fasebj.13.11.1303.

[25] C. Kirchhoff, S. Schröter, New insights into the origin, structure and role of CD52: A major component of the mammalian sperm glycocalyx, Cells Tissues Organs. 168 (2001) 93–104. https://doi.org/10.1159/000016810.

[26] T.C. McCauley, B.E. Kurth, E.J. Norton, K.L. Klotz, V.A. Westbrook, A.J. Rao, J.C. Herr, A.B. Diekman, Analysis of a human sperm CD52 glycoform in primates: Identification of an animal model for immunocontraceptive vaccine development, Biol. Reprod. 66 (2002) 1681–1688. https://doi.org/10.1095/biolreprod66.6.1681.

[27] J.C. Herr, C.J. Flickinger, M. Homyk, K. Klotz, E. John, Biochemical and morphological characterization of the intra-acrosomal antigen SP-10 from human sperm, Biol. Reprod. 42 (1990) 181–193. https://doi.org/10.1095/biolreprod42.1.181.

[28] A.B. Diekman, K.L. Klotz, V.A. Westbrook-Case, E.J. Norton, S. Naaby-Hansen, J.C. Herr, Biochemical characterization and purification of sperm agglutination antigen-1, a human sperm surface antigen implicated in gamete interactions, J. Reprod. Immunol. 34 (1997) 29–30. https://doi.org/10.1016/S0165-0378(97)90397-1.

[29] V. Chromikova, A. Mader, W. Steinfellner, R. Kunert, Evaluating the bottlenecks of recombinant IgM production in mammalian cells, Cytotechnology. 67 (2015) 343–356. https://doi.org/10.1007/s10616-014-9693-4.

[30] F. Samsudin, J.Y. Yeo, S.K.E. Gan, P.J. Bond, Not all therapeutic antibody isotypes are equal: The case of IgM: Versus IgG in Pertuzumab and Trastuzumab, Chem. Sci. 11 (2020) 2843–2854. https://doi.org/10.1039/c9sc04722k.

[31] A.J. MacPherson, K.D. McCoy, F.E. Johansen, P. Brandtzaeg, The immune geography of IgA induction and function, Mucosal Immunol. 1 (2008) 11–22. https://doi.org/10.1038/mi.2007.6.

[32] N.J. Mantis, N. Rol, B. Corthésy, Secretory IgA's complex roles in immunity and mucosal homeostasis in the gut, Mucosal Immunol. 4 (2011) 603–611. https://doi.org/10.1038/mi.2011.41.

[33] Y.Y. Wang, D. Harit, D.B. Subramani, H. Arora, P.A. Kumar, S.K. Lai, Influenza-binding antibodies immobilise influenza viruses in fresh human airway mucus, Eur Res J. 49 (2017) 1–4. https://doi.org/10.1183/13993003.01709-2016.

[34] J.M. Woof, M.A. Kerr, The function of immunoglobulin A in immunity, J. Pathol. 208 (2006) 270–282. https://doi.org/10.1002/path.1877.

[35] M. Paul, R. Reljic, K. Klein, P.M.W. Drake, C. Van Dolleweerd, M. Pabst, M. Windwarder, E. Arcalis, E. Stoger, F. Altmann, C. Cosgrove, A. Bartolf, S. Baden, J.K. Ma, Characterization of a plant-produced recombinant human secretory IgA with broad neutralizing activity against HIV, MAbs. 6 (2014) 1585–1597.

[36] V. Virdi, P. Juarez, V. Boudolf, A. Depicker, Recombinant IgA production for mucosal passive immunization, advancing beyond the hurdles, Cell. Mol. Life Sci. 73 (2016) 535–545. https://doi.org/10.1007/s00018-015-2074-0.

[37] K.T. Barnhart, M.J. Rosenberg, H.T. MacKay, D.L. Blithe, J. Higgins, T. Walsh, L. Wan, M. Thomas, M.D. Creinin, C. Westhoff, W. Schlaff, D.F. Archer, C. Ayers, A. Kaunitz, S. Das, T.R. Moench, Contraceptive efficacy of a novel spermicidal microbicide used with a diaphragm: A randomized controlled trial, Obstet. Gynecol. 110 (2007) 577–586. https://doi.org/10.1097/01.AOG.0000278078.45640.13.

[38] A. Mader, V. Chromikova, R. Kunert, Recombinant IgM expression in mammalian cells: A target

protein challenging biotechnological production, Adv. Biosci. Biotechnol. 04 (2013) 38–43. https://doi.org/10.4236/abb.2013.44a006.

[39] Y. Azuma, Y. Ishikawa, S. Kawai, T. Tsunenari, H. Tsunoda, T. Igawa, S.I. Iida, M. Nanami, M. Suzuki, R.F. Irie, M. Tsuchiya, H. Yamada-Okabe, Recombinant human hexamer-dominant IgM monoclonal antibody to ganglioside GM3 for treatment of melanoma, Clin. Cancer Res. 13 (2007) 2745–2750. https://doi.org/10.1158/1078-0432.CCR-06-2919.

[40] A.L. Nelson, E. Dhimolea, J.M. Reichert, Development trends for human monoclonal antibody therapeutics, Nat. Rev. Drug Discov. 9 (2010) 767–774. https://doi.org/10.1038/nrd3229.

[41] J.T. Huckaby, C.L. Parker, T.M. Jacobs, A. Schaefer, D. Wadsworth, A. Nguyen, A. Wang, J. Newby, S.K. Lai, Engineering Polymer-Binding Bispecific Antibodies for Enhanced Pretargeted Delivery of Nanoparticles to Mucus-Covered Epithelium, Angew. Chemie - Int. Ed. 58 (2019) 5604–5608. https://doi.org/10.1002/anie.201814665.

[42] J. Bearak, A. Popinchalk, L. Alkema, G. Sedgh, Global, regional, and subregional trends in unintended pregnancy and its outcomes from 1990 to 2014: estimates from a Bayesian hierarchical model Jonathan, Lancet Glob Heal. 6 (2018) 380–389. https://doi.org/10.1016/j.physbeh.2017.03.040.

[43] L.B. Finer, S.K. Henshaw, Disparities in Rates of Unintended Pregnancy In the United States, 1994 and 2001, Perspect. Sex. Reprod. Health. 38 (2006) 90–96. https://doi.org/10.1363/3809006.

[44] L.B. Finer, M.R. Zolna, Declines in Unintended Pregnancy in the United States, 2008–2011, N. Engl. J. Med. 374 (2016) 843–852. https://doi.org/10.1056/NEJMsa1506575.

[45] S.O. Skouby, Contraceptive use and behavior in the 21st century: A comprehensive study across five European countries, Eur. J. Contracept. Reprod. Heal. Care. 9 (2004) 57–68. https://doi.org/10.1080/13625180410001715681.

[46] J. Brynhildsen, Combined hormonal contraceptives : prescribing patterns , compliance , and benefits versus risks, Ther. Adv. Drug Saf. 5 (2014) 201–213. https://doi.org/10.1177/2042098614548857.

[47] W.W. Beck, Complications and Contraindications of Oral Contraception, Clin. Obstet. Gynecol. 24 (1981) 893–902. https://doi.org/10.1097/00003081-198109000-00016.

[48] D. Grossman, K. White, K. Hopkins, J. Amastae, M. Shedlin, J.E. Potter, Contraindications to combined oral contraceptives among over-the-counter compared with prescription users, Obstet. Gynecol. 117 (2011) 558–565. https://doi.org/10.1097/AOG.0b013e31820b0244.

[49] J.W. Roos-Hesselink, J. Cornette, K. Sliwa, P.G. Pieper, G.R. Veldtman, M.R. Johnson, Contraception and cardiovascular disease, Eur. Heart J. 36 (2015) 1728–1734. https://doi.org/10.1093/eurheartj/ehv141.

[50] K. Daniels, J. Daugherty, J. Jones, W. Mosher, Current Contraceptive Use and Variation by Selected Characteristics Among Women Aged 15–44: United States, 2011–2013, Natl. Cent. Heal. Stat. (2015) 1014–1018.

[51] J. Kremer, S. Jager, The Sperm-Cervical Mucus Contact Test: A Preliminary Report, Fertil. Steril.

27 (1976) 335–340. https://doi.org/10.1016/S0015-0282(16)41726-7.

[52] S. Komori, N. Yamasaki, M. Shigeta, S. Isojima, T. Watanabe, Production of heavy-chain class-switch variants of human monoclonal antibody by recombinant DNA technology, Clin. Exp. Immunol. 71 (1988) 508–516. https://doi.org/10.1007/978-3-211-89836-9_877.

[53] R. Vazquez-Lombardi, D. Nevoltris, A. Luthra, P. Schofield, C. Zimmermann, D. Christ, Transient expression of human antibodies in mammalian cells, Nat. Protoc. 13 (2018) 99–117. https://doi.org/10.1038/nprot.2017.126.

[54] G.Y. Wiederschain, The proteomics protocols handbook, Biochem. 71 (2006) 696–696. https://doi.org/10.1134/s0006297906060150.

[55] D. Some, H. Amartely, A. Tsadok, M. Lebendiker, Characterization of proteins by size-exclusion chromatography coupled to multi-angle light scattering (Sec-mals), J. Vis. Exp. 2019 (2019) 1–9. https://doi.org/10.3791/59615.

[56] P. Debye, Light scattering in solutions, J. Appl. Phys. 15 (1944). https://doi.org/10.1088/0150-536X/25/1/002.

[57] M. Andersson, B. Wittgren, K.G. Wahlund, Accuracy in multiangle light scattering measurements for molar mass and radius estimations. Model calculations and experiments, Anal. Chem. 75 (2003) 4279–4291. https://doi.org/10.1021/ac030128+.

[58] A. Real-Hohn, M. Groznica, N. Löffler, D. Blaas, H. Kowalski, nanoDSF: In vitro Label-Free Method to Monitor Picornavirus Uncoating and Test Compounds Affecting Particle Stability, Front. Microbiol. 11 (2020) 1–12. https://doi.org/10.3389/fmicb.2020.01442.

[59] W.H. Organization, Examination and processing of human semen, in: World Health, 2010: pp. 1–271. https://doi.org/10.1038/aja.2008.57.

[60] Y. Hirano, H. Shibahara, H. Obara, T. Suzuki, S. Takamizawa, C. Yamaguchi, H. Tsunoda, I. Sato, Relationships between sperm motility characteristics assessed by the computer-aided sperm analysis (CASA) and fertilization rates in vitro, J. Assist. Reprod. Genet. 18 (2001) 213–218. https://doi.org/10.1023/A:1009420432234.

[61] A. Mitra, R.T. Richardson, M.G. O'Rand, Analysis of Recombinant Human Semenogelin as an Inhibitor of Human Sperm Motility, Biol. Reprod. 82 (2010) 489–496. https://doi.org/10.1095/biolreprod.109.081331.

[62] H. Wu, D.S. Pfarr, S. Johnson, Y.A. Brewah, R.M. Woods, N.K. Patel, W.I. White, J.F. Young, P.A. Kiener, Development of Motavizumab, an Ultra-potent Antibody for the Prevention of Respiratory Syncytial Virus Infection in the Upper and Lower Respiratory Tract, J. Mol. Biol. 368 (2007) 652–665. https://doi.org/10.1016/j.jmb.2007.02.024.

[63] J.M. Newby, A.M. Schaefer, P.T. Lee, M.G. Forest, S.K. Lai, Convolutional neural networks automate detection for tracking of submicron-scale particles in 2D and 3D, Proc. Natl. Acad. Sci. U. S. A. 115 (2018) 9026–9031. https://doi.org/10.1073/pnas.1804420115.

[64] E. Garber, S.J. Demarest, A broad range of Fab stabilities within a host of therapeutic IgGs, Biochem. Biophys. Res. Commun. 355 (2007) 751–757.

https://doi.org/10.1016/j.bbrc.2007.02.042.

[65] R.M. Ionescu, J. Vlasak, C. Price, M. Kirchmeier, Contribution of Variable Domains to the Stability of Humanized IgG1 Monoclonal Antibodies, J. Pharm. Sci. 97 (2008) 1414–1426. https://doi.org/10.1002/jps.

[66] R.M. Sharpe, Sperm counts and fertility in men: A rocky road ahead. Science & Society Series on Sex and Science, EMBO Rep. 13 (2012) 398–403. https://doi.org/10.1038/embor.2012.50.

[67] D.S. Fordney Settlage, M. Motoshima, D.R. Tredway, Sperm Transport from the External Cervical Os to the Fallopian Tubes in Women: A Time and Quantitation Study, Fertil. Steril. 24 (1973) 655–661. https://doi.org/10.1016/s0015-0282(16)39908-3.

[68] C.A. Diebolder, F.J. Beurskens, R.N. De Jong, R.I. Koning, K. Strumane, M.A. Lindorfer, M. Voorhorst, D. Ugurlar, S. Rosati, A.J.R. Heck, J.G.J. Van De Winkel, I.A. Wilson, A.J. Koster, R.P. Taylor, E.O. Saphire, D.R. Burton, J. Schuurman, P. Gros, P.W.H.I. Parren, Complement is activated by IgG hexamers assembled at the cell surface, Science (80-. ). 343 (2014) 1260–1263. https://doi.org/10.1126/science.1248943.

[69] V. Sorensen, V. Sundvold, T.E. Michaelsen, I. Sandlie, Polymerization of IgA and IgM: roles of Cys309/Cys414 and the secretory tailpiece., J. Immunol. 162 (1999) 3448–55. http://www.ncbi.nlm.nih.gov/pubmed/10092800.

[70] K. Teye, K. Hashimoto, S. Numata, K. Ohta, M. Haftek, T. Hashimoto, Multimerization is required for antigen binding activity of an engineered IgM/IgG chimeric antibody recognizing a skin-related antigen, Sci. Rep. 7 (2017) 1–12. https://doi.org/10.1038/s41598-017-08294-2.

[71] A. Hirsh, Male subfertility, Br. Med. J. 327 (2003) 669–672. https://doi.org/https://doi.org/10.1136/bmj.327.7416.669.

[72] D. Li, A.J. Wilcox, D.B. Dunson, Benchmark Pregnancy Rates and the Assessment of Post-coital Contraceptives: An Update, Contraception. 91 (2015) 344–349. https://doi.org/10.1016/j.physbeh.2017.03.040.

[73] A. Hussain, F. Ahsan, The vagina as a route for systemic drug delivery, J. Control. Release. 103 (2005) 301–313. https://doi.org/10.1016/j.jconrel.2004.11.034.

[74] L. Zeitlin, R.A. Cone, K.J. Whaley, Using Monoclonal Antibodies to Prevent Mucosal Transmission of Epidemic Infectious Diseases., Emerg. Infect. Dis. 5 (1999) 54–64.

[75] D.H. Owen, D.F. Katz, A vaginal fluid simulant, Contraception. 59 (1999) 91–95. https://doi.org/10.1016/S0010-7824(99)00010-4.

[76] M. Johansson, N.Y. Lycke, Immunology of the human genital tract, Curr. Opin. Infect. Dis. 16 (2003) 43–49. https://doi.org/10.1097/00001432-200302000-00008.

[77] T. Moench, P. Blumenthal, R. Cone, K. Whaley, Antibodies may provide prolonged microbicidal activity due to their long residence time in the vagina, in: AIDS, 2001: p. S42.

[78] C. Zhao, M. Gunawardana, F. Villinger, M.M. Baum, M. Remedios-Chan, T.R. Moench, L. Zeitlin, K.J. Whaley, O. Bohorov, T.J. Smith, D.J. Anderson, J.A. Moss, Pharmacokinetics and

preliminary safety of pod-intravaginal rings delivering the monoclonal antibody VRC01-N for HIV prophylaxis in a macaque model, Antimicrob. Agents Chemother. 61 (2017) 1–16. https://doi.org/10.1128/AAC.02465-16.

[79] R. Racine, G.M. Winslow, IgM in microbial infections: Taken for granted?, Immunol. Lett. 125 (2009) 79–85. https://doi.org/10.1016/j.imlet.2009.06.003.

[80] R.K. Naz, X. Zhu, Recombinant Fertilization Antigen-1 Causes a Contraceptive Effect in Actively Immunized Mice, Biol. Reprod. 59 (1998) 1095–1100. https://doi.org/10.1095/biolreprod59.5.1095.

[81] R.K. Naz, S.C. Chauhan, Human Sperm-Specific Peptide Vaccine That Causes Long-Term Reversible Contraception, Biol. Reprod. 67 (2002) 674–680. https://doi.org/10.1095/biolreprod67.2.674.

[82] P. Primakoff, W. Lathrop, L. Woolman, A. Cowan, D. Myles, Fully effective contraception in male and female guinea pigs immunized with the sperm protein PH-20, Nature. 335 (1988) 543–546. https://doi.org/10.1038/335543a0.

[83] S.G. Goodson, S. White, A.M. Stevans, S. Bhat, C.Y. Kao, S. Jaworski, T.R. Marlowe, M. Kohlmeier, L. McMillan, S.H. Zeisel, D.A. O'Brien, CASAnova: A multiclass support vector machine model for the classification of human sperm motility patterns, Biol. Reprod. 97 (2017) 698–708. https://doi.org/10.1093/biolre/iox120.

[84] E.R. Boskey, T.R. Moench, P.S. Hees, R.A. Cone, A self-sampling method to obtain large volumes of undiluted cervicovaginal secretions., Sex. Transm. Dis. 30 (2003) 107–109. https://doi.org/10.1097/00007435-200302000-00002.

[85] L. Samanta, R. Parida, T.R. Dias, A. Agarwal, The enigmatic seminal plasma: A proteomics insight from ejaculation to fertilization, Reprod. Biol. Endocrinol. 16 (2018) 1–11. https://doi.org/10.1186/s12958-018-0358-6.

[86] T.L. Tollner, C.L. Bevins, G.N. Cherr, Multifunctional glycoprotein DEFB126-a curious story of defensin-clad spermatozoa, Nat. Rev. Urol. 9 (2012) 365–375. https://doi.org/10.1038/nrurol.2012.109.

[87] F. Ma, D. Wu, L. Deng, P. Secrest, J. Zhao, N. Varki, S. Lindheim, P. Gagneux, Sialidases on mammalian sperm mediate deciduous sialylation during capacitation, J. Biol. Chem. 287 (2012) 38073–38079. https://doi.org/10.1074/jbc.M112.380584.

[88] L.C.P. Molina, G.M. Luque, P.A. Balestrini, C.I. Marín-Briggiler, A. Romarowski, M.G. Buffone, Molecular basis of human sperm capacitation, Front. Cell Dev. Biol. 6 (2018) 1–23. https://doi.org/10.3389/fcell.2018.00072.

[89] M.A. Battistone, V.G. Da Ros, A.M. Salicioni, F.A. Navarrete, D. Krapf, P.E. Visconti, P.S. Cuasnicú, Functional human sperm capacitation requires both bicarbonate-dependent PKA activation and down-regulation of Ser/Thr phosphatases by Src family kinases, Mol. Hum. Reprod. 19 (2013) 570–580. https://doi.org/10.1093/molehr/gat033.

[90] D.F. Archer, C.K. Mauck, A. Viniegra-Sibal, F.D. Anderson, Lea's Shield®: A phase I postcoital study of a new contraceptive barrier device, Contraception. 52 (1995) 167–173.

https://doi.org/10.1016/0010-7824(95)00162-4.

[91] C.K. Mauck, J.M. Baker, S.P. Barr, W. Johanson, D.F. Archer, A phase I study of Femcapρ used with and without spermicide postcoital testing, Contraception. 56 (1997) 111–115. https://doi.org/10.1016/S0010-7824(97)00098-X.

[92] C.K. Mauck, M.D. Creinin, K.T. Barnhart, S.A. Ballagh, D.F. Archer, M.M. Callahan, S.W. Schmitz, R. Bax, A Phase I comparative postcoital testing study of three concentrations of C31G, Contraception. 70 (2004) 227–231. https://doi.org/10.1016/j.contraception.2004.02.001.

[93] C.K. Mauck, V. Brache, T. Kimble, A. Thurman, L. Cochon, S. Littlefield, K. Linton, G.F. Doncel, J.L. Schwartz, A phase I randomized postcoital testing and safety study of the Caya diaphragm used with 3% Nonoxynol-9 gel, ContraGel or no gel, Contraception. 96 (2017) 124–130. https://doi.org/10.1016/j.contraception.2017.05.016.

[94] C. Mauck, L.H. Glover, E. Miller, S. Allen, D.F. Archer, P. Blumenthal, B.A. Rosenzweig, R. Dominik, K. Sturgen, J. Cooper, F. Fingerhut, L. Peacock, H.L. Gabelnick, Lea's Shield®: A study of the safety and efficacy of a new vaginal barrier contraceptive used with and without spermicide, Contraception. 53 (1996) 329–335. https://doi.org/10.1016/0010-7824(96)00081-9.

[95] C. Mauck, M. Callahan, D.H. Weiner, R. Dominik, A comparative study of the safety and efficacy of femcap®, a new vaginal barrier contraceptive, and the ortho all-flex® diaphragm, Contraception. 60 (1999) 71–80. https://doi.org/10.1016/S0010-7824(99)00068-2.

[96] A. Burke, K. Barnhart, J. Jensen, M. Creinin, T. Walsh, L. Wan, C. Westhoff, M. Thomas, D. Archer, H. Wu, J. Liu, W. Schlaff, B. Carr, D. Blithe, Contraceptive Efficacy, Acceptability, and Safety of C31G and Nonoxynol-9 Spermicidal Gels, Obstet. Gynecol. 116 (2010) 1265–1273.

[97] J.L. Schwartz, D.H. Weiner, J.J. Lai, R.G. Frezieres, M.D. Creinin, D.F. Archer, L. Bradley, K.T. Barnhart, A. Poindexter, M. Kilbourne-Brook, M.M. Callahan, C.K. Mauck, Contraceptive efficacy, safety, fit, and acceptability of a single-size diaphragm developed with end-user input, Obstet. Gynecol. 125 (2015) 895–903. https://doi.org/10.1097/AOG.0000000000000721.

[98] K. Barnhart, C. Dart, K. Culwell, Efficacy, Safety, and Acceptability of Acidform (Amphora) and Nonoxynol-9 Contraceptive Vaginal Gels [16N], Obstet. Gynecol. 127 (2016) 118.

[99] J.D.S. Holt, D. Cameron, N. Dias, J. Holding, A. Muntendam, F. Oostebring, P. Dreier, L. Rohan, J. Nuttall, The sheep as a model of preclinical safety and pharmacokinetic evaluations of candidate microbicides, Antimicrob. Agents Chemother. 59 (2015) 3761–3770. https://doi.org/10.1128/AAC.04954-14.

[100] J.A. Moss, A.M. Malone, T.J. Smith, S. Kennedy, C. Nguyen, K.L. Vincent, M. Motamedi, M.M. Baum, Pharmacokinetics of a multipurpose pod-intravaginal ring simultaneously delivering five drugs in an ovine model, Antimicrob. Agents Chemother. 57 (2013) 3994–3997. https://doi.org/10.1128/AAC.00547-13.

[101] J.K. Ma, J. Drossard, D. Lewis, F. Altmann, J. Boyle, P. Christou, T. Cole, P. Dale, C.J. van Dolleweerd, V. Isitt, D. Katinger, M. Lobedan, H. Mertens, M.J. Paul, T. Rademacher, M. Sack, P.A.C. Hundleby, G. Stiegler, E. Stoger, R.M. Twyman, B. Vcelar, R. Fischer, Regulatory approval and a first-in-human phase I clinical trial of a monoclonal antibody produced in transgenic tobacco plants, Plant Biotechnol. J. 13 (2015) 1106–1120.

https://doi.org/10.1111/pbi.12416.

[102] S.S. Suarez, A.A. Pacey, Sperm transport in the female reproductive tract, Hum. Reprod. Update. 12 (2006) 23–37. https://doi.org/10.1093/humupd/dmi047.

[103] H.M. Behre, M. Zitzmann, R.A. Anderson, D.J. Handelsman, S.W. Lestari, R.I. McLachlan, M.C. Meriggiola, M.M. Misro, G. Noe, F.C.W. Wu, M.P.R. Festin, N.A. Habib, K.M. Vogelsong, M.M. Callahan, K.A. Linton, D.S. Colvard, Efficacy and safety of an injectable combination hormonal contraceptive for men, J. Clin. Endocrinol. Metab. 101 (2016) 4779–4788. https://doi.org/10.1210/jc.2016-2141.

[104] W.H. Organization, Contraceptive efficacy of testosterone-induced azoospermia and oligozoospermia in normal men, Fertil. Steril. 65 (1996) 821–829. https://doi.org/10.1016/s0015-0282(16)58221-1.

[105] W.H. Organization, Contraceptive efficacy of testosterone-induced azoospermia in normal men., Lancet. 336 (1990) 955–9. http://www.ncbi.nlm.nih.gov/pubmed/1977002.

[106] D.S. Guzick, J.W. Overstreet, P. Factor-Litvak, C.K. Brazil, S.T. Nakajima, C. Coutifaris, S.A. Carson, P. Cisneros, M.P. Steinkampf, J.A. Hill, D. Xu, D.L. Vogel, Sperm morphology, motility, and concentration in fertile and infertile men, N. Engl. J. Med. 345 (2001) 1388–1393.

[107] C. Garrett, D.Y. Liu, R.I. McLachlan, H.W.G. Baker, Time course of changes in sperm morphometry and semen variables during testosterone-induced suppression of human spermatogenesis, Hum. Reprod. 20 (2005) 3091–3100. https://doi.org/10.1093/humrep/dei174.

[108] D.Y. Liu, R. Johnston, H.W.G. Baker, Ability of spermatozoa to bind to the zona pellucida during oligozoospermia induced with testosterone during a male contraceptive trial, Int. J. Androl. 18 (1995) 39–44. https://doi.org/10.1111/j.1365-2605.1995.tb00637.x.

[109] Y.Q. Gu, X.H. Wang, D. Xu, L. Peng, L.F. Cheng, M.K. Huang, Z.J. Huang, G.Y. Zhang, A multicenter contraceptive efficacy study of injectable testosterone undecanoate in healthy Chinese men, J. Clin. Endocrinol. Metab. 88 (2003) 562–568. https://doi.org/10.1210/jc.2002-020447.

[110] C.K. Mauck, S. Allen, J.M. Baker, S.P. Barr, T. Abercrombie, D.F. Archer, An evaluation of the amount of nonoxynol-9 remaining in the vagina up to 4 h after insertion of a vaginal contraceptive film (VCFρ) containing 70 mg nonoxynol-9, Contraception. 56 (1997) 103–110. https://doi.org/10.1016/S0010-7824(97)00100-5.

[111] A.J. Wilcox, D. Dunson, D.D. Baird, The timing of the “fertile window” in the menstrual cycle: Day specific estimates from a prospective study, Br. Med. J. 321 (2000) 1259–1262. https://doi.org/10.1136/bmj.321.7271.1259.

[112] M. Mihm, S. Gangooly, S. Muttukrishna, The normal menstrual cycle in women, Anim. Reprod. Sci. 124 (2011) 229–236. https://doi.org/10.1016/j.anireprosci.2010.08.030.

[113] B. Kelly, Industrialization of mAb production technology, MAbs. 1 (2009) 443–452.

[114] Wellcome, IAVI, Expanding access to monoclonal products: A global call to action, 2020. https://wellcome.ac.uk/sites/default/files/expanding-access-to-monoclonal-antibody-based-products-executive-summary.pdf.

[115] V. Sorensen, I.B. Rasmussen, L. Norderhaug, I. Natvig, T.E. Michaelsen, I. Sandlie, Effect of the IgM and IgA secretory tailpieces on polymerization and secretion of IgM and IgG., J. Immunol. 156 (1996) 2858–2865.

[116] C.W. Skovlund, L.S. Mørch, L.V. Kessing, O. Lidegaard, Association of hormonal contraception with depression, JAMA Psychiatry. 73 (2016) 1154–1162. https://doi.org/10.1001/jamapsychiatry.2016.2387.

[117] L. Van Damme, G. Ramjee, M. Alary, B. Vuylsteke, V. Chandeying, H. Rees, P. Sirivongrangson, L. Mukenge-Tshibaka, V. Ettiegne-Traore, C. Uaheowitchai, S.S.A. Karim, B. Masse, J. Perriens, M. Laga, Effectiveness of COL-1492, a nonoxynol-9 vaginal gel, on HIV-1 transmission in female sex workers: a randomised controlled trial, Lancet. 360 (2002) 971–77.

[118] M.K. Stafford, H. Ward, A. Flanagan, I.J. Rosenstein, D. Taylor-Robinson, J.R. Smith, J. Weber, V.S. Kitchen, Safety study of nonoxynol-9 as a vaginal microbicide: Evidence of adverse effects, J. Acquir. Immune Defic. Syndr. Hum. Retrovirology. 17 (1998) 327–331. https://doi.org/10.1097/00042560-199804010-00006.

[119] J. Kreiss, E. Ngugi, K. Holmes, J. Ndinya-Achola, P. Waiyaki, P.L. Roberts, I. Ruminjo, R. Sajabi, J. Kimata, T.R. Fleming, A. Anzala, D. Holton, F. Plummer, Efficacy of Nonoxynol 9 Contraceptive Sponge Use in Preventing Heterosexual Acquisition of HIV in Nairobi Prostitutes, J. Am. Med. Assoc. 268 (1992) 477–482. https://doi.org/10.1001/jama.1992.03490040053025.

[120] R.A. Cone, K.J. Whaley, Monoclonal Antibodies for Reproductive Health: Part I. Preventing Sexual Transmission of Disease and Pregnancy With Topically Applied Antibodies, Am. J. Reprod. Immunol. 32 (1994) 114–131. https://doi.org/10.1111/j.1600-0897.1994.tb01102.x.

[121] D.J. Anderson, J.A. Politch, R.A. Cone, L. Zeitlin, S.K. Lai, P.J. Santangelo, T.R. Moench, K.J. Whaley, Engineering monoclonal antibody-based contraception and multipurpose prevention technologies, Biol. Reprod. 103 (2020) 275–285. https://doi.org/10.1093/biolre/ioaa096.

[122] A. Giritch, S. Marillonnet, C. Engler, G. Van Eldik, J. Botterman, V. Klimyuk, Y. Gleba, Rapid high-yield expression of full-size IgG antibodies in plants coinfected with noncompeting viral vectors, Proc. Natl. Acad. Sci. U. S. A. 103 (2006) 14701–14706. https://doi.org/10.1073/pnas.0606631103.

[123] V. Klimyuk, G. Pogue, S. Herz, J. Butler, H. Haydon, Production of Recombinant Antigens and Antibodies in Nicotiana benthamiana Using `Magnifection' Technology: GMP-Compliant Facilities for Small- and Large-Scale Manufacturing, in: K. Palmer, Y. Gleba (Eds.), Plant Viral Vectors, Springer Berlin Heidelberg, Berlin, Heidelberg, 2014: pp. 127–154. https://doi.org/10.1007/82_2012_212.

[124] G.P. Pogue, F. Vojdani, K.E. Palmer, E. Hiatt, S. Hume, J. Phelps, L. Long, N. Bohorova, D. Kim, M. Pauly, J. Velasco, K. Whaley, L. Zeitlin, S.J. Garger, E. White, Y. Bai, H. Haydon, B. Bratcher, Production of pharmaceutical-grade recombinant aprotinin and a monoclonal antibody product using plant-based transient expression systems, Plant Biotechnol. J. 8 (2010) 638–654. https://doi.org/10.1111/j.1467-7652.2009.00495.x.

[125] S. Marillonnet, C. Thoeringer, R. Kandzia, V. Klimyuk, Y. Gleba, Systemic Agrobacterium tumefaciens-mediated transfection of viral replicons for efficient transient expression in plants, Nat. Biotechnol. 23 (2005) 718–723. https://doi.org/10.1038/nbt1094.

[126] S. Cu-Uvin, K.H. Mayer, T. Moench, K.T. Tashima, J.G. Marathe, J.A. Politch, T.J. Nyhuis, L. Zeitlin, H.M. Spiegel, K. Whaley, D. Anderson, Phase 1 trial to assess safety and antiviral activity of MB66 vaginal film, in: Conf. Retroviruses Opportunistic Infect., Boston, Massachusetts, 2018. https://www.embase.com/search/results?subaction=viewrecord&id=L621729014&from=export.

[127] C.K. Mauck, K.L. Vincent, The postcoital test in the development of new vaginal contraceptives, Biol. Reprod. 103 (2020) 437–444. https://doi.org/10.1093/biolre/ioaa099.

[128] H. Hocini, A. Barra, L. Belec, Systemic and Secretory Humoral Immunity in the Normal Human Vaginal Tract, Scand. J. Immunol. 42 (1995) 269–274. https://doi.org/10.1111/j.1365-3083.1995.tb03653.x.

[129] A. Quesnel, S. Cu-Uvin, D. Murphy, R.L. Ashley, T. Flanigan, M.R. Neutra, Comparative analysis of methods for collection and measurement of immunoglobulins in cervical and vaginal secretions of women, J. Immunol. Methods. 202 (1997) 153–161. https://doi.org/10.1016/S0022-1759(97)00003-3.

[130] D.J. Anderson, R. Le Grand, Cell-Associated HIV mucosal transmission: The neglected pathway, J. Infect. Dis. 210 (2014) S606–S608. https://doi.org/10.1093/infdis/jiu538.

[131] T. Gong, W. Zhang, M.A. Parniak, P.W. Graebing, B. Moncla, P. Gupta, K.M. Empey, L.C. Rohan, Preformulation and Vaginal Film Formulation Development of Microbicide Drug Candidate CSIC for HIV Prevention, J. Pharm. Innov. 12 (2017) 142–154. https://doi.org/10.1007/s12247-017-9274-0.

[132] A.S. Ham, L.C. Rohan, A. Boczar, L. Yang, K.W. Buckheit, R.W.B. Jr., Vaginal Film Drug Delivery of the Pyrimidinedione IQP-0528 for the Prevention of HIV Infection, Pharm Res. 29 (2012) 1897–1907. https://doi.org/10.1016/j.physbeh.2017.03.040.

[133] K.E. Bunge, C.S. Dezzutti, L.C. Rohan, C.W. Hendrix, M.A. Marzinke, N. Richardson-Harman, B.J. Moncla, B. Devlin, L.A. Meyn, H.M.L. Spiegel, S.L. Hillier, A Phase 1 trial to assess the safety, acceptability, pharmacokinetics, and pharmacodynamics of a novel dapivirine vaginal film, J. Acquir. Immune Defic. Syndr. 71 (2016) 498–505. https://doi.org/10.1097/QAI.0000000000000897.

[134] A. Van Der Straten, J. Stadler, E. Montgomery, M. Hartmann, B. Magazi, F. Mathebula, K. Schwartz, N. Laborde, L. Soto-Torres, Women's experiences with oral and vaginal pre-exposure prophylaxis: The VOICE-C qualitative study in Johannesburg, South Africa, PLoS One. 9 (2014). https://doi.org/10.1371/journal.pone.0089118.

[135] C. Coggins, C.J. Elias, R. Atisook, M.T. Bassett, V. Ettiègne-Traoré, P.D. Ghys, L. Jenkins-Woelk, E. Thongkrajai, N.L. VanDevanter, Women's preferences regarding the formulation of over-the-counter vaginal spermicides, AIDS. 12 (1998) 1389–1403.

[136] W. Zhang, M. Hu, Y. Shi, T. Gong, C.S. Dezzutti, S.G. Sarafianos, M.A. Parniak, L.C. Rohan, Vaginal microbicide film combinations of two reverse transcriptase inhibitors, EFdA and CSIC, for the prevention of HIV-1 sexual transmission, Pharm Res. 32 (2015) 2960–2972. https://doi.org/10.1007/s11095-015-1678-2.Vaginal.

[137] A. Akil, B. Devlin, M. Cost, L.C. Rohan, Increased dapivirine tissue accumulation through vaginal film codelivery of dapivirine and tenofovir, Mol. Pharm. 11 (2014) 1533–1541.

https://doi.org/10.1021/mp4007024.

[138] A. Akil, M.A. Parniak, C.S. Dezzuitti, B.J. Moncla, M.R. Cost, M. Li, L.C. Rohan, Development and Characterization of a Vaginal Film Containing Dapivirine, a Non- nucleoside Reverse Transcriptase Inhibitor (NNRTI), for prevention of HIV-1 sexual transmission, 2011. https://doi.org/10.1007/s13346-011-0022-6.Development.

[139] C.J. Costanzo, Immune defense of the female lower reproductive tract and the use of monoclonal antibody-based topical microbicide films to protect against HIV infection, 2015.

[140] J. Li, G. Regev, S.K. Patel, D. Patton, Y. Sweeney, P. Graebing, S. Grab, L. Wang, V. Sant, L.C. Rohan, Rational design of a multipurpose bioadhesive vaginal film for co-delivery of dapivirine and levonorgestrel, Pharmaceutics. 12 (2020). https://doi.org/10.3390/pharmaceutics12010001.

[141] R. Cazorla-Luna, F. Notario-Pérez, A. Martín-Illana, L.M. Bedoya, A. Tamayo, J. Rubio, R. Ruiz-Caro, M.D. Veiga, Development and in Vitro/ Ex Vivo Characterization of Vaginal Mucoadhesive Bilayer Films Based on Ethylcellulose and Biopolymers for Vaginal Sustained Release of Tenofovir, Biomacromolecules. 21 (2020) 2309–2319. https://doi.org/10.1021/acs.biomac.0c00249.